IKU
SINTEF GROUP

Institutt for kontinentalsokkelundersøkelser og petroleumsteknologi A/S
Continental Shelf and Petroleum Technology Research Institute

S.P. Andersen veg 15 b * N-7034 Trondheim, Norway
Tel.: + 47 7 591100 * Telex: 55 434 iku n * Telefax: + 47 7 591102 (aut.)

REPORT

REG. NO.:	ACCESSIBILITY:
91.081	Confidential

REPORT TITLE:
SHALLOW DRILLING IN HOPENDJUPET, NORTHERN BARENTS SEA

REPORT NO.: 23.1529.00/01.91

AUTHORS:
Gunn Mangerud, Tom Bugge, Vidar Fjerdingstad, Geir B. Larssen, Leslie Leith, Fridtjof Riis, Robert W. Williams

DATE:	NO. OF PAGES:	NO. OF APPENDICES:	PROJECT MANAGER:	SIGN.:
4 July 1991	128	8	Tom Bugge	Tom Bugge

CLIENT:	APPROVED for	SIGN.:
Norwegian Petroleum Directorate (NPD)	Atle Mørk p.p. Helge H. Gabrielsen	

SUMMARY:

During the summer 1990, three shallow cores were drilled in the northern Barents Sea. Two cores were of Middle Triassic age, comprising about 15 metres of Anisian section (7532/02-U-01) on the Sentralbanken high and 89 metres of Ladinian section (7532/02-U-01) on the Gardarbanken high. An upper Jurassic - Lower Cretaceous core was drilled on the Sentralbanken high comprising 119 metres of section.

Totally 220 metres of core was obtained (core recovery 98.3%).

KEY WORDS:

Shallow Drilling	Triassic
Barents Sea	Jurassic
Hopendjupet	Cretaceous

Skipnes

CONTENTS

APPENDICES

P bør endres
Innledn. →
hvem hvor gjort hva

IKU SINTEF GRUPPEN

Preface

This project has been carried out by IKU on behalf of the Norwegian Petroleum Directorate (NPD) and comprises the shallow drilling operation and the analyses, evaluation of results and reporting. Scientists from the NPD as mentioned below have contributed with parts of the work performed. IKU has been responsible for the performance of the project and the content of the report.

Responsible contact person at NPD has been Fridtjof Riis. Project manager has been Tom Bugge and Kristin Dahlen Brønner has been project secretary. Gunn Mangerud has coordinated the laboratory work and reporting of the biostratigraphy. Leslie Leith was responsible for the organic geochemistry. The report is based on contributions from the following persons:

Field work:
Fridtjof Riis (NPD) and Stig Bakke, Tom Bugge, Vidar Fjerdingstad, Leslie Leith, Morten Smelror, Dag Arne Westgaard and Nils Århus from IKU.

Seismic interpretation:
Fridtjof Riis, NPD and Tom Bugge.

Sedimentology:
Geir Birger Larssen, NPD (core 7533/03-U-01).
Vidar Fjerdingstad (cores 7532/02-U-01 and 7427/03-U-01).

XRD interpretation:
Hans Rendall (core 7533/03-U-01).
Vidar Fjerdingstad (cores 7532/02-U-01 and 7427/03-U-01).

Palynology:
Robert Williams, NPD (core 7533/03-U-01).
Gunn Mangerud (cores 7532/02-U-01 and 7427/03-U-01).

Micropalontology:
Aase Moe, NPD and Jacob G. Verdenius (core 7533/03-U-01).

Ammonites:
Andrzej Wierzbowski (University of Warsaw) (core 7533/03-U-01).

Trace fossils:
Richard Bromley (Ichnos, Denmark).

Organic geochemistry:
Leslie Leith.

Laboratory work:
Grete Haugen, Sølvi Stene, Torunn Vinge, Unni Merete Wang, IKU.
Aase Moe, Finn Moe, NPD.

Drawing:
Rolf Angell-Petersen, Inger Lisbet Berg, Ingrid Brandslet, Britt Egeland, Kåre Holst, Jan Helge Johansen.

Computing:
Stig Bakke.

Text processing:
Kristin Dahlen Brønner, Jorunn B. Lundhaug.

Printing:
Geir Herje

Preparation of slabs and core photographs:
Øistein How, Sølvi Stene, Unni Merete Wang.

Ron Steel, University of Bergen contributed to the interpretation of the Jurassic/Cretaceous core 7533/03-U-01. Nils Århus edited the biostratigraphy of core 7533/03-U-01. Joar Sættem contributed to the discussion about the glaciotectonics and origin of the crater structures. Atle Mørk reviewed most of the report. All these persons are acknowledged, in addition to the crew on board the drillig vessel M/S "Bucentaur", the personnel from Fugro-McClelland BV, A/S Geoteam and Dia-Team A/S for excellent work during the drilling operation.

1. INTRODUCTION

This report gives the result from bedrock coring at three sites in Hopendjupet in the northern Barents Sea (Figure 1.1). The project has been carried out on behalf of the Norwegian Petroleum Directorate (NPD) with the objective of supplying data for the hydrocarbon evaluation and further planning of activity in this part of the Barents Sea. Personnel from the NPD has contributed in the planning as well as in the accomplishment of the work (see Preface).

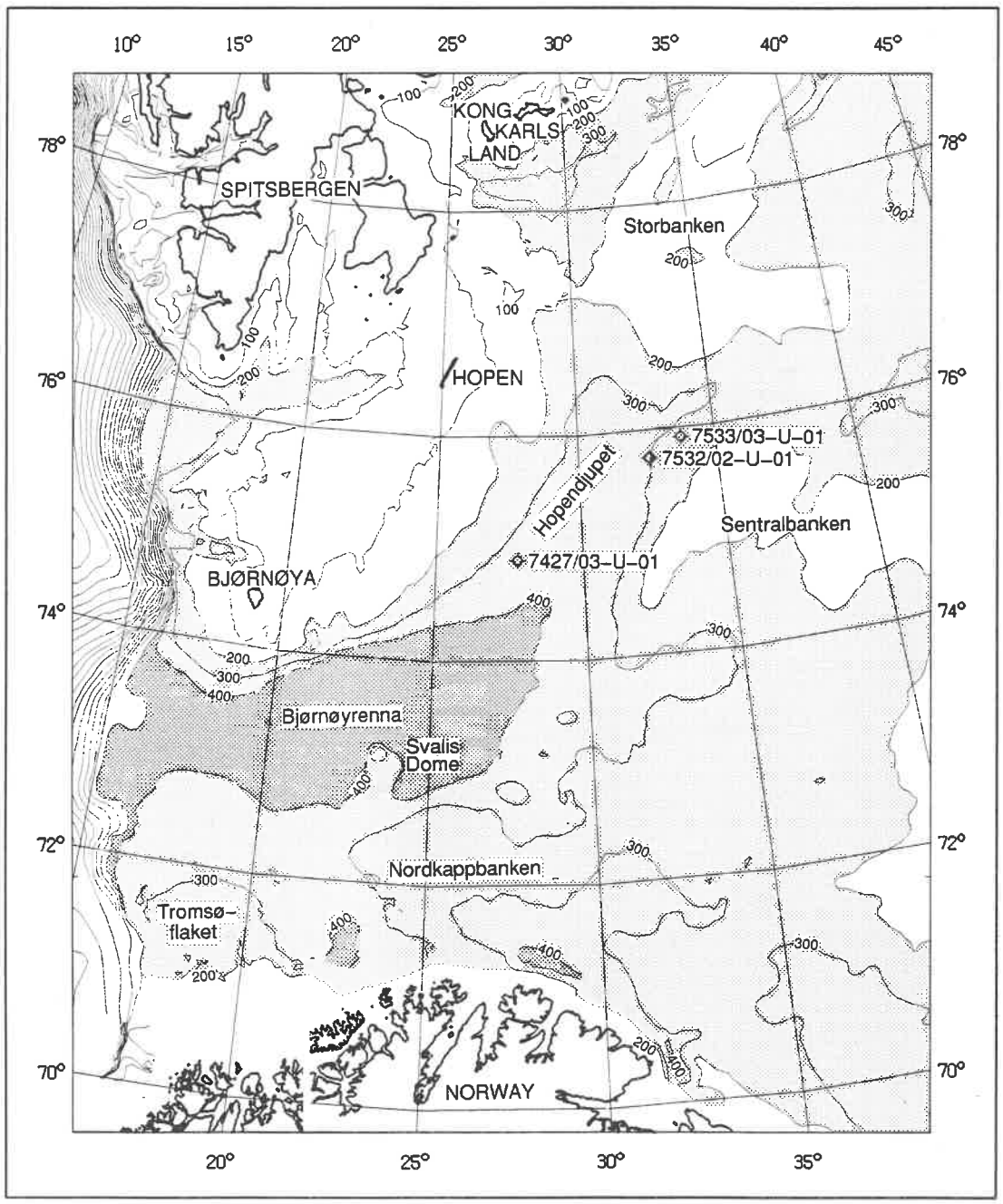

Figure 1.1 *Shallow drilling was carried out at three sites in Hopendjupet in the Barents Sea in 1990, comprising the Middle Triassic and the Upper Jurassic/Lower Cretaceous section.*

Data from the Triassic succession in Hopendjupet will later in 1991 be incorporated in two separate correlation studies. One comprises a detailed investigation for organic geochemistry, while the other comprises biostratigraphic correlation where data from Spitsbergen, the Svalis Dome, shallow drillings and selected exploration wells in the Barents Sea will be included.

Due to budgetary restrictions, no high resolution seismic data could be acquired for this project. Although some analog sparker data existed, detailed planning of the drill sites beforehand and detailed correlation with the seismic after the drilling was therefore limited. This accounts particularly for the shortest, Anisian core, which was drilled on a faulted anticline. The other two cores are fairly reliably correlated.

The shallow drilling operation in Hopendjupet succeeded IKU's drilling in the Troms III area lasting for about 7 days during July/August 1990 (excluding four days of sailing time). The operation followed IKU's normal procedures for shallow drilling programs with exception of the relatively short holes (120.55, 90.30 and 19.92 metres) drilled and no petrophysical logging carried out.

The report is organized in the same way as previous IKU-shallow drilling reports. Data for each core are presented (Chapters 3-5) with a short summary of each core followed by a discussion of the local tie to the seismic data, sedimentology, biostratigraphy, and organic geochemistry results. In Chapter 6 the results are put in a regional context, including correlation of the cored intervals. Emphasis is put on the paleogeography of the Middle Triassic and the Early Cretaceous. The migrated hydrocarbons are discussed separately.

The Appendix section includes:

A.1 Summary sheets of each core (scale 1:250)
A.2 Organic geochemical summary of all cores
A.3 Biostratigraphical range charts
A.4 Field work - drilling operation
A.5 Navigation
A.6 Analytical methods
A.7 Organic geochemical data
A.8 Core photos

2. SUMMARY AND CONCLUSIONS

The project "Shallow drilling in Hopendjupet, Northern Barents Sea" was performed on behalf of the NPD in 1990/91. Three cores were drilled. The oldest core was drilled on the Sentralbanken high (Figure 2.1), and comprised sand and shales of Middle Triassic (Anisian) age (core 7532/02-U-01). One core was drilled on the Gardarbanken high and contained shales of Middle Triassic (Ladinian) age (core 7427/03-U-01). One core was drilled on the Sentralbanken high close to the Olga basin, comprising shales of Middle/Late Jurassic age overlain by limestone/siltstone/sandstone of Early Cretaceous age (core 7533/03-U-01). Key data from the three drillings are shown in Tables 2.1 and 2.2.

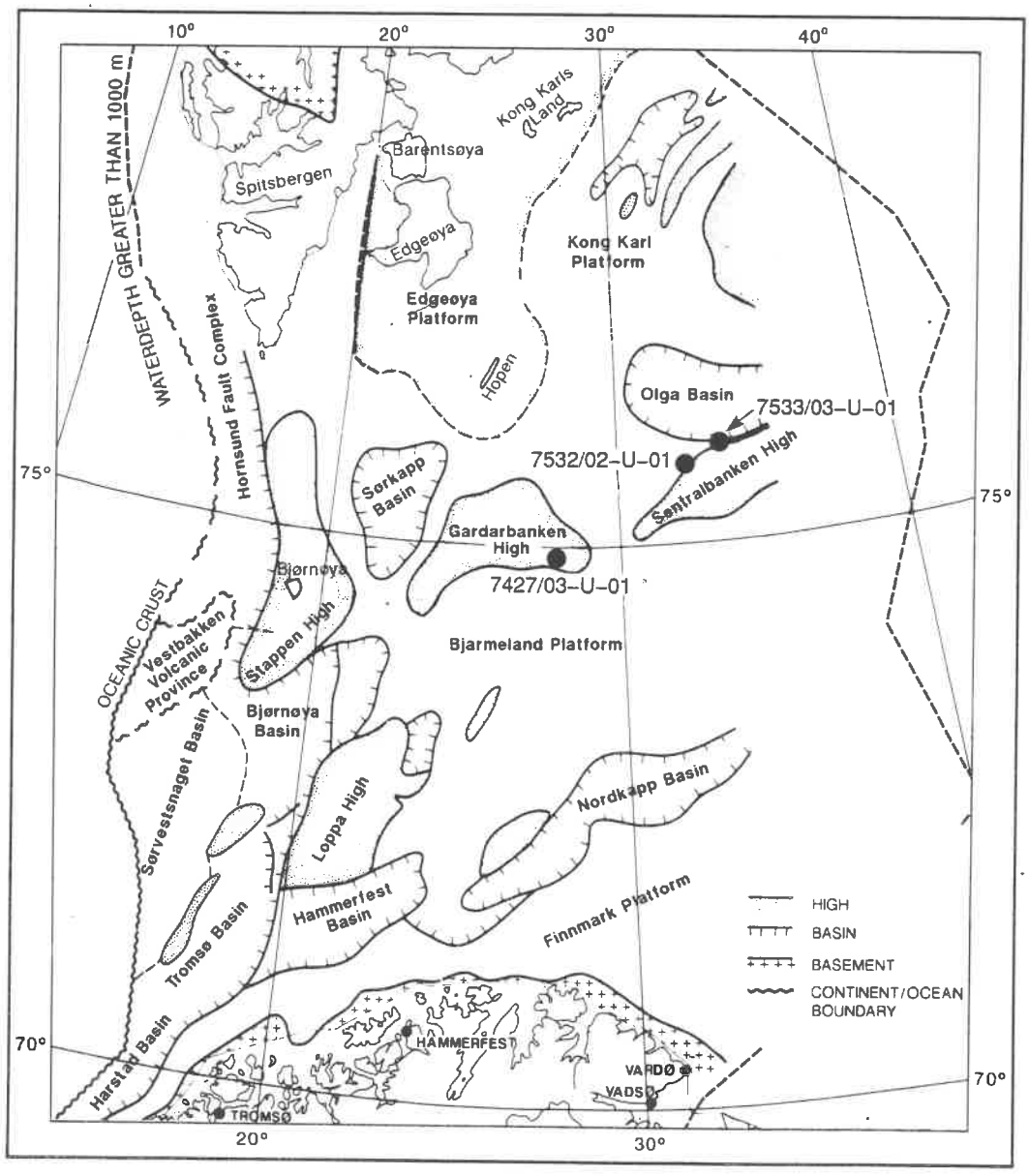

Figure 2.1 Tectonic framework of the Barents Sea Region. The two Middle Triassic cores (7427/03-U-01, 7532/02-U-01) and the Jurassic/Cretaceous core (7533/03-U-01) drilled during the survey are shown on the map.

Table 2.1 Technical data of the three drillings in Hopendjupet.

Core no.	Seismic line	Shotpoint	Water-depth	Quat.-over-burden	Penetration in bedrock	Core length	Core recovery	Total depth below seabed
7427/03-U-01	D-10-82 (sparker) D-10-87 (konv.seism)	5349.5 * 2215	340 m	1.5 m	88.80 m	88.23 m	99.4%	90.30 m
7532/02-U-01	7545-87	6103	306 m	4.6 m	15.32 m	14.79 m	96.5%	19.92 m
7533/03-U-01	3345-87	10287	263 m	1.8 m	118.71 m	116.13 m	97.8%	120.55 m
Sum/(average)			(303 m)	7.9 m	222.83 m	219.15 m	(98.3%)	

* Line D-10-87 (conventional seismic) and line D-10-82 (analog sparker) are parallel and 80 m apart. Drill site 7427/03-U-01 was localized between the two lines, 15 m NNE of shotpoint 2349.5 on the sparker line and 65 m SSW of shotpoint 2215 on the conventional seismic line D-10-87.

Table 2.2 Final positions of the drill sites (ED50 and UTM Zone 35 with central meridian 27°E).

Core no.	Geographical		UTM	
	Latitude	Longitude	Northing	Easting
7427/03-U-01	74°54'55.94"	27°45'42.31"	8314559	522129
7532/02-U-01	75°45'01.00"	32°32'28.40"	8414692	652054
7533/03-U-01	75°56'16.88"	33°44'59.09"	8438962	682704

Middle Triassic (Anisian - Ladinian)

The Anisian core 7532/02-U-01 was drilled on the Sentralbanken high in the platform area to the southeast of the paleo-shelf edge. The purpose was to retrieve a datapoint in order to obtain stratigraphic control, and the core-hole was terminated approximately 20 m below seabed. The core consisted of 7 metres homogeneous sand overlain by shale and more silty sand with sandstone layers in the upper 3.5 metres. The Quaternary overburden comprised glaciotectonically influenced bedrock ("glacitectonite"). The sandstone is interpreted to represent a deltaic environment, while the shale and silty sand probably represent more distal delta front deposits. A general regressive trend throughout the Anisian was identified from shallow cores drilled at the Svalis Dome, where a major transgression was recognized in the latest Anisian.

7427/03-U-01

IKU SINTEF GRUPPEN

7533/03–U–01

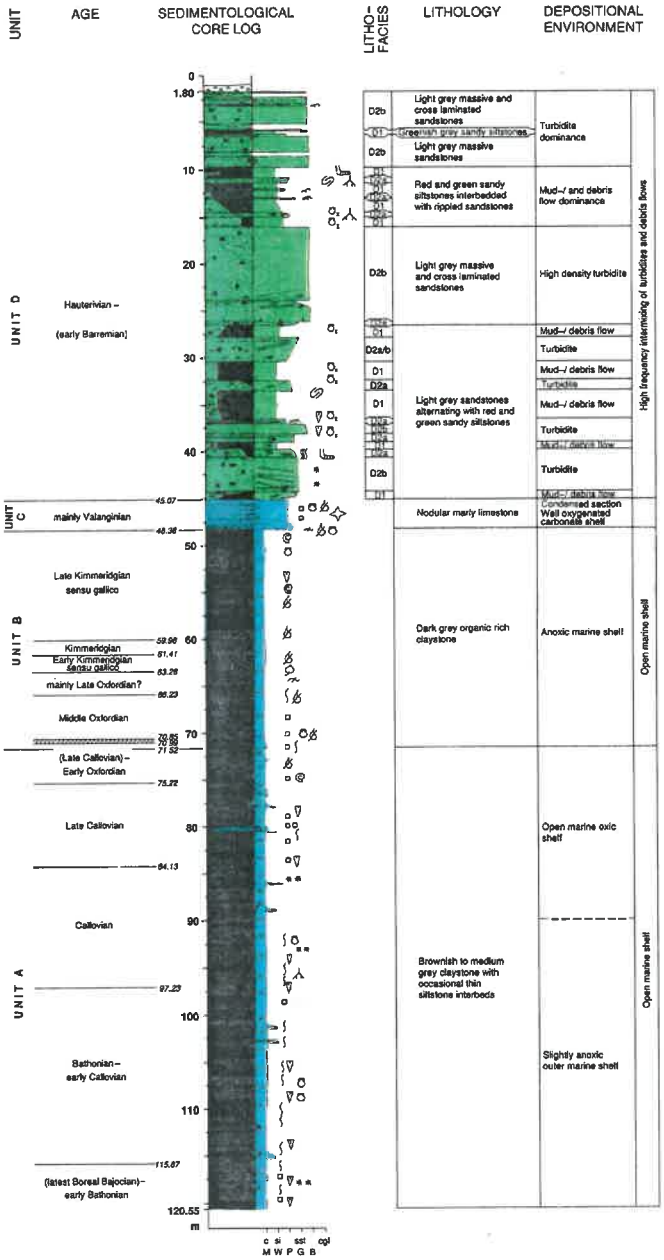

7532/02–U–01

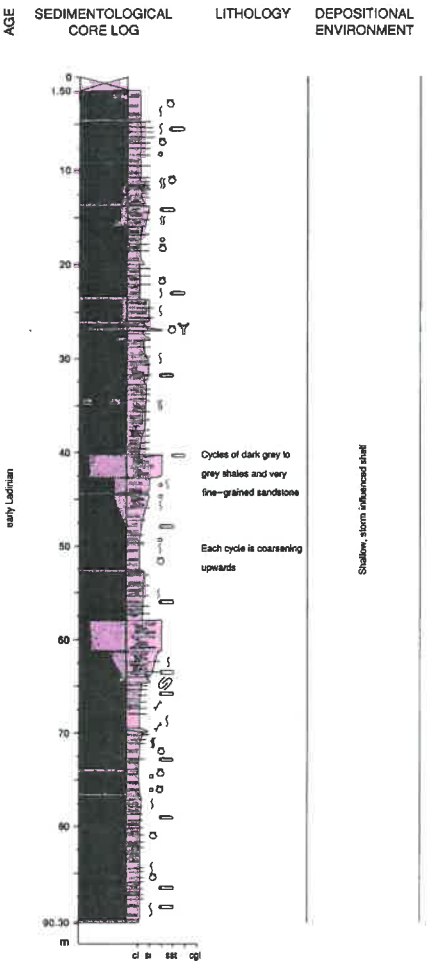

7532/02-U-01

7427/03–U–01

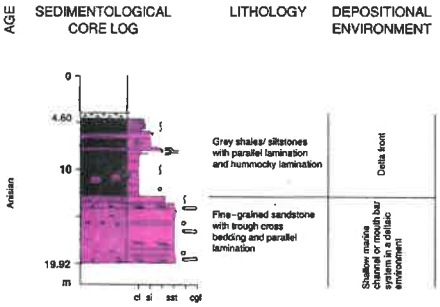

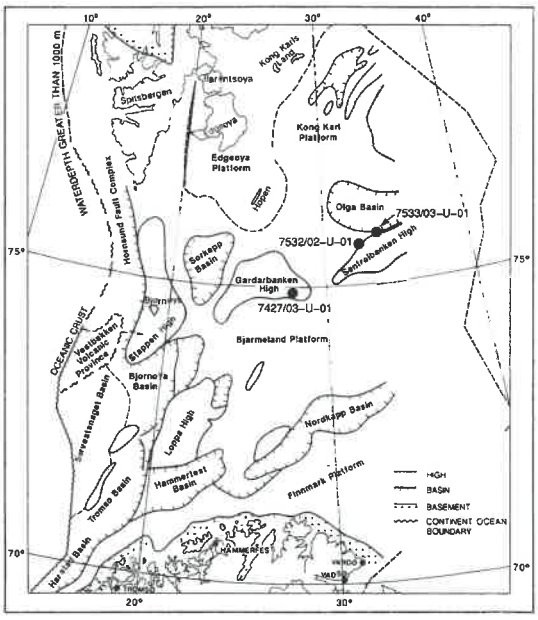

Figure 2.2 Summary figure of three cores in Hopendjupet.

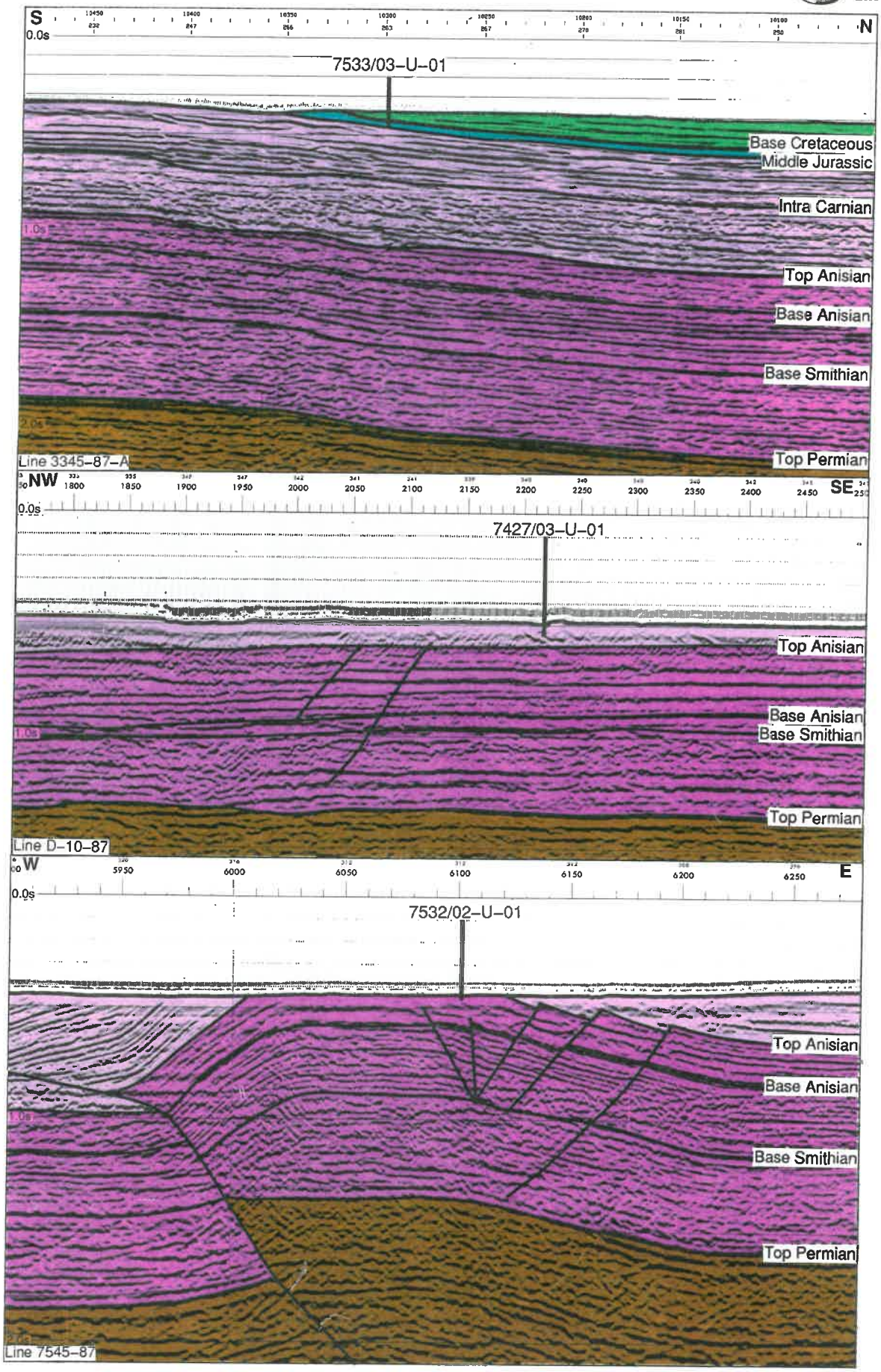

Figure 2.3 Seismic sections at the three drill sites.

The same boundary is correlated with a seismic reflector subcropping close to the core-hole. The reflector corresponds to a stratigraphic level 50 metres above the core.

Interpretation of seismic data from the Barents Sea indicates a north-northwestern prograding shelf edge resulting in clinoforms recognized in the area between the Svalis Dome and Hopendjupet. The sediments most probably were derived from the southeastern Barents Sea, where the Uralian front (including Novaya Zemlya) was eroded resulting in a thick Triassic clastic succession. There are no indications of tectonic activity during this period. The top of the clinoform unit seems to correspond with the latest Anisian transgression.

Core 7427/03-U-01 of early Ladinian age was drilled on the Gardarbanken high, and the core-hole was terminated about 90 m below seabed. The core consisted of alternating shale- and siltstone comprising several coarsening upward units interpreted to be deposited in a shallow, storm influenced environment in a lower shoreface to upper offshore setting. The land area was probably still located to the southeast. The drill site was localized east of where the Anisian clinoform sequence subcrops below the Ladinian sediments, landward of the shelf edge. From the base of the core-hole there are about 120 metres down to the reflector believed to represent the late Anisian transgression.

Visible oil-staining was evident in sandstones and siltstones in the Ladinian core 7427/03-U-01, where relatively light, non-undegraded oil was exuded from the core on recovery. Evidence for additional oil-staining is present in the Anisian-age sandstones at the base of core 7532/02-U-01. The source of the oil in these cores is currently uncertain, but preliminary studies suggest that the oil in core 7427/03-U-01 is similar to artificial oil produced from Anisian shales at Svalis Dome. The type III kerogen analysed for core 7532/02-U-01 was early mature, while the type III kerogen analysed from core 7427/03-U-01 was mature.

Upper Jurassic/Lower Cretaceous

The Middle Jurassic to Lower Cretaceous core 7533/03-U-01 was drilled on the northern flank of the Sentralbanken high/southern margin of the Olga basin. The lowermost 50 metres (Unit A) of the 120 metres long core comprise shales and siltstones of Bajocian/Bathonian - Late Kimmeridgian age and are correlated with the Fuglen Formation in the southwestern Barents Sea. With a transitional boundary, Unit A is overlain by dark grey, organic rich shales

correlated with the Hekkingen Formation. Total organic content is up to 10-20% and the organic matter is dominated by thermally immature type II and type II/III kerogen. The shales are dated to Middle Oxfordian - Late Kimmeridgian. With a probable erosional contact, the shales are overlain by a condensed unit (3.3 m thick) of nodular marly limestone dated as Valanginian. The upper approximately 44 m consist of alternating siltstones and sandstones dated as Hauterivian - early Barremian.

The sediments of the Middle/Upper Jurassic Unit A are interpreted to represent an open shelf environment. They were deposited in a generally stable tectonic period lasting from the Triassic to the middle Jurassic. The organic rich shales of Unit B were deposited in an anoxic shelf environment during the last part of a transgressional period. The late Jurassic/early Cretaceous was an active tectonic period and NNE-SSW oriented anticlines were formed in the northern Barents Sea. Core 7533/03-U-01 was localized close to one of these anticlines. There is a time span from Late Kimmeridgian to Valanginian from the shales of Unit B to the nodular, marly limestone of Unit C. This is probably partly due to erosion, but a marked, relative lowering of the sea level obviously occurred. The marly limestone unit is a condensed section deposited on a well oxygenated carbonate shelf.

As a result of the tectonic activity, some of the anticlines were probably subaerially exposed and we interpret the reddish and greenish coloured sediments within Unit D to be derived from such an anticline. They were probably transported as mud- or debris flows. The sandy intervals are interpreted as high density turbidites derived from a prograding delta front. The sandstone has high permeability, partly in excess of 3000-4000 mD.

The organic-rich, Upper Jurassic black shales of core 7533/03-U-01 represent the only potential hydrocarbon source interval penetrated by the shallow cores. These shales are comparable with the most organic-rich samples described from the Hekkingen Formation elsewhere in the Barents Sea during previous shallow drilling cruises. However, the thermal immaturity of the kerogen in these shales restricts their hydrocarbon generation potential as sampled in the above core.

3. RESULTS AND INTERPRETATION CORE 7532/02-U-01

3.1 Summary

Core 7532/02-U-01 penetrated 15.32 m into bedrock, below 4.6 m of Quaternary overburden. A core recovery of 96.5% was obtained. Three lithological units are recognized: a lower sandstone unit (19.92 - 13.02 m) consisting of homogeneous, fine-grained sand, overlain by an upwards coarsening shale unit (13.02 - 8.01 m) and at top a more silty shale with sandstone layers (8.01 - 4.6 m). The sandstone was probably deposited in a deltaic environment, while the finer grained units most probably represent more distal delta front deposits. From palynology the core has been dated to Anisian.

The rocks analysed from core 7532/02-U-01 contain moderate amounts of early mature type III kerogen with no appreciable hydrocarbon generation potential. There is indirect evidence of oil-staining in the sandstones below ca. 14 m.

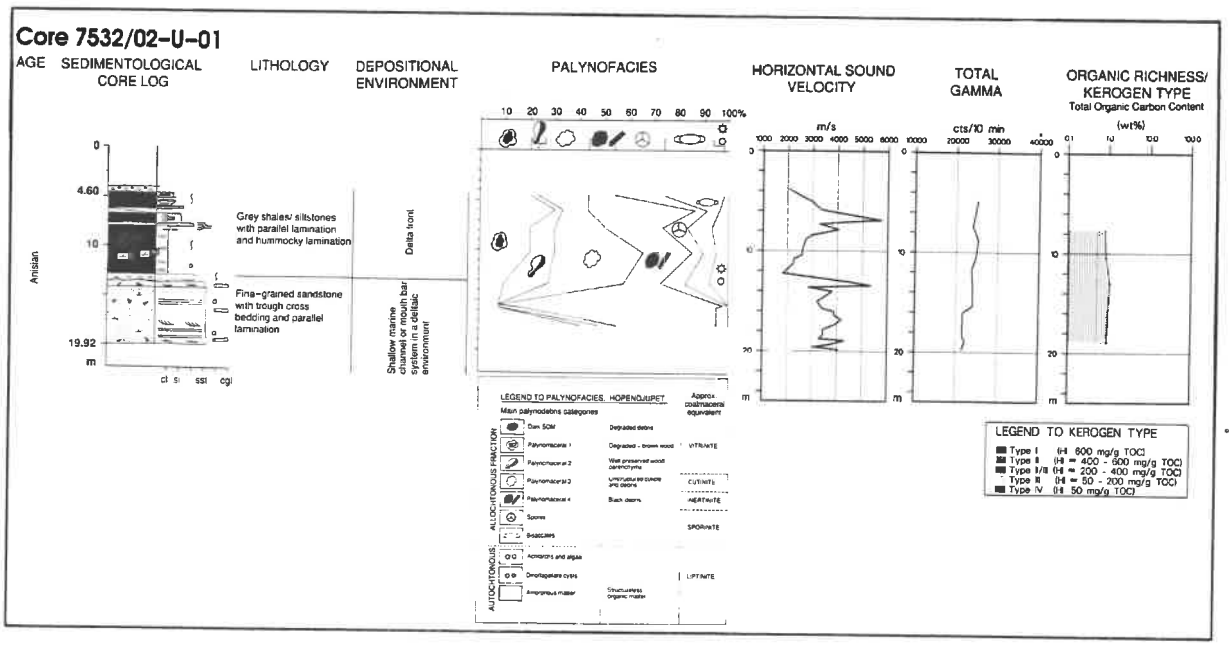

Figure 3.1 Summary of core 7532/02-U-01.

3.2 Seismic interpretation

Core 7532/02-U-01 was drilled on the Sentralbanken high, 165 km to the northeast of site 7427/03-U-01, on seismic line 7545-87 at shotpoint 6103. The overburden was 4.6 m thick and consisted of overconsolidated till.

The objective of this drilling was to core some of the oldest strata subcropping close to the seabed in this area. There are no digital high resolution seismic data available at this site and a detailed seismic correlation is therefore not possible. The changes in lithology from silty shale to shale and sand are reflected in the sound velocity measured on the core (Figure 3.1). These and similar changes are probably the reason for the high frequency reflection pattern seen in the seismic data. In the analog sparker data (Figure 3.2) a seismic reflection seems to correspond with the boundary between the shale and the underlying sand at 13.0 m. Other reflections probably correspond to the above mentioned lithological changes.

The reflector interpreted to represent top Anisian subcrops close to the drill site. There seems to be an approximately 30 ms (45-50 m) thick Anisian section above the top of the core.

3.3 Sedimentology

Core description

Core 7532/02-U-01 penetrated 15.32 m of rock between 4.60 m and 19.92 m below seabed. A subdivision into three lithological units can be made; a sandstone unit between 19.92 m and 13.02 m, a shale unit between 13.02 m and 8.01 m, and between 8.01 m and 4.60 m a shale with some sandstone layers and a higher silt content than in the unit below.

The sandstone is relatively homogeneous with respect to grain size and sorting. It is fine-grained with slightly coarser material below approximately 19 m, but it is still characterized as fine-grained. Parts of the core is homogeneous (Figure 3.3C), while most intervals show alternating trough-cross bedding (Figure 3.3B), and parallel bedding and lamination. Small coal particles, often concentrated along laminae and thus revealing the sedimentary structures, are present throughout the unit. Grey angular to subrounded shale clasts (Figure 3.3A) occur at several levels in this unit. They occur in both

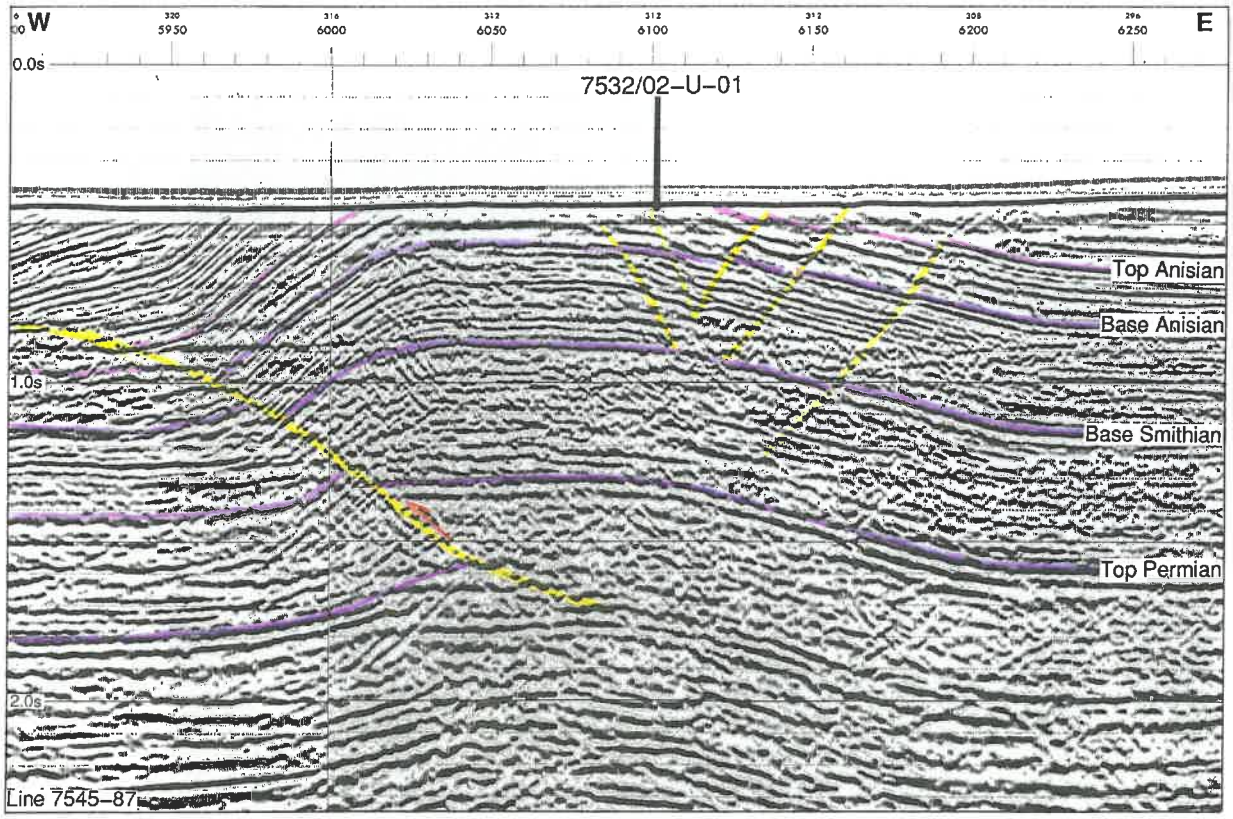

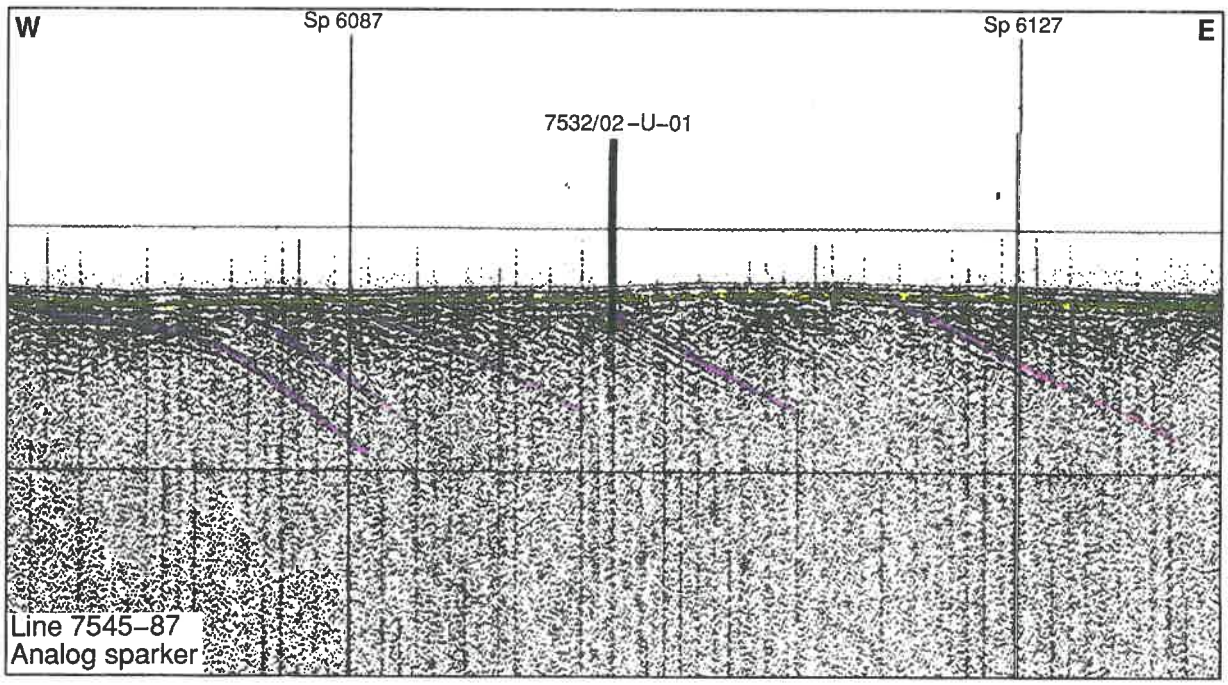

Figure 3.2 *Seismic correlation of core 7532/02-U-01. The core was drilled on an anticline probably formed in the Cretaceous, where all younger sediments than Middle Triassic have been eroded. The reflector interpreted as top Anisian (blue) correspond to a level approximately 30 ms (45-50 m) above the core.*

crossbedded and parallel laminated layers. In the upper part of the sandstone unit there are also two thin shale-layers, 3-6 cm thick (at 13.75 m and at 13.27 m).

Thin sections from this interval show well sorted, angular to sub-rounded grains in the lower fine-grained range (125-190 μm) except for a slightly coarser fraction below 19 m (190-250 μm). The grains comprise mainly polycrystalline (chert) and monocrystalline quartz, plagioclase, shale clasts, schistose rock fragments and mica. Black to reddish-brown translucent organic matter occurs either as scattered particles or as accumulations along laminae. There are several types of polycrystalline quartz grains registered in the thin sections. Grains showing metamorphic textures as interlobate and straight grain boundaries, and schistose fragments are present, as well as microcrystalline chert fragments.

Plagioclase is the more abundant feldspar in the examined samples. It is occasionally etched or partly replaced by calcite cement. No authigenic plagioclase is observed. The present alkali-feldspars show different degrees of alteration. Some twinned microcline grains are seemingly unaltered while untwinned grains are commonly leached and partly illitized.

The most common cements are evenly scattered pore-filling calcite and pyrite, both occurring partly poikilotopic. Calcite cement seems evenly distributed. Some porosity is left except for the upper tens of centimetres (13.60-13.02 m) which are totally cemented. Pyrite occurs in scattered crystals and occasionally as concretions. Based on a visual impression, the porosity is moderate to low. Cement, altered rock fragments, mica, and squeezed shale fragments reduce, however, the permeability to a very low level, generally below 50 mD (see core summary sheet in Appendix A.1.1).

The shale unit between 13.02 m and 8.01 m consists of medium grey to light grey shale (Figure 3.4B) with scattered, tiny pyrite crystals and a few pyrite concretions. The shale is parallel laminated with some thin (<1 cm) dolomite cemented laminae. Bioturbation is scarce, but shows a gradual increase upwards to about 8.7 m. *Planolites?* occur at about 9.5 m. The colonization is, however, only opportunistic (Richard G. Bromley, pers.comm.).

The unit above 8.01 m has a thin basal layer (20 cm) of very fine-grained sandstone with erosive contact to the shale. The lowermost 1.1 m of this lithological unit is generally coarser grained than the upper part. A very fine-grained sandstone and a sandy shale occurring in the lower 30 cm are

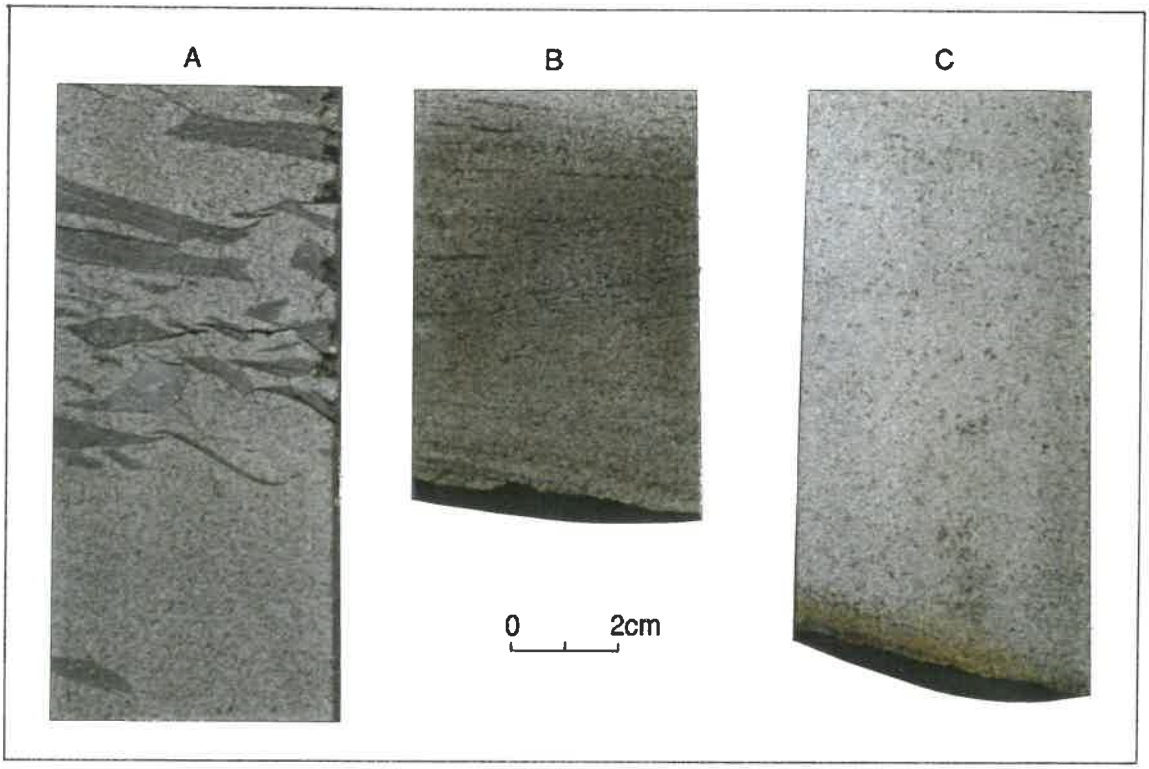

Figure 3.3 *Photographs of core 7532/02-U-01, lower sandstone unit.*
A. Sandstone with shale clasts (15.34 m)
B. Trough-cross-bedded sandstone with drapes of coal particles (16.19 m).
C. "Homogeneous" sandstone at 16.61 m.

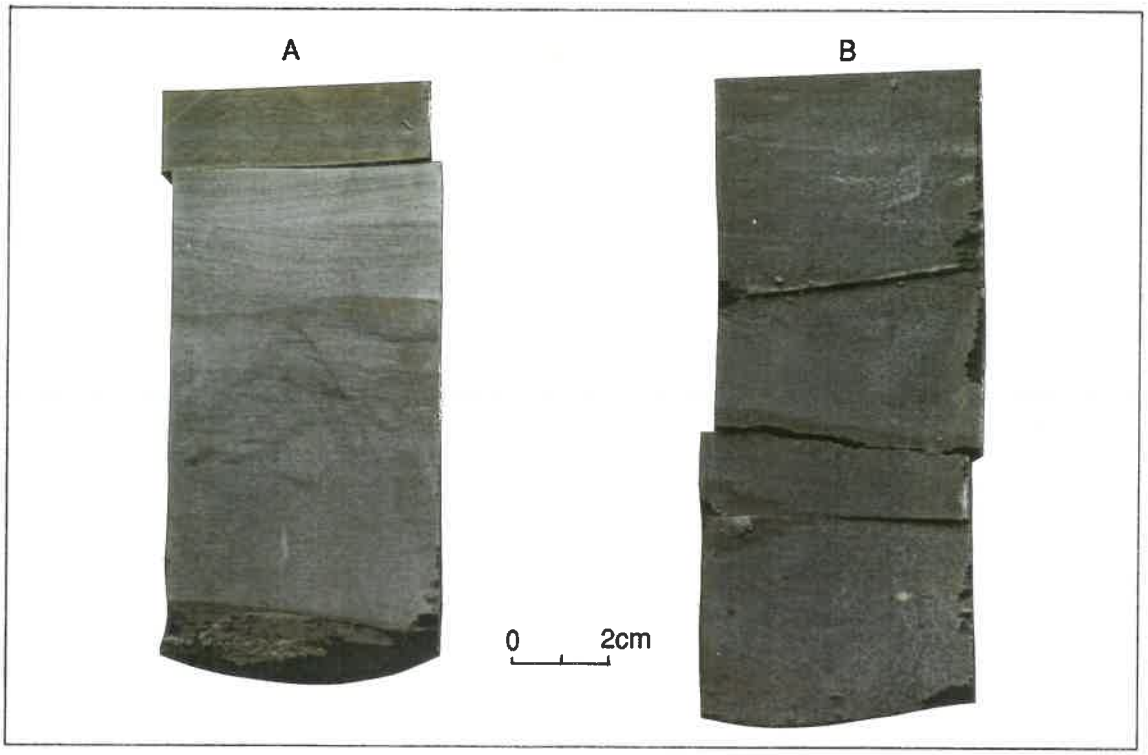

Figure 3.4 *Photographs of core 7532/02-U-01, units 2 and 3.*
A. Fining upwards layers from unit 3 showing cross laminated sandy shale (7.27 m)
B. Grey, parallel laminated shale in unit 2 (10.98 m).

crossbedded. Upwards to 6.87 m, thin, fining upwards layers of sandy/silty shale are present. The layers show mainly parallel-lamination with some examples of small scale hummocky lamination and ripples (Figure 3.4A). The finer grained upper part of the core consists of medium grey to light grey parallel laminated shale. The silt content is slightly higher than in the shale unit below.

Burrows are present but not abundant in this uppermost unit. *Planolites?* and *Chondrites?* are present at 7.35 m and 7.00 m, respectively. The ichnodiversity increases upwards (R.G. Bromley, pers.comm.).

Generally, there is a gradual increase in bioturbation at intervals upwards in units 2 and 3, but not more than opportunistic colonization until about 5.45 m.

Tectonic influence from an overriding glacier is observed down to the base of the shale unit at 13.02 m. The deformation was concentrated along a few centimetres thick horizontal zones which are turned into glaciotectonic fault gauge (glaciotectonite) and in some tens of centimetres thick intervals where larger rock fragments are still intact. A glaciotectonic origin of these zones is strongly suggested by their horizontal boundaries. There is a gradual transition from the bedrock into the Quaternary till above 4.6 m (Figure 3.5).

Mineralogical composition

Five shale samples have been analysed by X-ray powder diffraction (Table 3.1). The samples show very little variation with respect to mineralogical composition. Smectite is absent or minor and mixed layered, illite-dominated, illite-smectite is present. The latter appears as a shoulder on the low angle side of the illite reflection (basal spacing between 10Å and 13Å) in the diffractogrammes, and is probably of detrital origin.

There is some variation in the kaolinite/chlorite ratio. In the upper sample, the abundance of kaolinite is about twice that of chlorite. In the upper part of the shale interval, between about 10 m and 8 m, chlorite to kaolinite is about 1:1, while below 10 m kaolinite is 6 to 10 times more abundant. The compositional variation can be due to variation in the sediment source, but more likely it is an effect of grain size and/or diagenesis. The two lowermost

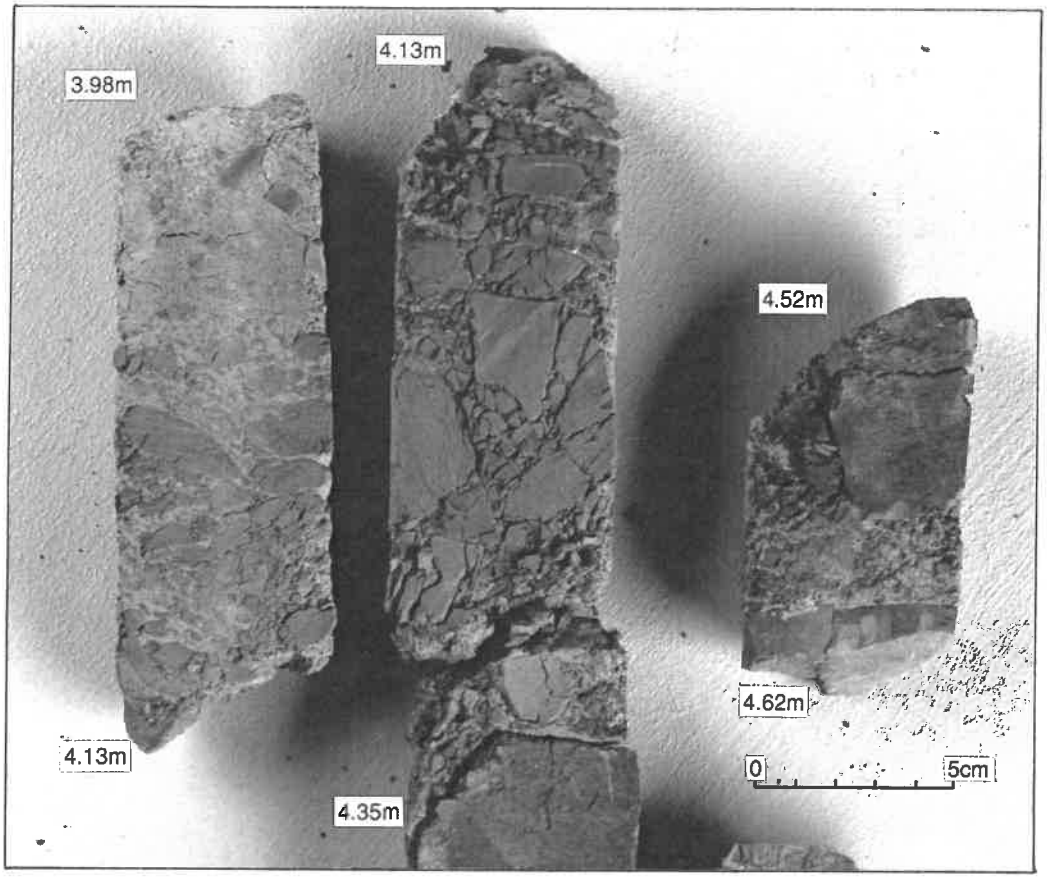

Figure 3.5 *Glacially influenced bedrock. The sediment is classified as a glaciotectonite and the "base Quaternary" is set at 4.60 m. Upwards increase in glacial influence can be observed, from zones of crushed rock (4.60-4.57 m), through zones with whole rock pieces between broken bedrock, to sediment of dominating glacial matrix with rock fragments. Crushed zones like the one at 4.60 - 4.57 m occur down to the base of the shale at 13.02 m. Note the horizontal deformation boundary.*

samples contain abundant dolomite and pyrite cement, and are therefore not directly comparable with the two other samples from the same interval.

Quartz and feldspar show only small variation with grain size. Similar to what we observed in the thin sections of the underlying sandstone, plagioclase is also the more abundant feldspar phase in the shale. Potassium feldspar is absent or present only as a trace in the diffractogrammes. One must, however, remember that the detection limit for this type of analysis is in the range 1-5%. The distribution of the feldspar phases suggests the same provenance for the shale/siltstone and the underlying sandstone. Siderite cement is present in all the samples.

Table 3.1 *Mineralogical whole rock composition of shale samples from core 7532/02-U-01 (semi-quantitative wt%). (Tr - trace).*

Depth (m)	Sm	Mix	Chl	Kao	Mic	Qtz	Kfl	Pl	Cal	Dol	Sid	Py
4.65	1	6	8	19	18	22	tr	20	-	-	5	1
8.02	-	12	13	11	22	18	-	16	-	-	8	-
9.32	-	8	11	11	25	21	-	15	tr	1	2	6
11.19	-	4	1	11	19	9	-	5	-	53	1	6
12.69	-	9	3	19	18	21	-	14	-	1	1	14*

* Pyrite and trace of marcasite

Palynofacies

In addition to conventional sedimentological analyses, palynofacies studies are here included as a tool for interpretation of the depositional environment in the cored sequences. These analyses are based on the total acid-resistant organic residues. The palynodebris categories applied in the present study are those described by Whitaker (1984) and Van der Zwan (1990). The classification and approached model proposed by Whitaker and van der Zwan is preferred because it is largely based on the sedimentary properties of the organic matter (i.e. buoyancy and sensitivity to degradation processes), and thus these palynodebris categories provide useful means in the recognition of various marine and non-marine subenvironments. The components are divided into an allochthonous and an autochthonous fraction.

The palynofacies development in core 7532/02-U-01 is shown in Figure 3.1. In this core two different palynofacies types are recognized as follows:

17.61 - 15.63 m and 5.98 m

In this intervals palynofacies is characterized by a dominance of medium-sized equidimensional palynomaceral 4 (40-90 %), with blade-shaped fragments nearly absent. At some levels palynomaceral 1 is an important component, while palynomacerals 3 and 4 represent minor constituents. Palynomorphs are rare.

This palynofacies corresponds Whitaker's (1984) palynofacies VIII, which is characteristic in high energy settings where most of the constituents are separated out. Samples completely dominated by palynomaceral type 4 characterize reworked and redistributed sediments. The sediments are therefore interpreted to probably represent delta front to upper shoreface environment.

13.22 - 7.66 m and 4.64 m

Palynofacies is here characterized by medium sized palynomacerals 1,2,3 and 4 with moderate proportions of pollen and spores. Acritarchs are present in minor amounts. Analysis of the relative distribution of main palynomorph groups shows that bisaccate pollen represent about 20-50 % of the microfloral assemblage, while cavate spores from plants known to grow in a more mangrove type of vegetation, represent about 30-70 %. Marine palynomorphs represent only 1-2 % of the total palynoflora. Dominance of palynomacerals 1,2 and 3 is characteristic for a depositional environment where more buoyant constituents start to settle as a result of decrease of energy conditions at sea bottom. This type of palynofacies corresponds to Whitakers's (1984) palynofacies VII/VI, which is interpreted to represent lower to upper shoreface depositional environments.

Depositional environment

The lower sandstones (19.92 - 13.02 m) are mineralogically immature and the grains are well sorted. Sedimentary structures comprise parallel lamination and, trough-cross bedding, while homogenized intervals are present. In addition, cm-sized grey to light grey shale clasts are present. From palynofacies a high energy setting is indicated. Based on all data the sandstone is interpreted to have been deposited in a shallow marine channel or mouth bar system in a deltaic environment. The finer grained units (13.02 - 4.60 m) of grey to light grey shales/siltstones may represent slightly more distal delta front deposits.

3.4 Biostratigraphy

Core 7532/02-U-01 has been analysed for palynomorphs, while no records of age-diagnostic macrofossils were made. The eight samples analysed for palynomorphs revealed poor to well preserved acritarchs, pollen and spores (Figure 3.6), with the two latter as dominant groups. The samples from the sand below 13.02 m revealed poor and less diverse assemblages than the shaly sequence above. Selected specimens are illustrated in Figures 3.7 and 3.8.

The recovered palynomorphs suggest an Anisian age throughout.

19.92 m (TD) - 4.6 m, Anisian

The palynomorph assemblage recorded is indicative of an Anisian age, based on presence of the spore *Jerseyiaspora punctaspinosa* (syn. *Raistrickia sp.*) appearing together with *Asseretospora* group (syn. *Duplexisporites*-group). The first mentioned ranges from the late Spathian to late Anisian in the Barents Sea area (Hochuli et al. 1989, Mangerud & Rømuld in press), but is regularly present and most common in the late Spathian to middle Anisian. It is also recorded from Anisian beds in Libya (Kar et al. 1972) and in Israel (Eshet & Cousminer 1986, fig. 6.3). *Asseretospora*-group appears for the first time in base Anisian in the Arctic (Fisher 1979, Mangerud & Rømuld in press), and develops throughout the Late Triassic and Jurassic. Its first appearance is therefore a significant event.

The total assemblage characteristics with abundant *Aratrisporites* and bisaccate pollen was also noted from ammonite dated Anisian beds at the Svalis Dome. The assemblage also correlates with assemblage K of Hochuli et al. (1989) dated as late Anisian, although several of their lowest occurrences are not recorded in core 7532/02-U-01. The regular presence of *Jerseyiaspora punctispinosa* and the monosaccate genera *Cordaitina gunyalensis* was noted from the upper part of the middle Anisian on the Svalis Dome (Mangerud & Rømuld in press). These two genera appear regularly, and although the recovered palynomorphs give no direct evidence for precise dating in the Anisian succession, a middle to late Anisian age would be preferred. This is also supported by negative evidences, such as lack of *Densoisporites nejburgii* which ranges up into basal Anisian beds.

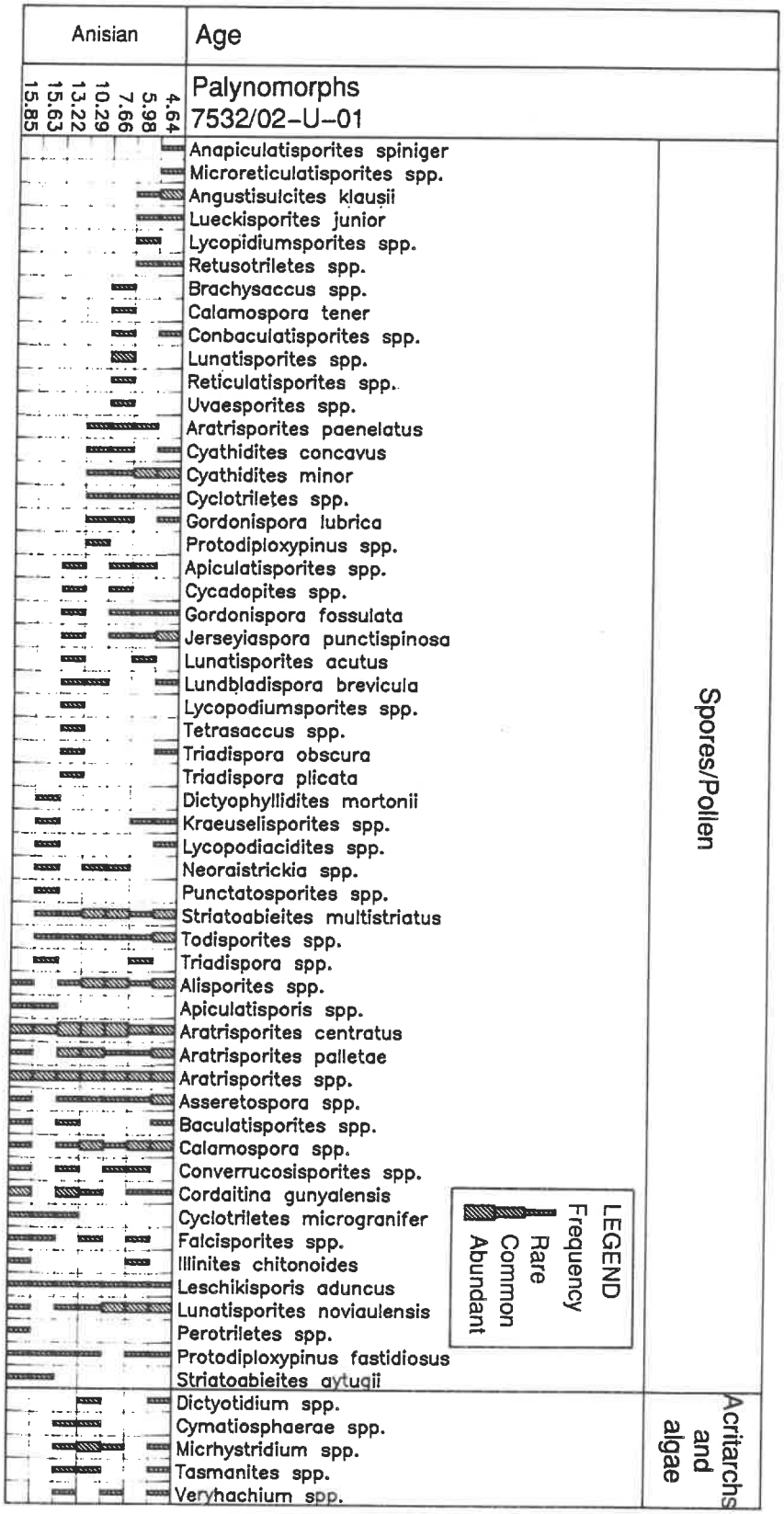

Figure 3.6 *Range chart of palynomorphs in core 7532/02-U-01 sorted according to earliest occurence.*

Figure 3.7 *Selected spores from core 7532/02-U-01. Magnification indicated by 50 µm scale bar. Taxon name is followed by sample depth in metres, and coordinates to Leitz Aristoplan microscope.*

1. *Calamospora* sp. 4.64 m 50-101.6
2. *Retusotrilets* sp. 4.64 m 56-113.9
3. *Gordonispora lubrica* 4.64 m 64-100
4. *Baculatisporites* sp. 4.64 m 65-102.2
5. *Verrucosisporites* sp. 4.64 m 57-93.5
6. *Verrucosisporites* sp. 13.22 m 65.99
7. *Jerseyiaspora punctispinosa* 13.22 m 52-109
8. *Lycopodiaciedites* sp. 4.64 m 60-95
9. *Lundbladispora* 13.22 m 48-95
10. *Asseretospora complex* 4.64 m 45-103
11. *Microreticulatisporites* sp. 4.64 m 46-103
12. Unidentified 4.64 m 63-106
13. *Aratrisporites palettae* 4.64 m 57-95
14. *Aratrisporites paenelatus* 4.64 m 59.5 -106.4
15. *Aratrisporites centratus* 13.22 m 50.3-94

Figure 3.8 *Selected pollen and marine palynomorphs from core 7532/02-U-01. Magnification indicated by 50 µm scale bar. Taxon name is followed by sample depth in metres, and coordinates to Leitz Aristoplan microscope.*

1. *Falcisporites* sp. 4.64 m 47-107
2. *Triadispora plicata* 13.22 m 51-96
3. *Lunatispories noviaulensis* 4.64 m 66.5-100.2
4. *Cordaitina gunyalensis* 13.22 m 58-95
5. *Striatoabieites multistriatus* 13.22 m 60.5-95.5
6. *Lueckisporites junior* 4.64 m 65-99
7. *Tasmanites* sp. 4.64 m 62.95
8. *Veryhachium* sp. 4.64 m 61.2-95.7
9. *Accinctisporites circumdatus* 13.22 m
10. *Dictyotidium* sp. 10.29 m 57.5-95.3
11. *Dictyotidium* sp. 4.64 m 50-90.
12. *Cymatiosphaerae* sp. 13.22 m 63-93

Core 7532/02-U-01

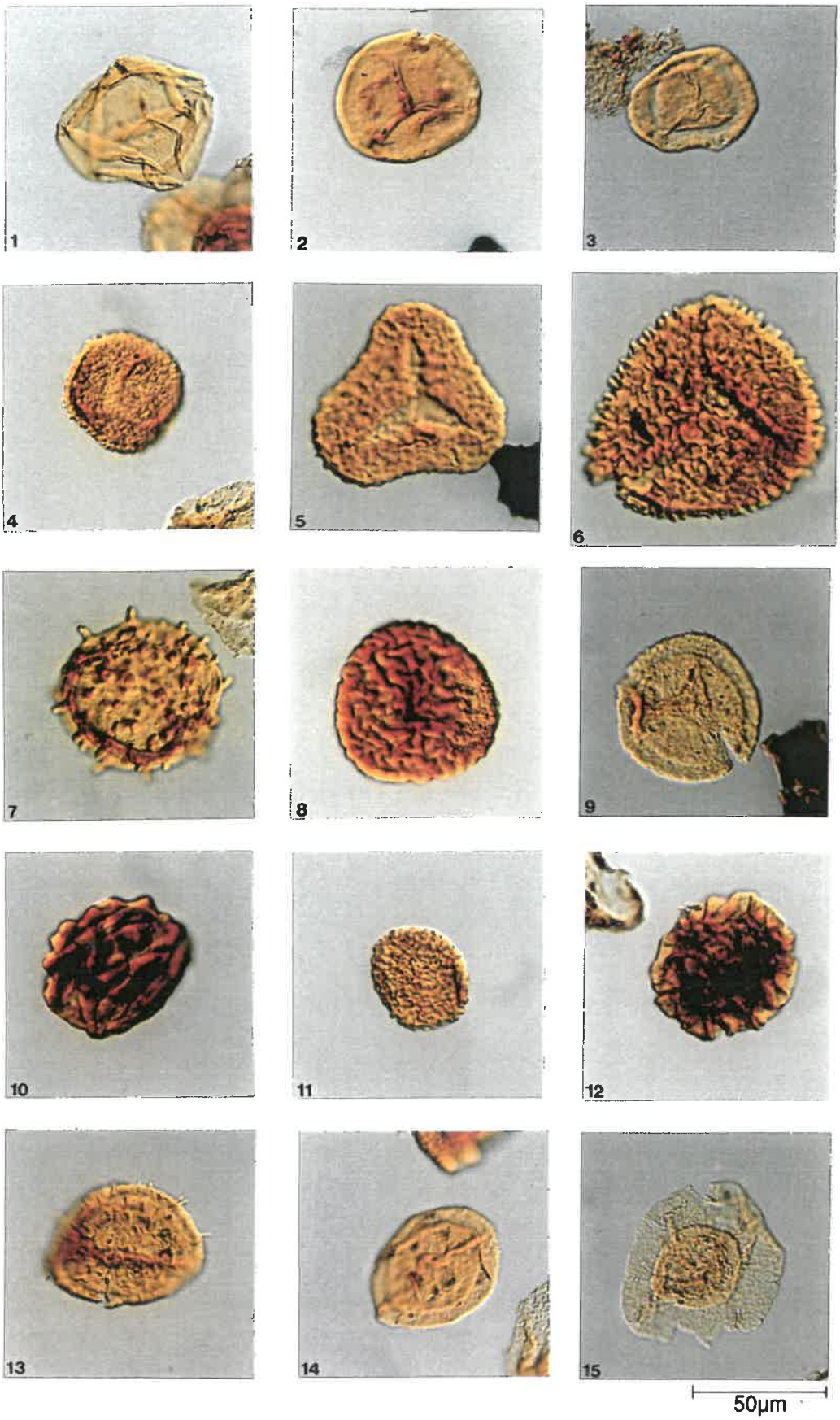

Figure 3.7

Core 7532/02-U-01

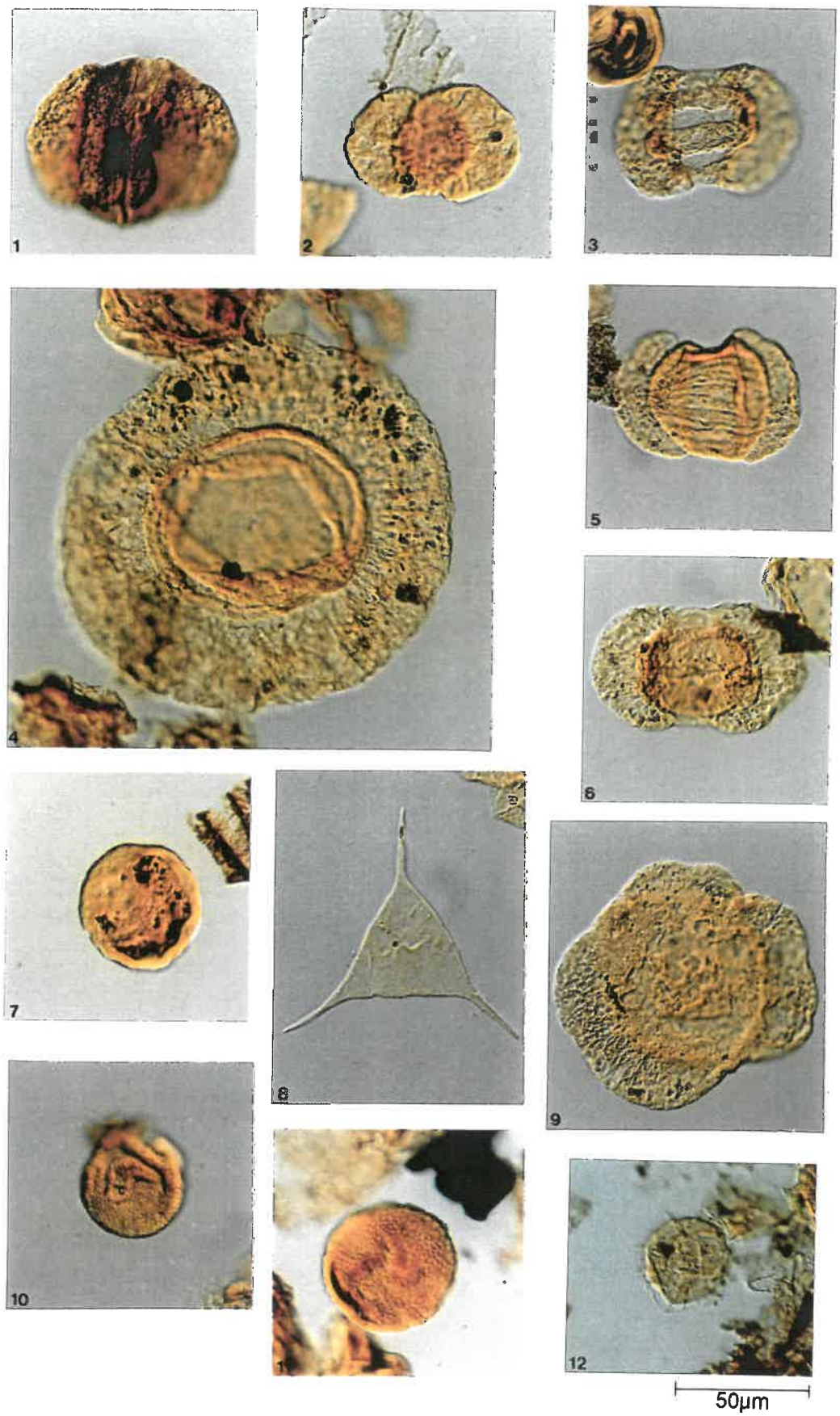

Figure 3.8

3.5 Organic Geochemistry

Four canned samples were collected from core 7532/02-U-01 for analysis and description of the headspace and occluded gas fractions (Figure 3.9). Methane was the major hydrocarbon constituent of the two gas fractions, C_{2+} hydrocarbons only accounting for a few hundred µl/kg.

The two the lowermost samples at 18.81 m and 13.74 m were found to contain appreciable concentrations of C_{5+} hydrocarbons. These two samples come from the sandstone unit occurring towards the base of the core. Stable carbon and deuterium isotope values from the adsorbed gas in the sample at 13.74 m suggest that the gas in these samples may be associated with oil (Figure 3.10), although no visible evidence of oil-staining was observed in the rocks.

Nine samples were selected for total organic carbon (TOC) content determination. All of the samples had TOC contents of ca 1 wt%, regardless of lithological variation (Figure 3.11). Rock-Eval pyrolysis data from four selected samples suggest that the kerogen in these rocks is largely type III or type III/IV kerogen (Figure 3.12). Palynofacies data suggest that the hydrogen index values reflect the presence of largely terrestrial debris with little hydrocarbon source potential. Tmax values of ca 434-439°C in the three upper samples suggest that the kerogen is approaching thermal maturity with respect to hydrocarbon generation.

Relatively high hydrogen index values were observed in the two lowermost samples analysed, i.e. from the lower sandstone unit. The highest hydrogen index value of 156 mg/gTOC occurs in the sample at 18.80 m, where it is associated with a high production index of 0.63 and an anomalously low Tmax value of 414°C. Considered together with the high C_{5+} hydrocarbon content of this sample, these Rock-Eval data are considered to reflect the presence of oil-staining, rather than the character of the kerogen.

In conclusion, the rocks contain moderate amounts of the near-thermally mature type III to type III/IV kerogen, with no appreciable hydrocarbon generation potential as sampled in this core. Headspace/occluded/adsorbed gas data and Rock-Eval data indicate the presence of oil-staining in the lower sandstone of this core. This material could not be characterized in detail within the scope of the project.

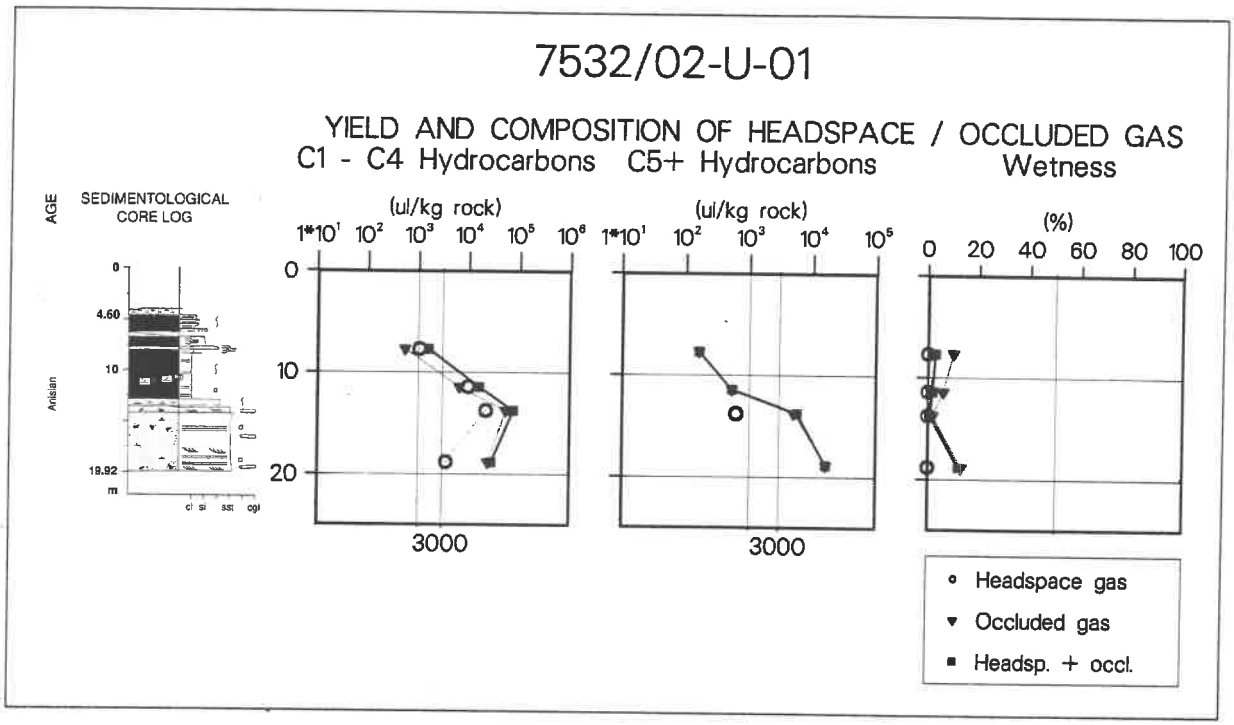

Figure 3.9 *Yield and composition of headspace/occluded gas in core 7532/02-U-01.*

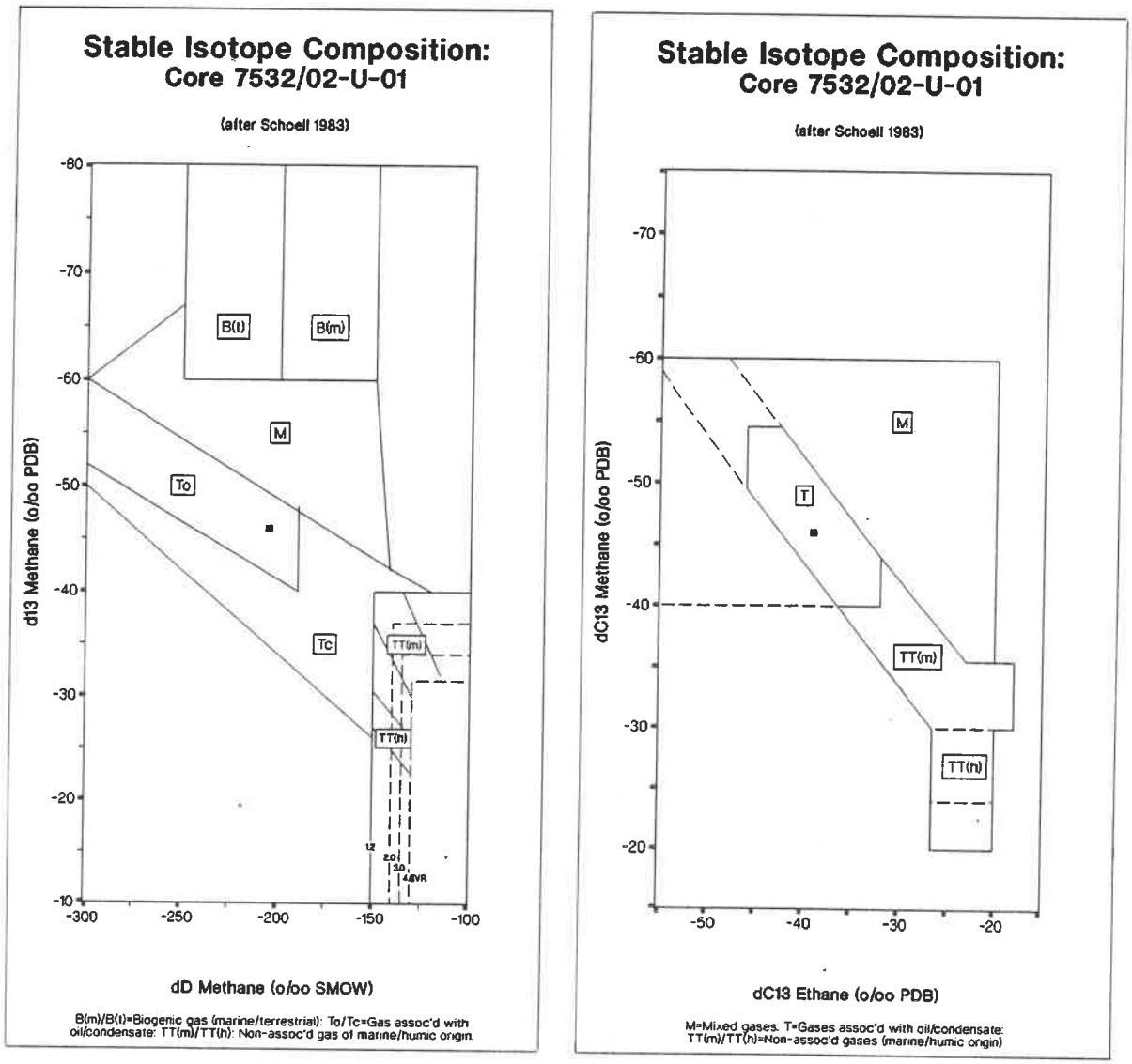

Figure 3.10 *Summary diagrams of stable carbon and deuterium isotope composition of adsorbed methane and ethane in core 7532/02-U-01.*

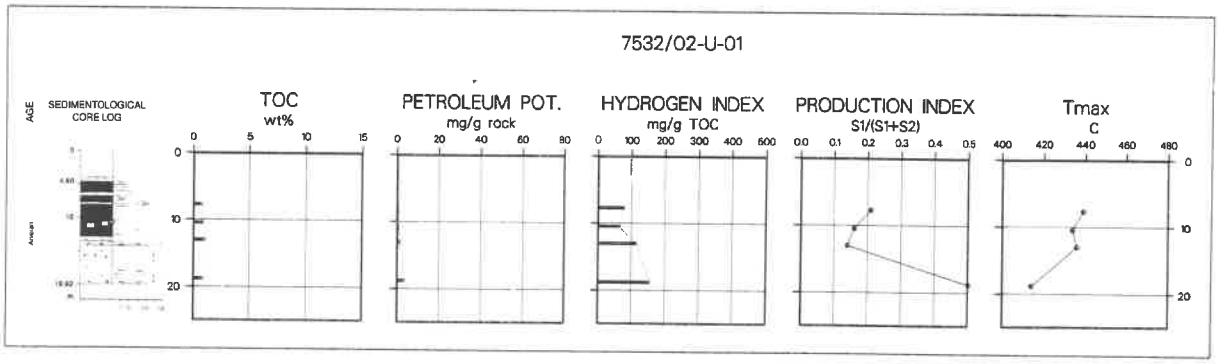

Figure 3.11 *Total organic carbon content and data from Rock-Eval data from core 7532/02-U-01.*

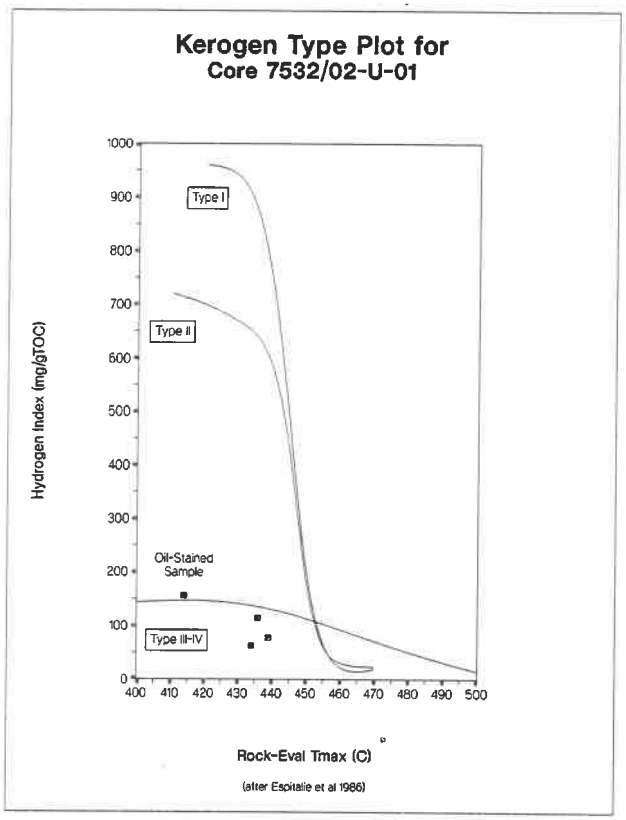

Figure 3.12 Kerogen type/maturation summary plot for core 7532/02-U-01.

4. RESULTS AND INTERPRETATION CORE 7427/03-U-01

4.1 Summary

Core 7427/03-U-01 penetrated 88.8 m into bedrock below 1.5 m of Quaternary overburden. A core recovery of 99.4% was obtained. The core consists of dominantly shales with several coarsening upwards units (5-20 cm thick). The basal parts of each unit comprise a dark grey parallel laminated shale which grades into silty shales. Storm deposited layers occur towards the top. Some silty layers have hummocky and ripple lamination. Palynofacies is dominated by wood particles in different stages of degradation. The core is interpreted to have been deposited in a shallow storm influenced environment, with an oscillating sea level. From palynomorphs the core has been assigned an early Ladinian age.

Fine-grained sandstone and siltstone intervals in the central part of this core are visibly oil-stained with a relatively light, undegraded oil. The moderate amounts of mature type III, largely terrestrial, kerogen which is present in most of the rocks has no hydrocarbon generation potential, and is unlikely to be the source of the oil-staining.

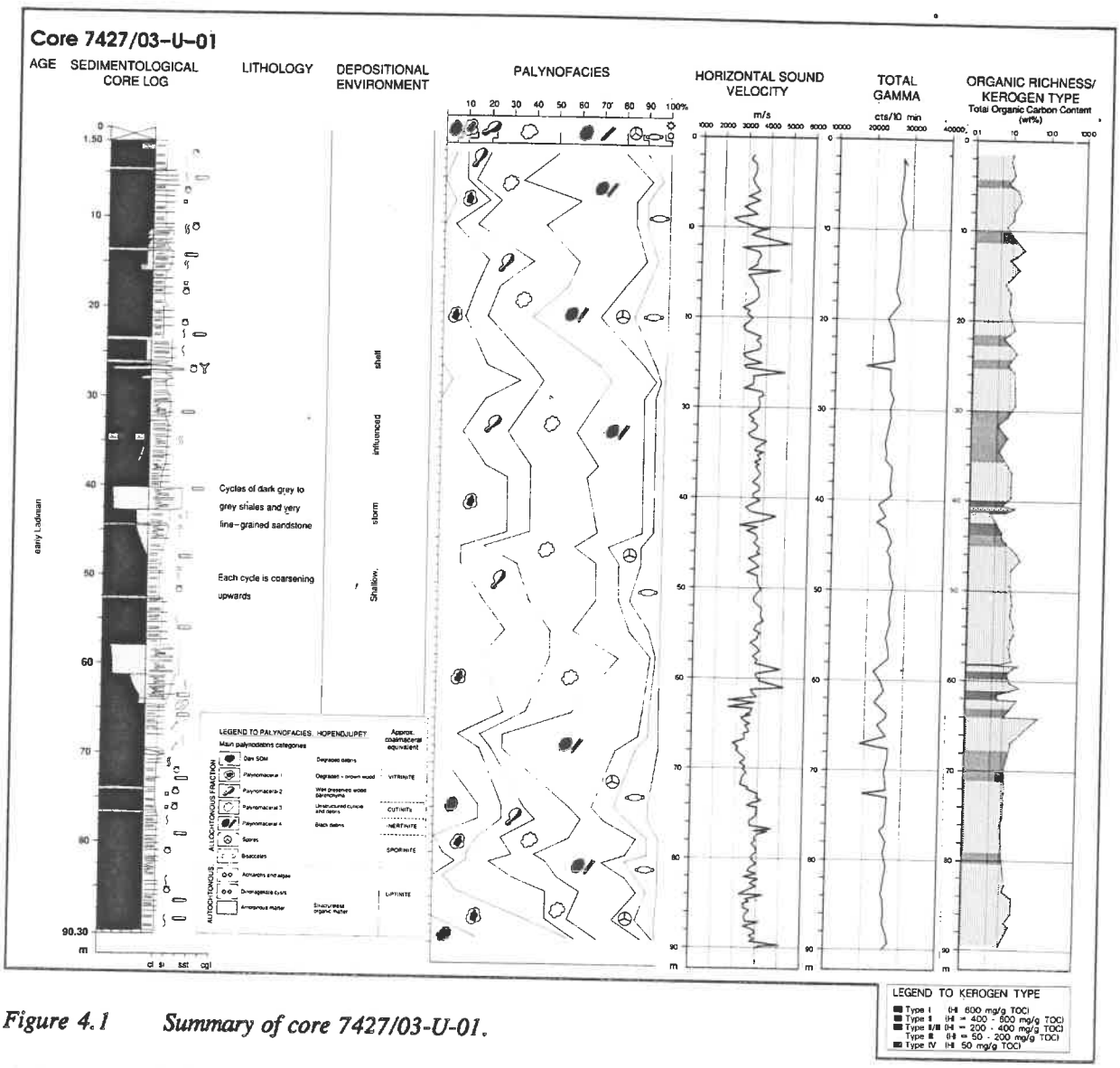

Figure 4.1 Summary of core 7427/03-U-01.

4.2 Seismic interpretation

Core 7427/03-U-01 was drilled on the Gardarbanken high, on seismic line D-10 (Figure 4.2). It was localized 65 m to the SSW of shotpoint 2215 on the conventional seismic line D-10-87 and 15 m to the NNE of shotpoint 2349.5 on the analog sparker line D-10-82. The drill site was in a local depression on the seabed, approximately 10 m deep. Investigating the origin of this and similar depressions in the neighbouring area and see their potential relationship to hydrocarbon occurrence was part of the objective with this drilling. The overburden consisted of 1.5 m of soft clay, probably of Holocene age, and the glacial till that seems to occur elsewhere in the area, was not present in the depression. This implies that the depression is Holocene or latest Pleistocene in age.

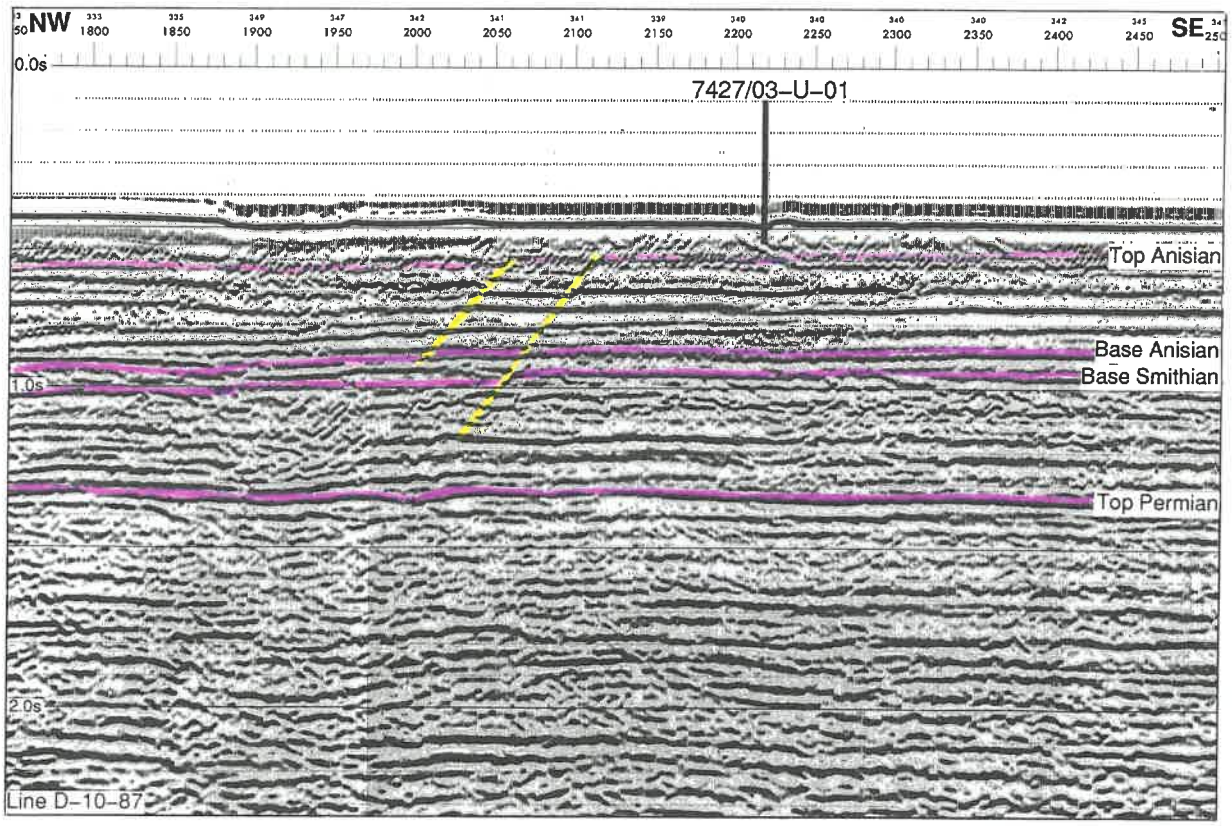

Figure 4.2 *Seismic correlation of core 7427/03-U-01. The core was drilled in a 10 m deep depression on the seabed. The base of the core-hole is approximately 120 m above the reflector interpreted as top Anisian.*

The primary objective of this drilling was to penetrate a seismic reflector interpreted as the upper boundary of a prograding unit with clinoforms

observed in the seismic data. Lacking high resolution digital seismic data, it was hard to say exactly where this reflector subcrops and the exact depth of the reflector at the drill site. At about 58 m in the core there is a boundary with sand below silty shale. Above the sand, the measured sound velocity is about 3800 m/s, in the sand it is 4000-5000 m/s and below it is about 3500 m/s. In the analog sparker data there is a faint reflection at about 35 ms which could correspond to this boundary.

As discussed in Chapter 6, the upper boundary of the clinoforms coincides with the Anisian/Ladinian transition at the Svalis Dome. Considering the age of the present core (?early Ladinian) and the available seismic data, we suggest that the core was drilled above the clinoform unit and that a reflection approximately 115 ms below seabed (595 ms below the sea surface) represents the Anisian/Ladinian boundary at the drill site. Applying the sound velocities measured on the core, the base of the core-hole was situated about 50 ms below seabed. The section from this down to the top of the clinoforms was 65 ms thick, which is about 120 m when extrapolating the sound velocities of the core downward. The Anisian/Ladinian boundary is therefore believed to be about 120 m below the base of the core-hole.

4.3 Sedimentology

Core 7427/03-U-01 penetrated totally 88.80 m of bedrock between 1.50 m and 90.30 m below seabed (Figure 4.1). The length of the core is 88.23 m which represents a recovery of 99.4%. The cored sequence consists of several 5-20 cm thick coarsening upward units of dark grey to grey shales/siltstones with thin siderite beds.

The general pattern of each unit is a development from dark grey parallel laminated clayey shales at the base to parallel, small scale hummocky and ripple laminated silty shales towards the top. Occasionally the upper part of a unit consists of very fine-grained sandstone.

Between 90.30 m and 76.60 m the lowermost 2.5 m consist mainly of dark grey, parallel laminated shale with small bivalves. A siderite cemented bed (10 cm thick) is situated at the base, while thinner (<5 cm) siderite cemented beds occur elsewhere throughout the interval. The siderite cemented bed at the base is completely bioturbated with cm-sized structures and good diversity. In the siderite beds within the shale *Helminthopsis* is commonly present. The upper 11.2 m of this unit consist of beds that are commonly 2-5 cm thick, parallel

laminated with siltstone at the base and clayey shale at the top. Occasionally the beds show erosive boundaries. In some of the silty beds hummocky lamination and ripple lamination occur.

In the thin graded beds ichnodiversity is low. *Helminthopsis* is common below about 83 m, while *Chondrites* is more common above this level. Two 15-25 cm thick siderite cemented beds occur within the upper 0.5 m of the unit. Primary sedimentary structures are visible in the lower cemented part, while the upper bed is more complex, possibly due to bioturbation.

A similar evolution is also seen in the interval between 76.60 m and 58 m. Dark grey, parallel laminated shale with scattered bivalves in the lower part and input of coarser material towards the top is seen. The difference is the frequency and thickness of the graded silty beds which here increase towards the top of the unit where layers of very fine-grained oil stained sandstone occur. The sandstone layers show parallel lamination and small scale hummocky lamination.

Chondrites is common in the silty and sandy units of this interval, while *Helminthopsis* are present in the dark grey clayey shales.

Between 58 m and about 40.3 m a second unit showing development from dark grey shales into very fine-grained oil stained sandstone is recorded. The shale (Figure 4.3 A & B) has parallel lamination with thin siderite layers and small bivalves present. In the sandstone layers (Figure 4.4 A & B) hummocky lamination is common and is also seen in the more silty, commonly parallel laminated layers (Figure 4.4B). The ichno-diversity is higher in the silty and sandy parts of the interval than in the dark grey shale. In addition to *Helminthopsis*, *Diplocraterion parallelum* and *Spirophyton* are registered in the upper part of the unit.

Between 40.3 m and 1.50 m, three major coarsening upwards intervals with boundaries at 23.8 m and 11.3 m can be distinguished. The units show the same development as described below. Shales grading into fining upwards laminae and layers of silty shales are present. Sandstones are only seen as a very thin, very fine-grained layer at about 27 m, containing fossil fragments of bivalves.

Siderite cemented layers are present throughout the core, nearly always present at the boundaries between coarsening upwards units. Fragments of plants, usually small coal particles, are present in all lithologies.

Glaciotectonic influence (see Chapter 3.3) is observed at least down to 16.3 m below seabed. The Quaternary overburden was 1.5 m thick and consisted of soft clay of supposed Late Pleistocene/Holocene age.

Mineralogical composition

Eleven shale samples and one concretion were analysed by X-ray powder diffraction (Table 4.1). In addition, six thin sections of carbonate cemented beds were analysed.

The mineralogical variation observed in the shales is minor, and can be ascribed the grain size distribution in the samples. There is no variation indicating change in the provenance.

"Pure" smectite is very low or absent in these samples. Even the recorded abundances of 1-2 wt% may be too high since the calculations is based on the 14Å basal reflection which interfers with chlorite. The mixed layered illite-smectite is illite dominated and appears as a shoulder on the low angle side of the 1. order illite reflection. It probably represents weathered or leached detrital mica/illite rather than diagenetic illitization of smectite, as the latter would show a better defined reflection.

The abundance of kaolinite is 2-3 times higher than chlorite in most samples. Of the feldspars, only plagioclase is present as a major component. The concretion or cemented bed at 34.15 m contains only siderite in addition to the detrital components.

The thin sections of six cemented layers at 13.90 m, 26.14 m, 44.53 m, 52.47 m, 74.03 m and 89.70 m show the same, i.e. no detectable amounts of calcite or dolomite/ankerite, but abundant siderite in addition to detrital components.

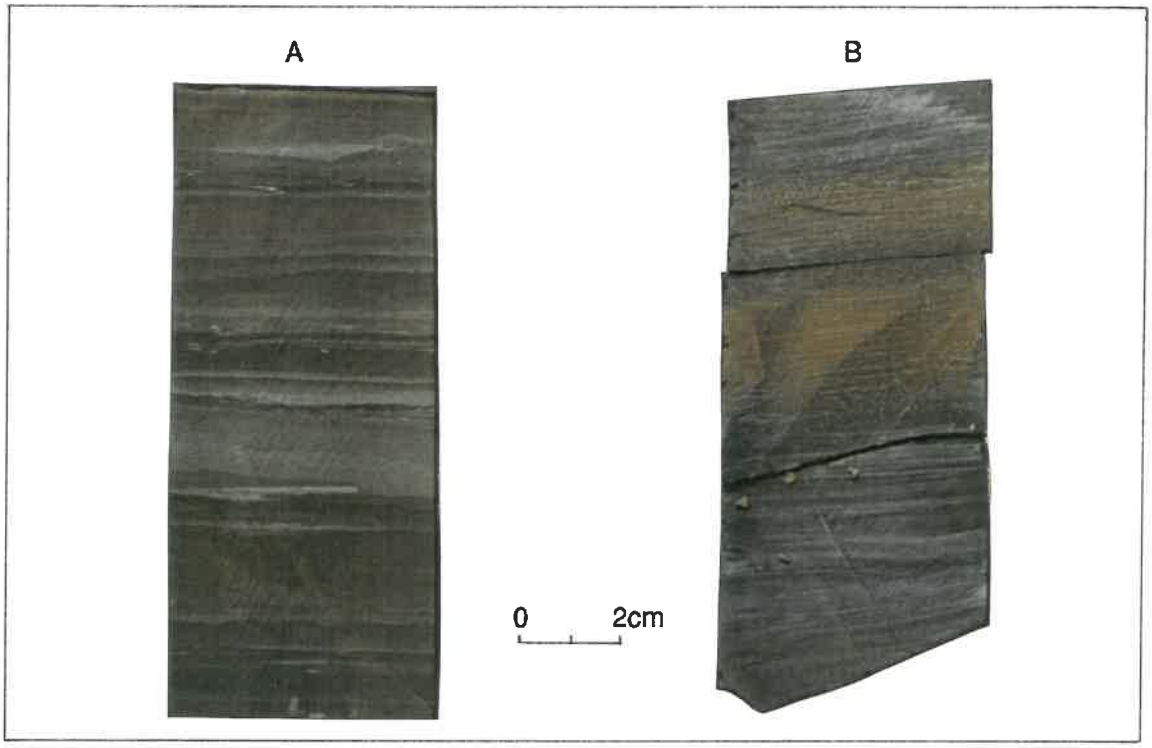

Figure 4.3 *Photographs of core 7427/03-U-01.*
A. Thin, storm influenced, fining upwards layers at 46.40 m.
B. Dark grey shale with thin siderite cemented layers at 53.35 m.

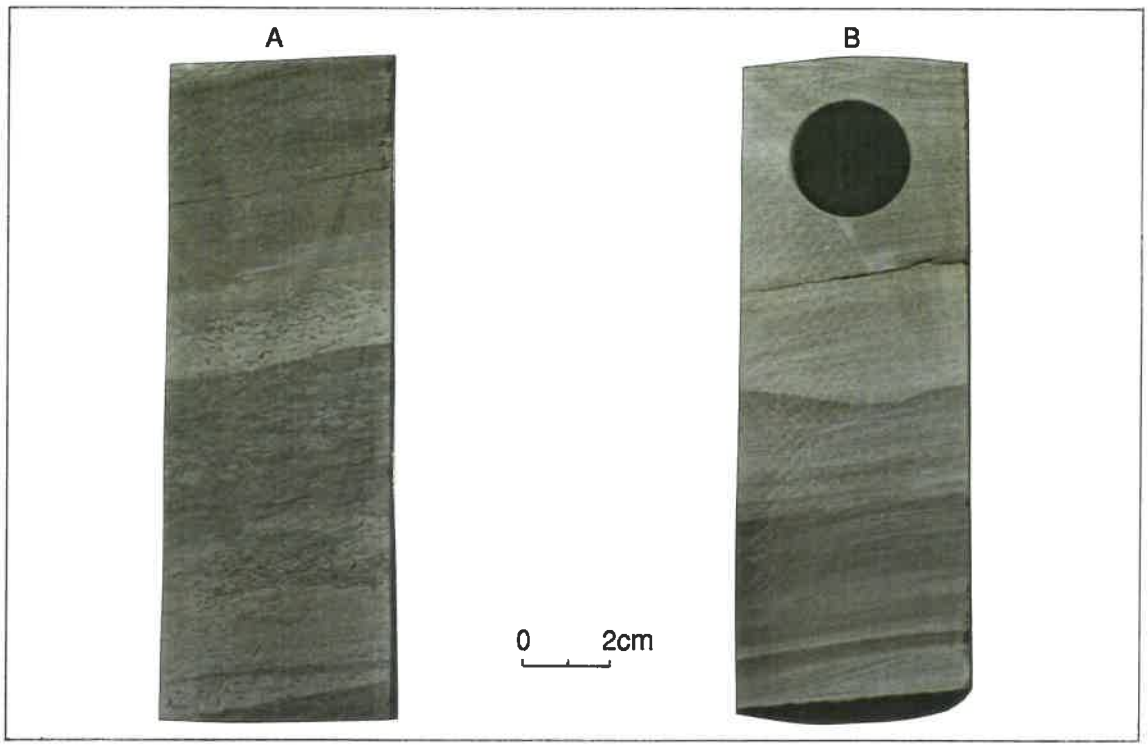

Figure 4.4 *Photographs of core 7427/03-U-01.*
A. Sandy layers fining upwards to dark grey siltstone (43.97 m). The burrows are Helminthopsis.
B. Sandy layers with hummocky lamination (44.96 m).

Thin sections of the silty layers show mainly monocrystalline quartz. Chert is not observed. The high and uniform content of plagioclase and only small or minor amounts of alkali-feldspars indicate that the major source of the sediment did not change during deposition of the cored sequence. The thin sections show that the plagioclase is detrital.

Table 4.1 *Mineralogical whole rock compositions of shale samples from core 7427/03-U-01 (semi-quantitative wt%). (Tr - trace).*

Depth (m)	Sm	Mix	Chl	Kao	Mic	Qtz	Kfl	Pl	Cal	Dol	Sid	Py
2.95	2	4	8	17	14	33	-	18	tr	1	1	1
7.02	1	4	8	19	19	30	-	16	-	-	3	tr
21.82	tr	6	9	19	13	30	-	19	-	-	4	tr
34.15*	-	2	9	3	5	12	-	10	-	-	56	3
39.80	tr	6	10	29	13	24	-	15	-	-	2	1
45.79	1	5	12	17	18	23	1	14	-	-	7	2
67.53	2	4	8	18	15	30	-	14	-	-	9	tr
72.46	tr	7	11	25	11	28	-	13	tr	-	5	tr
74.10	1	6	10	28	15	23	-	13	-	-	4	tr
78.84	1	6	5	21	9	33	-	21	-	-	2	2
84.87	2	6	8	21	16	26	-	14	-	-	7	-
89.44	-	6	12	15	17	26	-	13	-	-	9	2

* concretion

Palynofacies

The same approach to palynofacies as used for depositional environment analysis given in Chapter 3.3 is applied.

The palynofacies development in core 7427/03-U-01 is shown in Figure 4.1. The following mixed palynofacies are recognized (89.48 - 2.32 m):

There is a rather high frequency of medium-sized palynomacerals 1,2 and 3 through the cored sequence. At some levels palynomaceral 4 is an important constituent comprising both equidimensional and blade-shaped fragments. At a few levels, e.g. 89.48, 76.04, 74.01 m, dark structureless organic material is seen, but this constituent seems to be from the allochtonous fraction. Spores, pollen and acritarchs are present in all examined samples. Bisaccate pollen dominate throughout, although different spore complexes dominate at different levels.

The palynomaceral 4 fraction varies from representing about 10 % of the total organic content to representing a major part at some levels. The low amount of blade-shaped fragments reflects a certain portion of energy, because this fraction is extremely buoyant and normally is transported over long distances. Although marine palynomorphs are present, they represent a very minor constituent throughout the cored unit. This type of palynofacies corresponds to Whitaker's (1984) palynofacies types VI/V representing inner shelf and storm deposits. In a lower shoreface to upper offshore environment where the sea level has oscillated, a similar mixed palynofacies would occur. Such small-scale oscillations might be very local, caused by delta switches, and reflected in the variation in the allochtonous fraction.

Depositional environment

The whole core is interpreted to be deposited in a shallow, storm influenced shelf to shallow marine environment or shallow pro-delta environment. The overall coarsening upwards trends are probably due to several cycles of regressive development with transgressions at the onsets of sedimentation of dark grey shale possibly due to delta switches. Only in two of the units there is a development into sandstone. The sandstone layers may be relatively shallow storm deposits or they may represent lower shoreface deposits.

4.4 Biostratigraphy

Core 7427/03-U-01 has been analysed for palynomorphs, while no age-diagnostic macrofossils were recorded. The thirty-one samples analysed for palynomorphs yielded moderately to well preserved acritarchs, algae, pollen and spores (Figure 4.5). Generally non-taeniate bisaccate pollen yielded more than 50 % of the assemblages, together with a small proportion of taeniate bisaccate pollen. A diverse spore assemblage was present throughout, while marine palynomorphs only were represented by a small percentage in each sample. The palynomorphs suggests an early Ladinian age. Selected specimens are illustrated (Figures 4.6 - 4.9).

90.30 m (TD)- 1.5 m, early Ladinian

The age-diagnostic monolete spore *Echinitosporites iliacoides* is recorded throughout the cored interval. This spore is a Ladinian marker in the Barents Sea (Hochuli et al. 1989), as well as in the Alpine Triassic of Europe (Visscher & Brugman 1981). It appears together with a very characteristic assemblage which in general consists of more than 50% bisaccate pollen, some of which have their first occurrence in the Ladinian (e.g. *Ovalipollis pseudoalatus, Triadispora verrucata, Protodiploxypinus ornatus, Staurosaccites quadrifidus*. Comparable assemblages have been described from the Svalis Dome (Vigran et al. 1988, Follow-up studies, Dia Structure Shallow Drilling) as well as from exploration wells in the Barents Sea (Hochuli et al. 1989). They described an early Ladinian assemblage I based on down-hole appearance of *Cordaitina gunyalensis (syn. Heliosaccus dimorphus)* and lower limit a.o. of *Echinitosporites iliacoides, Kraeuselisporites cooksonae, Thomsonisporites toralis* and *Schizaeoisporites worsleyi*. All these species are recorded throughout core 7427/03-U-01, suggesting an early Ladinian age for this core.

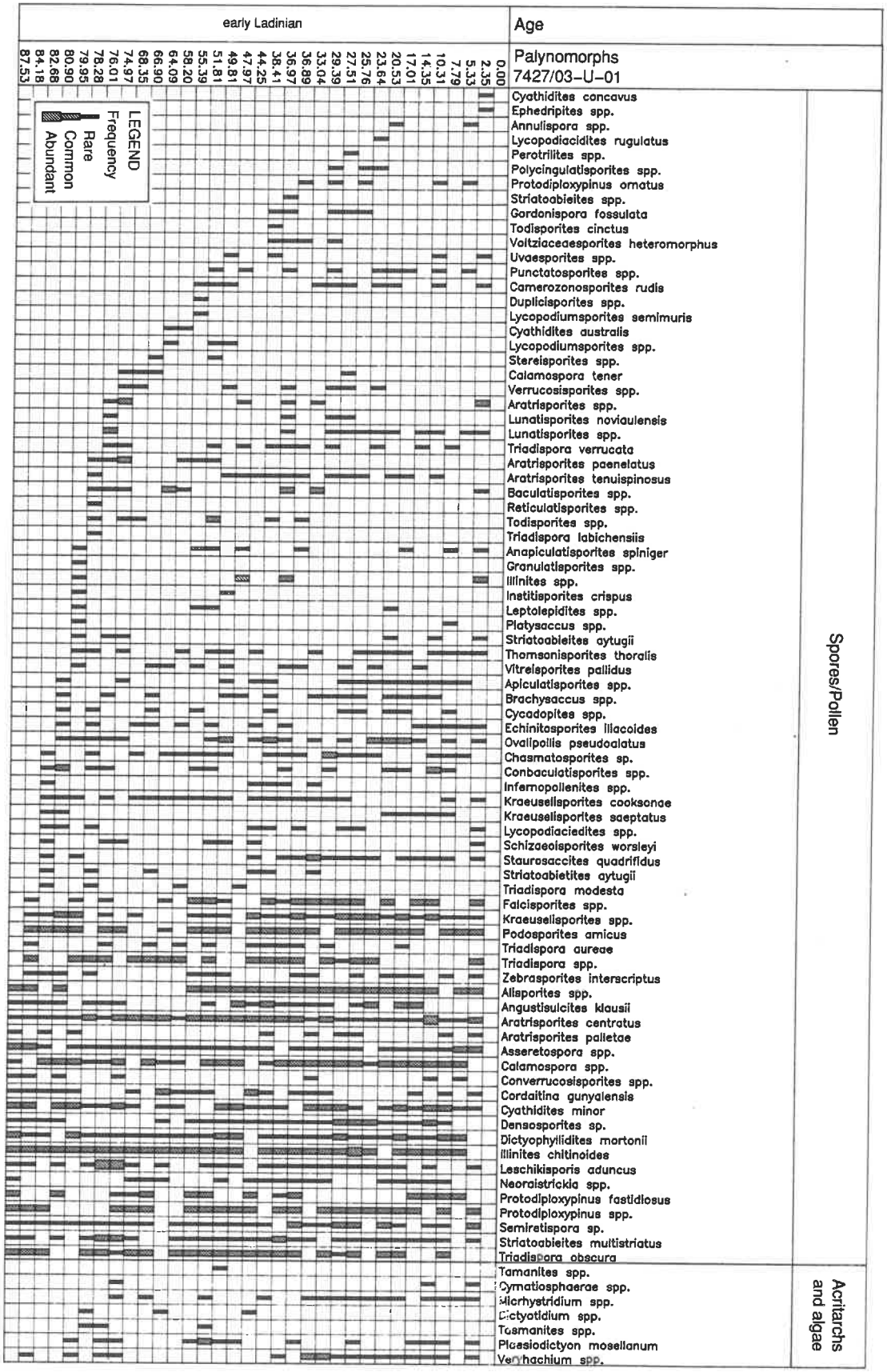

Figure 4.5 Range chart of palynomorphs in core 7427/03-U-01 sorted according to earliest occurrence.

Figure 4.6 *Selected spores from core 7427/03-U-01. Magnification indicated by 50 µm scale bar. Taxon name is followed by sample depth in metres and coordinates to Leitz Aristoplan microscope.*

1. *Calamospora* sp. 36.97 m 56-97.2
2. *Cyathidites minor* 47.97 m 50-101.2
3. *Dictyophyllidites mortonii* 74.97 m 24.9-95
4. *Conbaculatisporites* sp. 72.45 m 22-103.2
5. *Conbaculatisporites* sp. 52.75 m 26.1-102
6. Unidentified 74.97 m 36-94
7. *Anapiculatisporites spiniger* 17.01 m 64.8-100.8
8. *Apiculatisporites* sp. 36.89 m 59-91
9. *Zebrasporites interscriptus* 55.39 m 65-93
10. *Lycopodiacidites semimuris* 55.39 m 66-95
11. *Lycopodiacidites* sp. 75.45 m 24-107
12. *Annulispora* sp. 20.53 m 60-97
13. *Gordonispora fossulata* 36.97 m 68-102
14. *Asseretospora*-complex 76.01 m 44.8-104
15. *Asseretospora*-complex 74.97 m 30.2-110

Figure 4.7 *Selected spores from core 7427/03-U-01. Magnification indicated by 50 µm scale bar. Taxon name is followed by sample depth in metres and coordinates to Leitz Aristoplan microscope.*

1. *Thomsonisporites toralis* 52.75 m 41-110.5
2. *Semiretispora* sp. 72.45 m 34.3-109.6
3. *Semiretispora* sp. 55.39 m 63-93.2
4. *Kraeuselisporites* sp. 66.35 m 55-108
5. *Kraeuselisporites cooksonae* 7.79 m 46.2-96
6. *Kraeuselisporites* sp. 52.75 m 36-114
7. *Densosporites* sp. 55.39 m 59-93
8. Unidentified spore 52.75 m 41.9-93.2
9. *Leschikisporis aduncus* 76.01 m 53.5-93
10. *Echinitosporites iliacoides* 51.81 m 46-93.5
11. *Echinitosporites iliacoides* 7.79 m 52-110.5
12. *Schizaeoisporites worsleyii* 51.81 m 66-105
13. *Aratrisporites palletae* 47.97 m 66-91
14. *Aratrisporites centratus* 74.97 m 42-92.2
15. *Aratrisporites* sp. 49.81 m 62-95.5

Figure 4.8 *Selected pollen from core 7427/03-U-01. Magnification indicated by 50 µm scale bar. Taxon name is followed by sample depth in metres and coordinates to Leitz Aristoplan microscope.*

1. *Brachysaccus* sp. 38.41 m 47-100
2. *Protodiploxypinus fastidiosus* 36.89 m 59-91
3. *Protodiploxypinus ornatus* 36.89 m 59-100
4. *Podosporites amicus* 51.81 m 53.9-97.7
5. *Podosporites amicus* 64.09 m 66-112.2
6. *Ovalipollis pseudoalatus* 74.97 m 22-96
7. *Staurosaccites quadrifidus* 33.04 m 52-97.3
8. *Illinites chitonoids* 38.41 m 51.3-94
9. *Angustisulcites klausii* 45.86 m 65.5-97
10. *Triadispora aureae* 76.01 m 33.3-94
11. *Triadispora* sp. 51.81 m 52-97.5
12. *Institisporites crispus* 49.81 m 64-97.2
13. *Lunatisporites* sp. 20.53 m 69.7-95.2
14. *Striatoabieites multistriatus* 76.01 m 50.7-105.3
15. *Striatoabieites aytugii* 33.04 m 52-98.3

Figure 4.9 *Selected pollen, marine palynomorphs and algae from core 7427/03-U-01. Magnification indicated by 50 µm scale bar. Taxon name is followed by sample depth in metres and coordinates to Leitz Aristoplan microscope.*

1. *Chasmatosporites* sp. 51.81 m 64-94
2. *Chasmatosporites* sp. 47.97 m 50.8-102.3
3. Sulcate pollen 36.89 m 67.4-101.5
4. *Veryhachium* sp. 33.04 m 63-94
5. *Veryhachium* sp. 76.01 m 61-105.3
6. *Veryhachium* 33.04 m 64-91
7. *Micrhystridium* sp. 33.04 m 58-104
8. *Cymatiosphaerae* sp. 10.31 m 53.5-97
9. *Plaesiodictyon mosellanum* 55.39 m 53-102.5
10. Palynofacies 40.09 m
11. Palynofacies 10.90 m

IKU SINTEF GRUPPEN

Core 7427/03-U-01

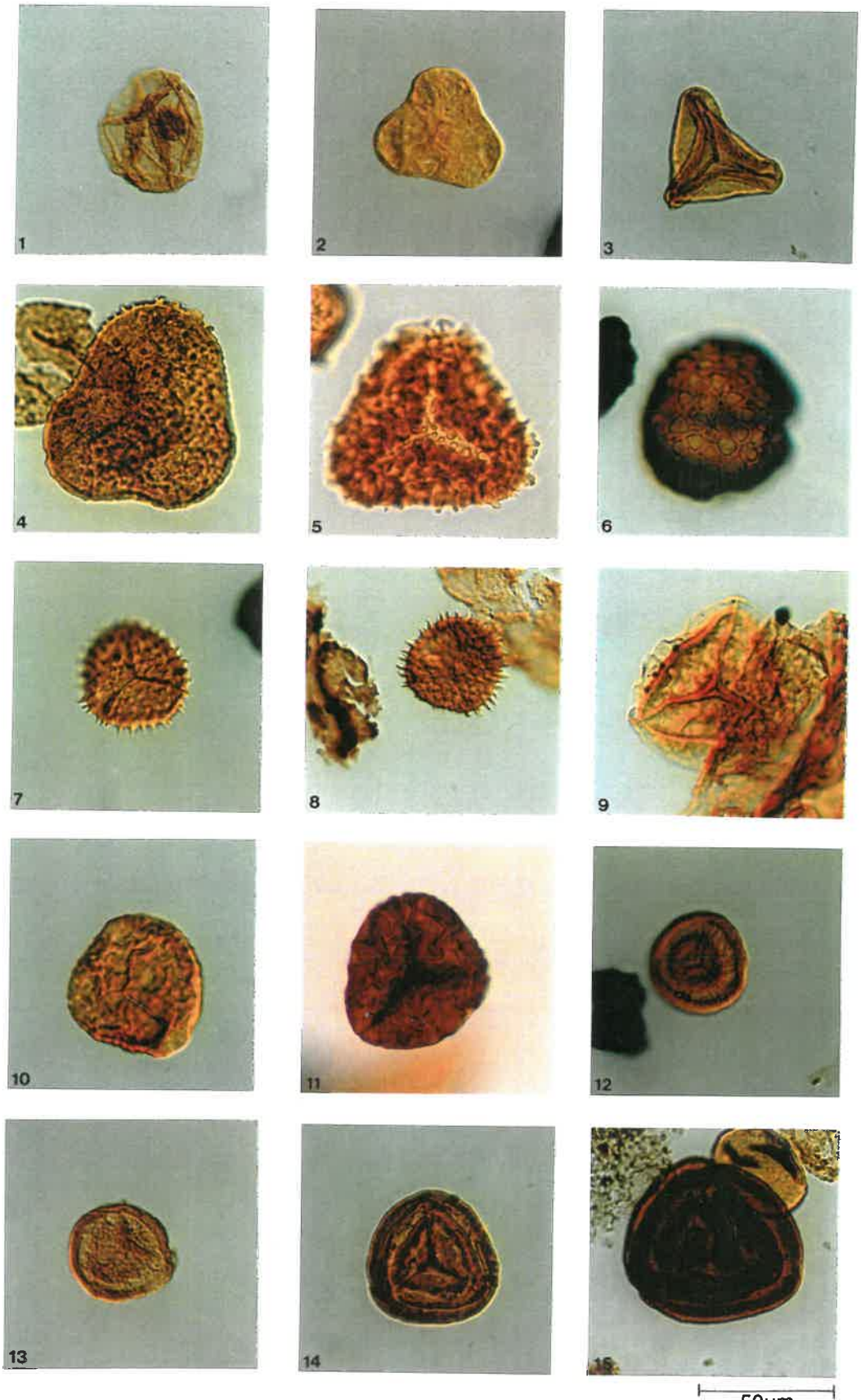

Figure 4.6

IKU SINTEF GRUPPEN

Core 7427/03-U-01

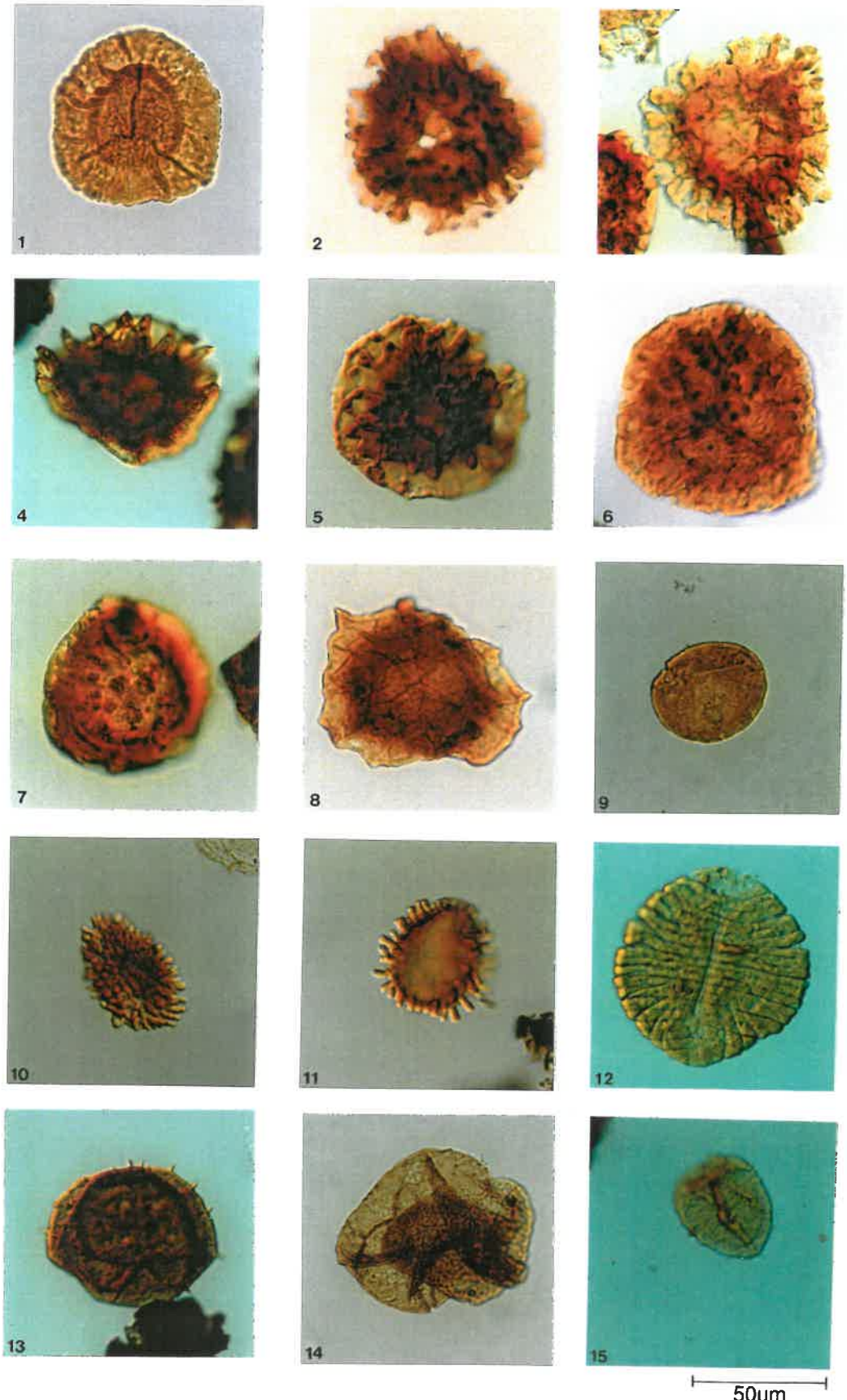

Figure 4.7

IKU SINTEF GRUPPEN

Core 7427/03-U-01

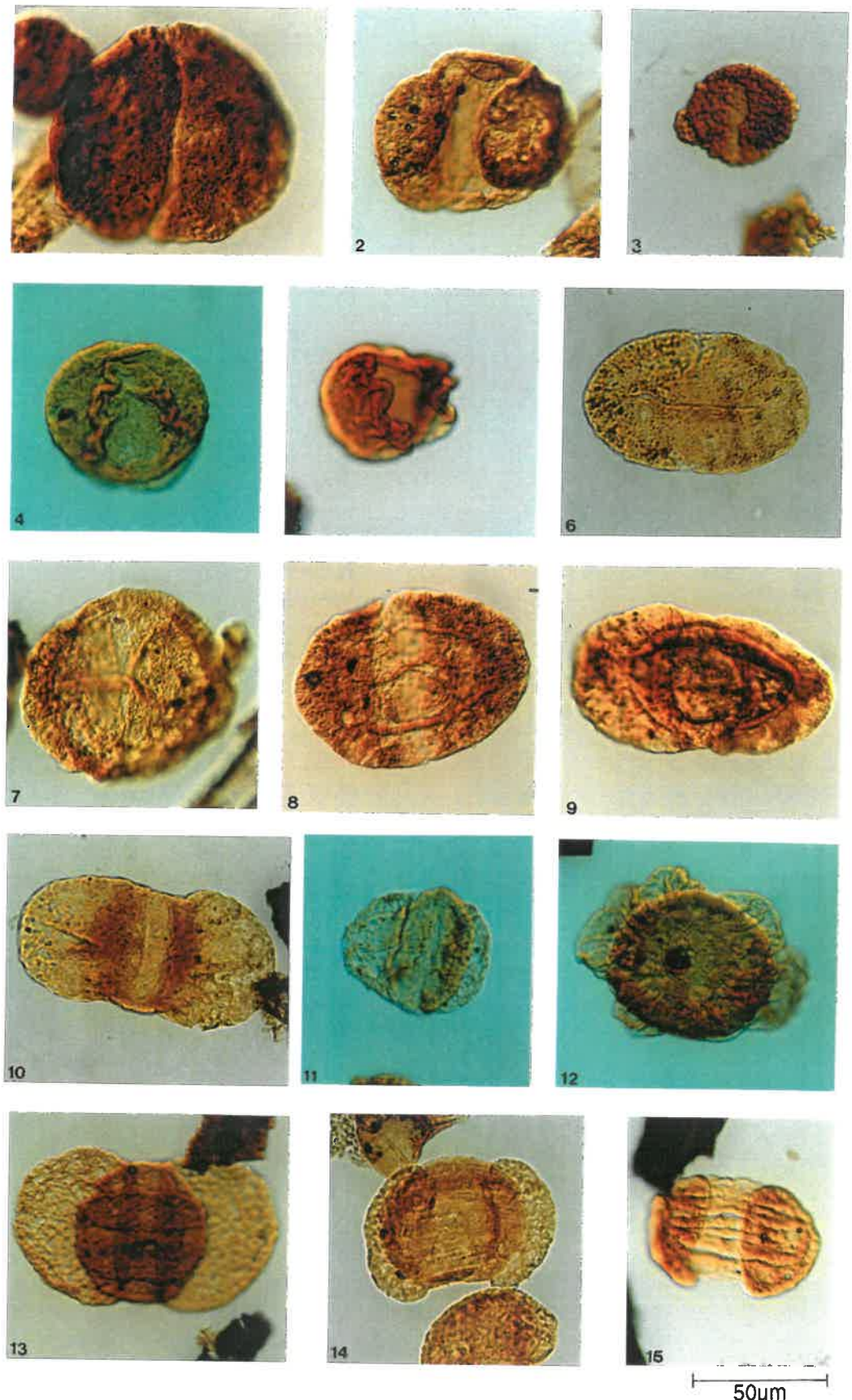

Figure 4.8

IKU SINTEF GRUPPEN

Core 7427/03–U–01

Figure 4.9

4.5 Organic Geochemistry

A total of twenty-eight canned samples was collected from core 7427/03-U-01 to permit analysis and characterization of the headspace and occluded gas fractions. With the exception of the oil-stained intervals between 60 m and 40 m depth, methane is the main constituent of both gas fractions. This is especially true of the core section below ca 84 m, between ca 70-65 m, and above ca 30 m, where the C_{2+} gaseous hydrocarbons are nearly absent (Figure 4.10).

Within the visibly oil-stained sandstones and siltstones which occur between ca 64 m and 40 m, the C_{2+} hydrocarbons are more abundant than methane, giving rise to relatively high gas wetness values of between 20% and 90%. Similar high values are typically associated with oil reservoirs. In spite of the high gas wetness values associated with the oil-stained intervals, the iC_4/nC_4 ratio values associated with the gas from these intervals were slightly higher than might be expected, with values of 0.4 and higher. Lower values of 0.2 to 0.3 were only found in six of the analysed samples at 60.80 m, 59.30 m, 56.41 m, 54.88 m, 46.63 m and 41.37 m, and are not always associated with particularly high gas wetness values (i.e. the most stained intervals).

Stable carbon and deuterium isotope analysis of the adsorbed methane and ethane in seven samples from this core suggested that the gas in the core samples is associated with oil, as might be expected from the visible oil-staining in the core (Figure 4.11). Slightly elevated δD ratios are not wholly reconcilable with the apparently petroliferous source of the gas and may suggest that either some fractionation has occurred, or that the gases contain a slight biogenic contribution. The low degree of scatter in the data suggests that all the gases are derived from a common source and have experienced a similar history.

A total of seventy-five samples was analysed for organic carbon content and bulk pyrolysis character. The samples were distributed fairly evenly throughout the core at intervals of ca 1 m. The majority of the samples analysed from the core have total organic carbon (TOC) contents of ca 1 wt% (Figure 4.12). There is no obvious pattern evident in the TOC content of the samples, although the lowest TOC contents tend to occur in sandstones and siltstones. The presence of oil-staining does not appear to influence the TOC content of the samples to any significant degree. The highest TOC content of ca 9 wt% was observed in a claystone sample at 64.15 m, which appears to directly underlie an unconformity.

Not surprisingly, the Rock-Eval data show more evidence of oil-stain influence in the central part of the core where visibly oil-stained intervals occur (Figure 4.12). In these intervals, hydrogen indices of 200-300 mg/gTOC are associated with high production index values in excess of 0.5. The data from these intervals (43.56-40.60 m and 61.58-58.32 m) are consequently considered to be unreliable as regards kerogen character and maturity.

The remainder of the samples from the cored succession are characterized by low pyrolytic yields, with hydrogen indices typical of type III or type III/IV kerogen (Figures 4.12 and 4.13). Production indices of 0.1 to 0.2 are not considered indicative of appreciable oil-staining given the generally high maturity level of the samples indicated by Tmax values of ca 440°C. Visual kerogen and palynofacies assessments suggest that structured terrestrial debris is the major kerogen component in the cored rocks. This description is consistent with the Rock-Eval data, suggesting that the kerogen in these rocks is unlikely to have generated significant amounts of oil.

Gas chromatograms of oil collected after it had seeped from the core are shown in Figure 4.14. These oils (41.25-41.05 m and 43.52-43.37 m) are characterized by a unimodal n-alkane distribution which decreases smoothly from a maximum peak height at nC_{15} to a minimum at nC_{31}. Both oils are very similar in composition, with pristane/phytane ratios of ca 2.0. The relative smoothness of the n-alkane envelope and the relative absence of biomarker peaks suggest a relatively mature oil.

The two oil samples show no evidence of biodegradation or water-washing as might be expected in oil samples from such shallowly buried rocks. This may suggest that either seabed temperatures are sufficiently low to inhibit microbial activity, or that the oil is currently being replenished in the cored aquifer. The saturated hydrocarbon composition of the two oil samples is similar to that of artificial oils generated from Spathian to Anisian age shales from the Svalis Dome, although a more positive correlation will require further data.

In conclusion, the succession penetrated by this core contains claystones, siltstones and sandstones with an organic carbon content of ca 1 wt% which is mostly comprised of type III or type III/IV kerogen with poor hydrocarbon source potential. However, the relatively high thermal maturity level of the kerogen leaves open the possibility that the kerogen in some of these rocks may originally have had some hydrocarbon potential. Thermally mature, undegraded oil occurs as visible oil-staining in the central part of the core.

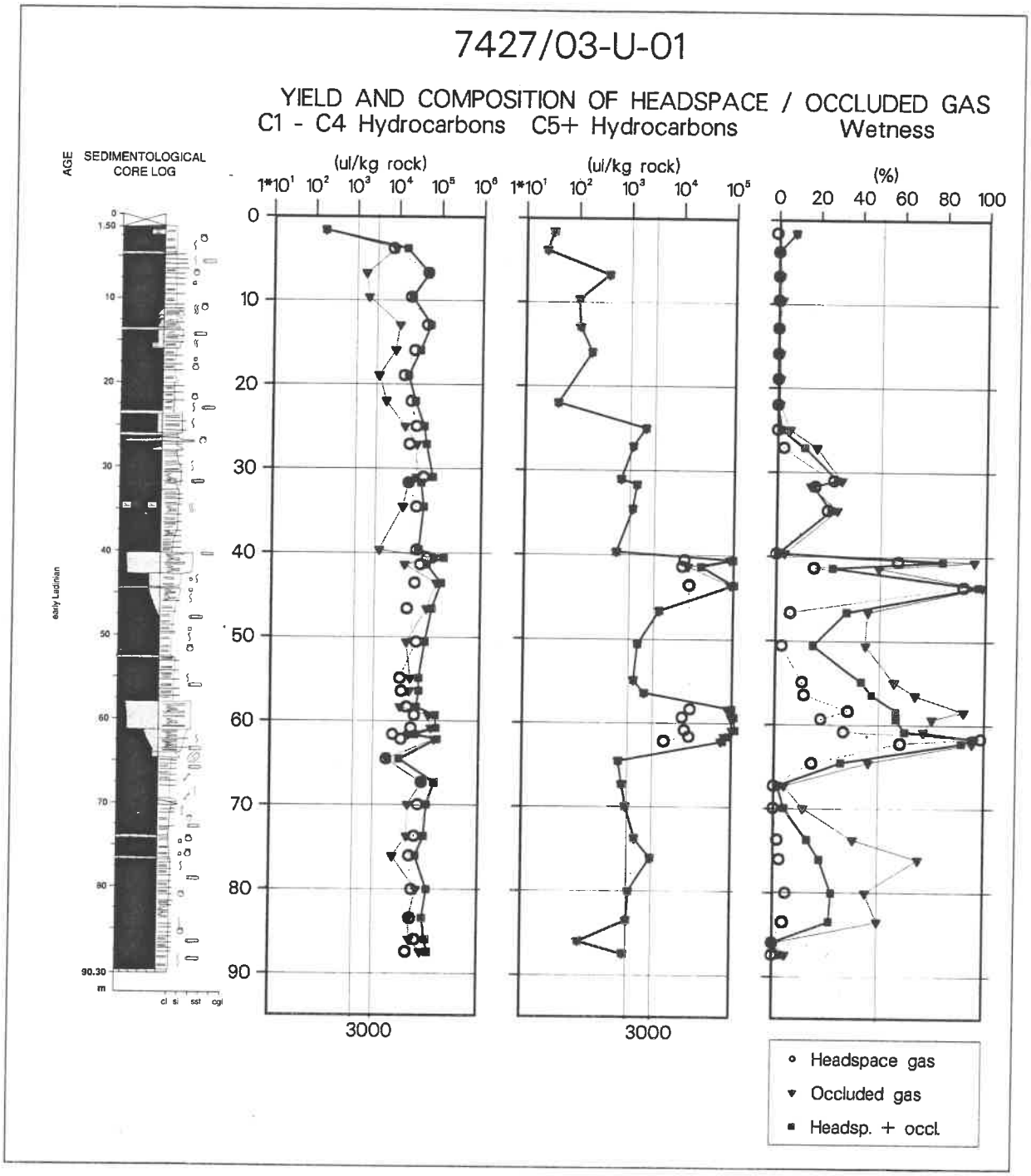

Figure 4.10 Yield and composition of headspace/occluded gas in core 7427/03-U-01.

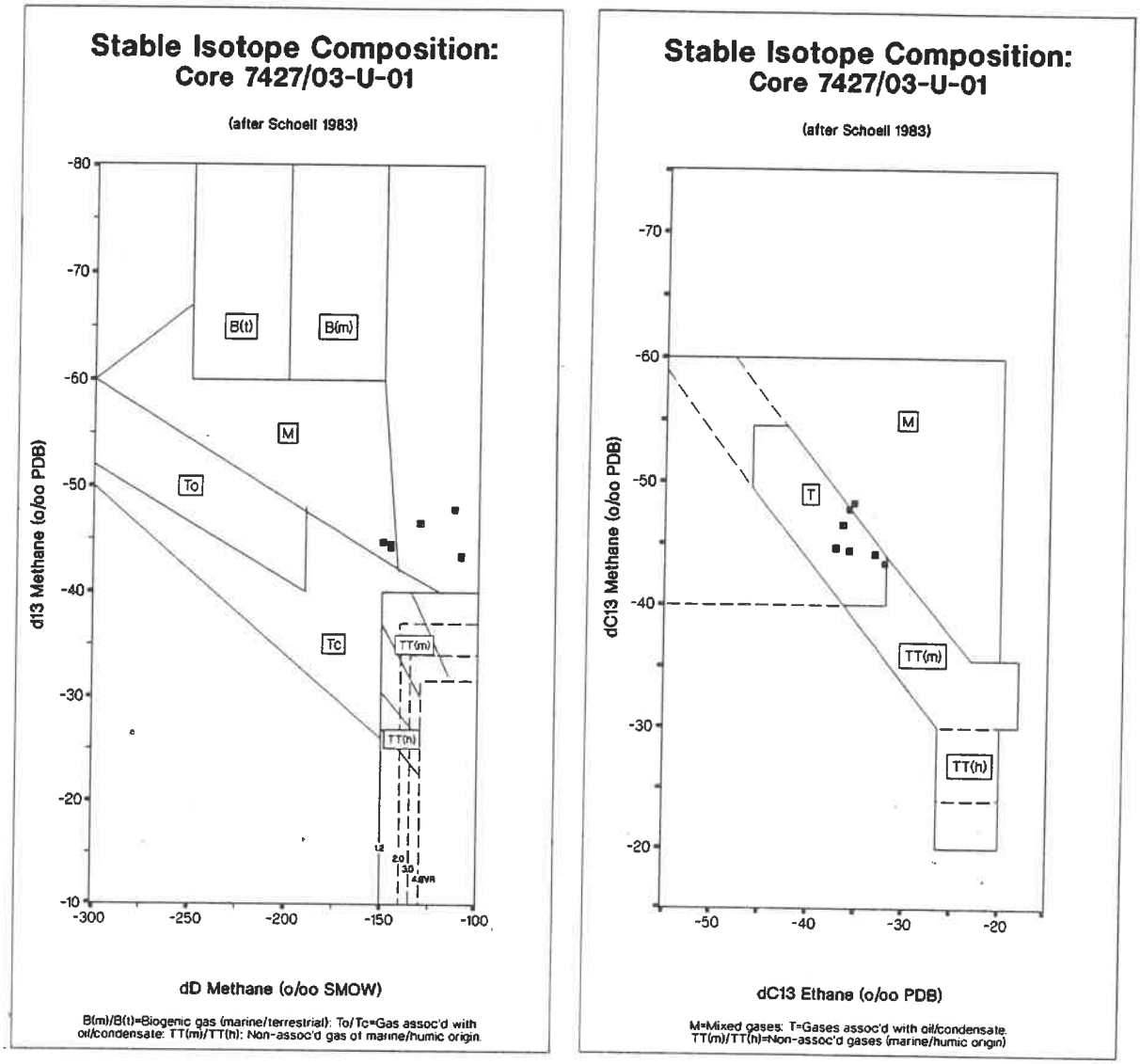

Figure 4.11 *Summary diagrams of stable carbon and deuterium isotope composition of adsorbed methane and ethane in core 7427/03-U-01.*

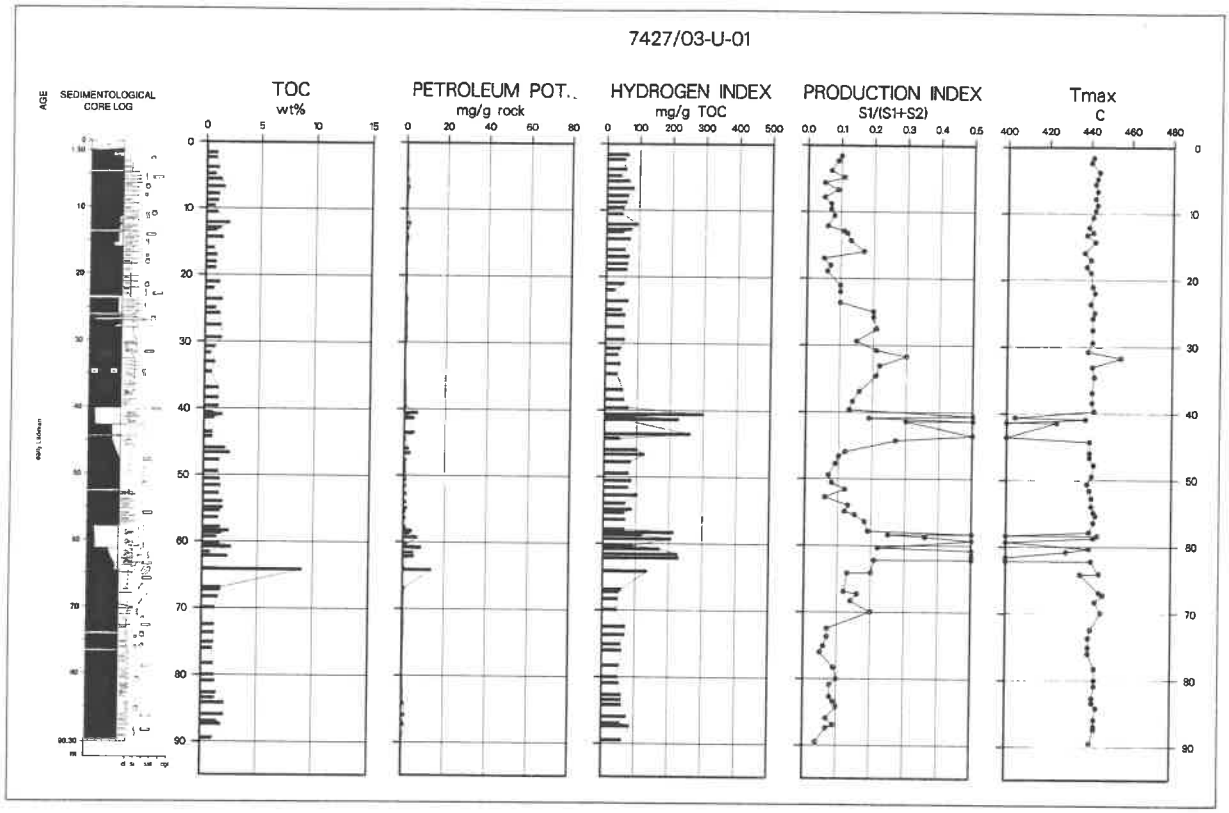

Figure 4.12 *Total organic carbon content and data from Rock-Eval data from core 7427/03-U-01.*

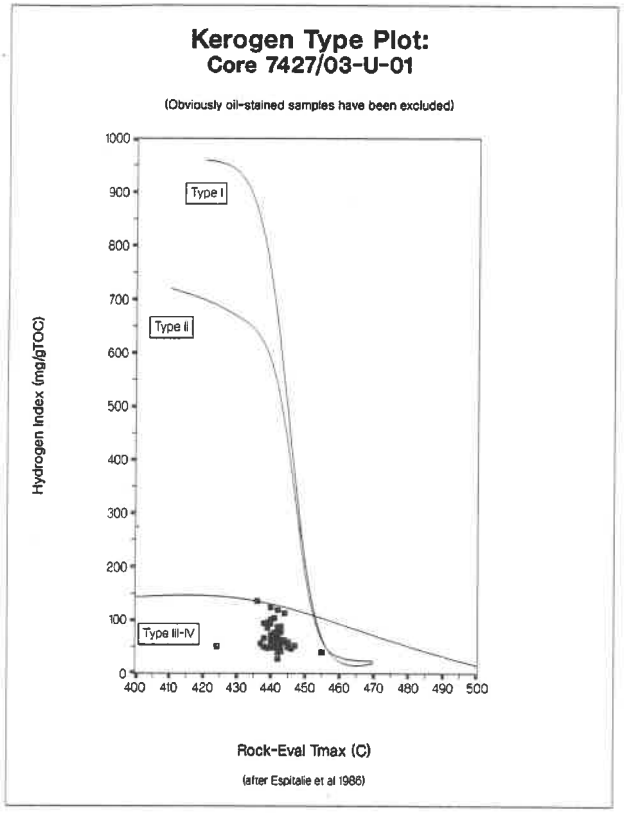

Figure 4.13 Kerogen type/maturation summary plot for core 7427/03-U-01.

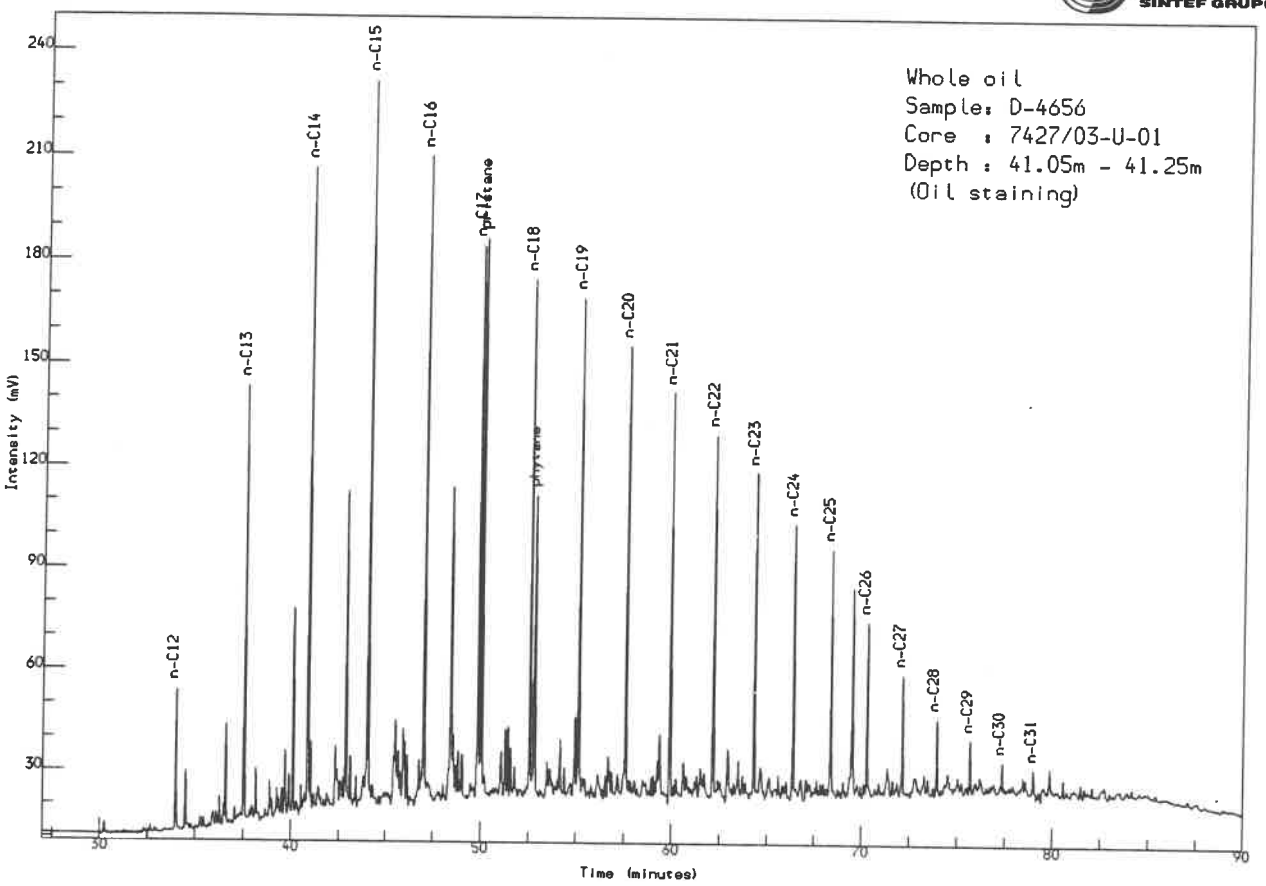

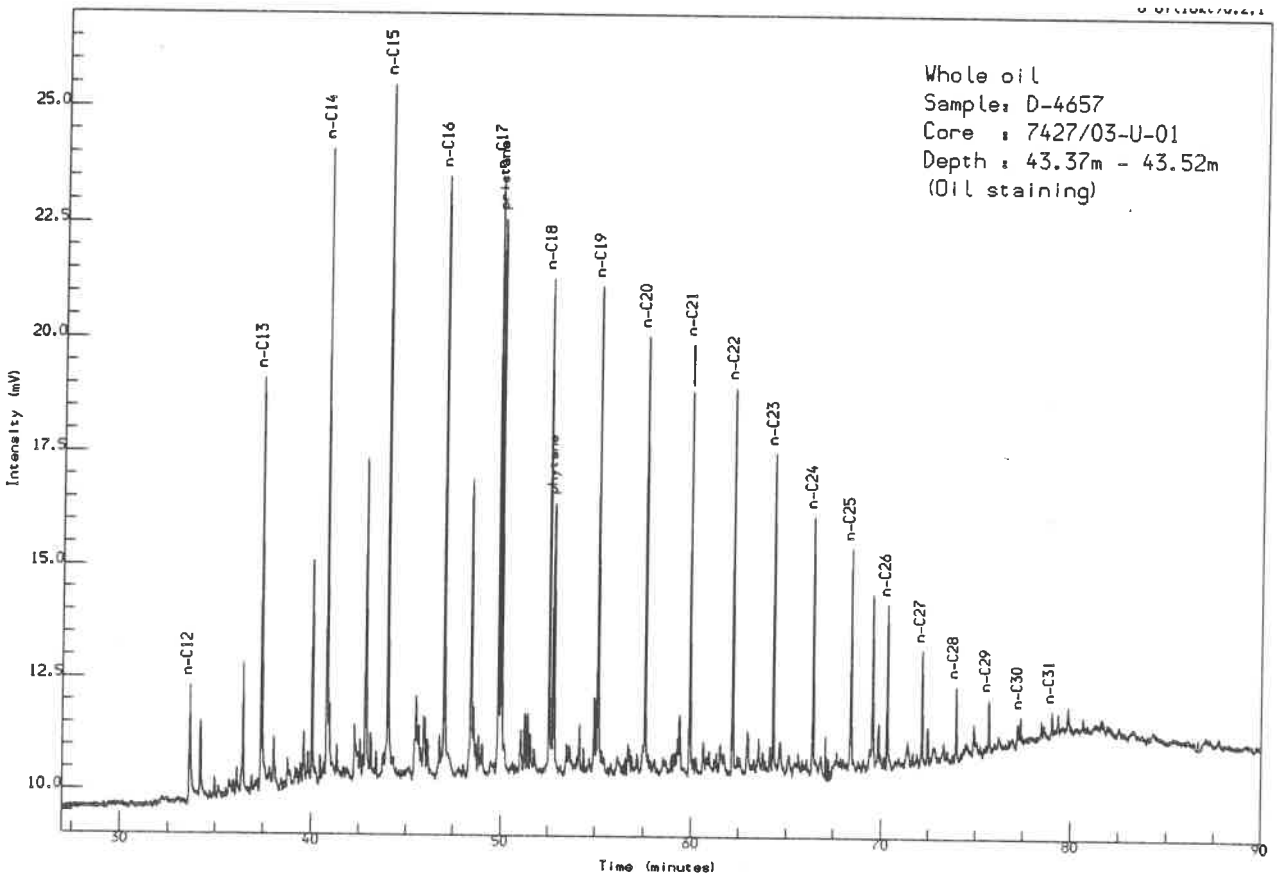

Figure 4.14 Whole oil gas chromatograms of oil-stain from core 7427/03-U-01.

5. RESULTS AND INTERPRETATION CORE 7533/03-U-01

5.1 Summary

Core 7533/03-U-01 penetrated 118.75 metres into bedrock, below 1.8 metres of Quaternary overburden. The core has been divided into four lithological units of which Unit A is correlated to the Fuglen Formation and Unit B is correlated to Hekkingen Formation. A limestone representing a condensed interval is referred to as Unit C, and it is overlain by Unit D comprising alternating sandstones and siltstones.

The lowermost Unit A (120.55 - 71.52 m) consists of medium dark grey shales and siltstones suggested to represent an open shelf environment. From ammonites and palynomorphs it is dated as uppermost Boreal Bajocian to Upper Callovian.

Unit B (71.52 - 48.38 m) consists of dark grey claystone believed to represent a anoxic shelf environment. From ammonites and palynomorphs it is dated as Middle Oxfordian to Upper Kimmeridgian.

Unit C (48.38 - 45.07 m) consists of nodular, marly limestone. This condensed interval known to exist in large parts of the Barents Shelf is interpreted to represent a shallow marine shelf, periodically influenced by storm deposits. A Valanginian age is proposed from nannofossils and foraminifera.

Unit D (45.07 - 1.80 m) consists of reddish brown and greenish, grey sandy siltstone. It is divided into two lithofacies where D1 consists of reddish brown and greyish green sandy siltstone, with variable amount of fossil fragments. D2 consists of fine-grained, light grey, rippled laminated sandstone and well sorted light grey massive sandstone. The bimodal rhytmically interchanging sediment recorded in this core is believed to represent derivation from two different source areas. The siltstones in lithofacies D1 are interpreted as mud-/debris flow deposits and the sandstones in lithofacies D2 as high density turbidites. Unit D was assigned a Hauterivian - early Barremian age, based on palynomorphs and foraminifera.

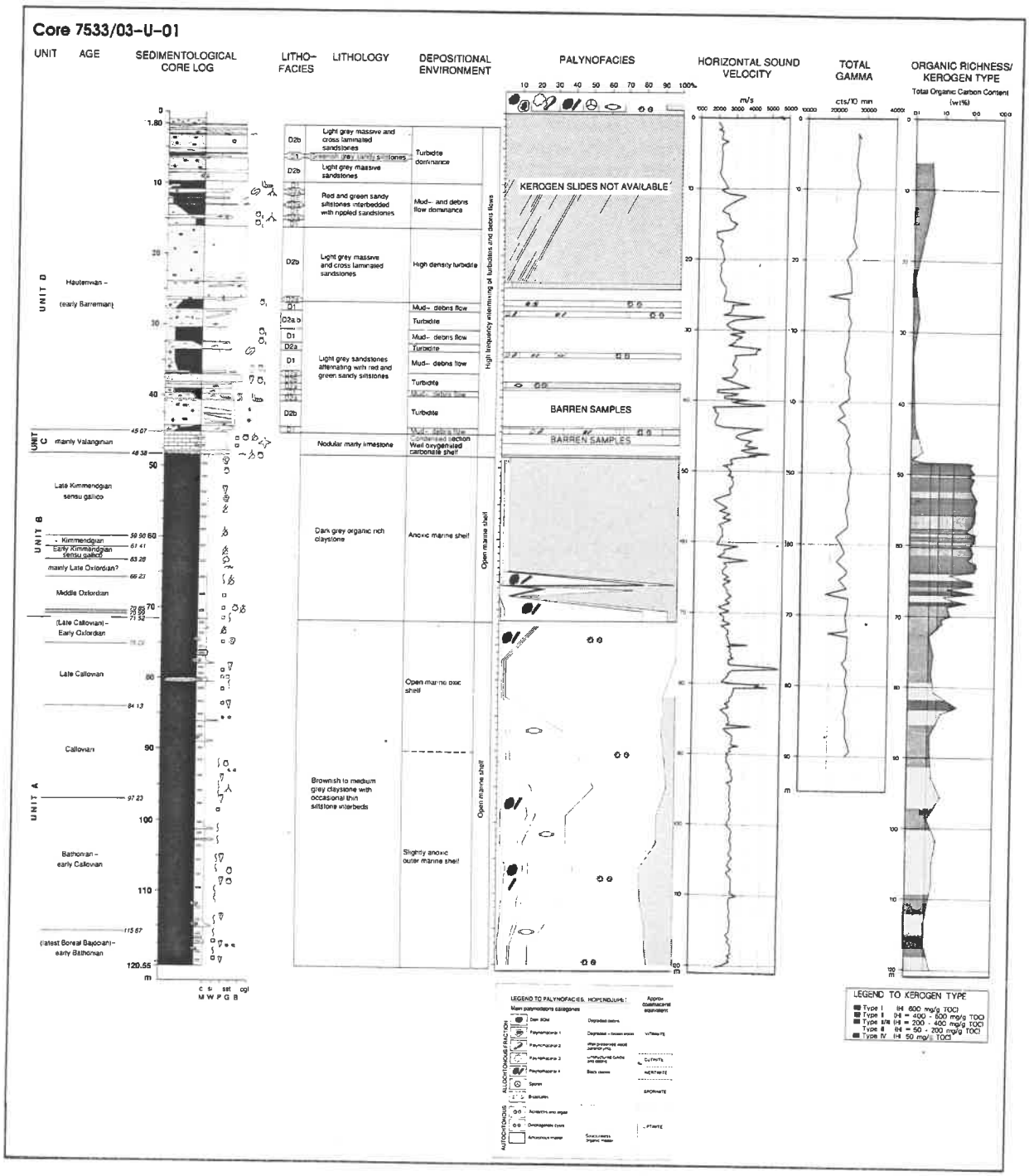

Figure 5.1 Summary figure of core 7533/03-U-01.

The ca 20 m thick shaly Unit B in the central part of this core contains excellent amounts of thermally immature type II and type II/III kerogen. This interval will represent an excellent hydrocarbon source rock with increased maturation. The majority of the core, however, is characterized by organic carbon contents of 1 wt% and less, consisting mainly of type III and type IV kerogen. These rocks have no appreciable hydrocarbon generation potential.

5.2 Seismic interpretation

Core 7533/03-U-01 was drilled 40 km to the northeast of core 7532/02-U-01, on seismic line 3345-87-A at shotpoint 10287. The overburden was 1.8 m thick and consisted of overconsolidated till.

The objective of the drilling was to core the lowermost part of the Cretaceous and the upper Jurassic. From some seabed samples obtained by the Norwegian Polar Research Institute (Antonsen et al. in press), the Cretaceous was expected to contain sandstone. The upper Jurassic was further believed to contain organic rich shale.

One very strong seismic reflection was penetrated. This probably correlates with the top of the high velocity layer of limestone/sandstone below approximately 44 m. (The lithological unit boundary is set at 45 m). The density also seems to increase rapidly, as evaluated from the lithology and measured permeability. The boundary between the two lithologically defined Units A and B is tentatively set at a lithologic change at 71.52 m. There are some peak values in the measured sound velocity at 78-80 m. They may correspond to a weak, but continuous seismic reflection about 30 ms below the reflection from the top of the limestone. The richest source rock is found within this interval. Applying the measured sound velocity values, the base of the core is approximately 84 ms below seabed, which means that the corehole nearly penetrated down to the blue seismic reflector in Figure 5.2. Based on age evidence we tentatively correlate this reflector with a top Stø Formation equivalent (Worsley et al. 1988).

It was planned to core a few metres of the unit above the Cretaceous sandstone, but because of navigation problems during the seismic acquisition, the site was probably placed farther to the south on seismic line 3345-87-A, relatively seen. It is known from the observers log that frequent "lane slips" occurred during this part of the seismic survey,while the navigation during the drilling was accurate. From the seismic data (Figure 3.2) the sandstone

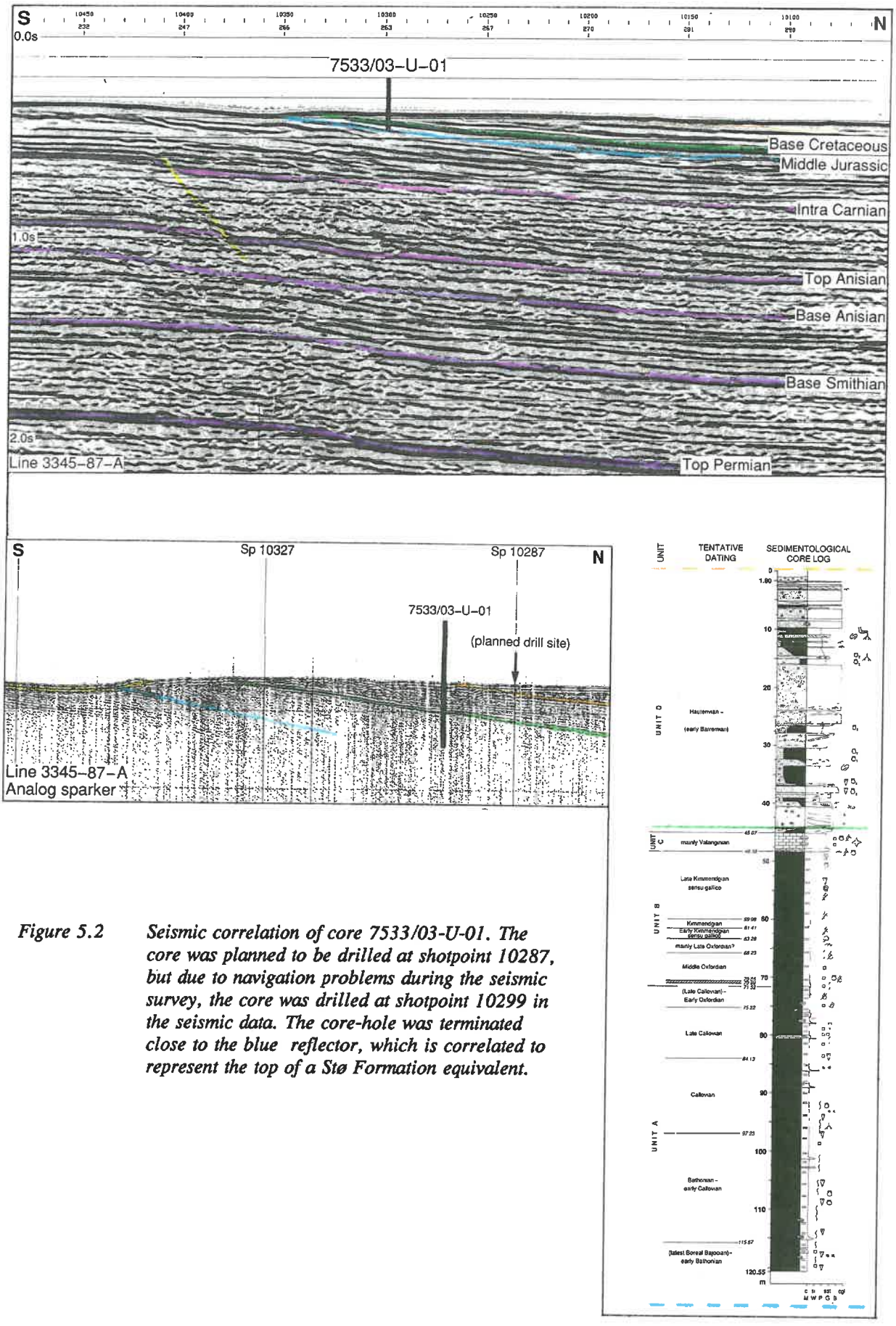

Figure 5.2 *Seismic correlation of core 7533/03-U-01. The core was planned to be drilled at shotpoint 10287, but due to navigation problems during the seismic survey, the core was drilled at shotpoint 10299 in the seismic data. The core-hole was terminated close to the blue reflector, which is correlated to represent the top of a Stø Formation equivalent.*

unit seems to be about 33 ms thick. Using the sound velocity measured on the core, this corresponds to approximately 44 m, which is also the depth down to the limestone. This implies that the core probably was drilled close to the truncation point of the reflector representing the top of the limestone. We may therefore conclude that the seismic line at this locality should be moved about 300 m (12 shotpoints) to the north.

5.3 Sedimentology

At site 7533/03-U-01 totally 118.75 m of bedrock was drilled between 1.8 m and 120.55 m below seabed. The drilled interval has been divided into four lithological units (Figure 5.1). Unit A (120.55 - 71.52 m) is dominated by shale with some silt, Unit B (71.52 - 48.38 m) contains dark grey shale, Unit C is a 3.3 m thick layer of nodular, marly limestone and Unit D consists of alternating sandstones and siltstones.

Unit A (120.55 m (TD) - 71.52 m)

Unit A consists of brownish to medium grey, weakly laminated shales and claystones with occasional thin interbeds of siltstone (Figure 5.3A).

Siderite beds or nodules are occasionally seen throughout the interval. Pyrite appears as smaller concretions (1-2 cm) and also associated with burrows in the lowermost and upper part of the unit. Glauconite occurs as scattered silt to fine sand grains and also as concentrations in the sediment.

A 44 cm thick marly limestone with patchy pyrite and calcite filled fractures, occurs close to the top of the unit.

Small scale, mainly horizontal bioturbation, dominated by *Planolites* sp., appears with a low (to moderate) bioturbation grade. Possible *Chondrites* sp. are also observed (96.27 m).

Macrofossils occur throughout the unit. Belemnites dominate, but also ammonites and bivalves occur.

Kerogens are characterized by an abundance of marine microplankton throughout this interval (Figure 5.1). From 120.0 m to 87.19 m, the number of bisaccate sporomorphs show an increasing trend, whereas marine amorphous material shows a slight decrease. From 87.19 m to the interval top (72.37 m), the marine microplankton component dominates, while amorphous and bisaccate components are virtually nonexistent.

Paleoenvironment

The macrofossil assemblage is dominated by pelagic forms and demonstrates a clear marine environmental setting for the sediment. Absence of features indicating high energy environments, suggests that sedimentation took place in open shelf environments. The palynofacies study indicates a transgressive phase in an outer shelf depositional environment. From 120.0 m to 87.19 m, sea floor conditions were slightly anoxic with very low depositional energies. This is indicated by the large fraction of amorphous material and bisaccate pollen. Above 87.19 m, depositional energy was higher (bisaccates disappear), and bottom water was more oxic (amorphous material disappears). The total dominance of marine microplankton at 77.15 m may indicate either an increase in surface water organic productivity, or simply a decrease in terrestrial organic input as a result of shifting hydrography at sea level maximum.

Unit B (71.52 - 48.38 m)

Unit B consists of medium dark grey to dark grey (to black) laminated claystones (Figure 5.3B). The organic content increases rapidly upwards through a relatively thin transitional zone (71.52-63.80 m), which is reflected in a change to high gamma ray readings (Figure 5.1).

The transition from Unit A to Unit B is very gradational and vague. The boundary is drawn on the basis of a slight increase in silt content and a colour change from medium grey to medium dark grey shale. Unspecified horizontal and vertical bioturbation occurs in the uppermost 10 centimetres of Unit A, and belemnites are found on the bedding plane where we have defined the boundary. An interval with oscillations in palynofacies starts around the base of the unit.

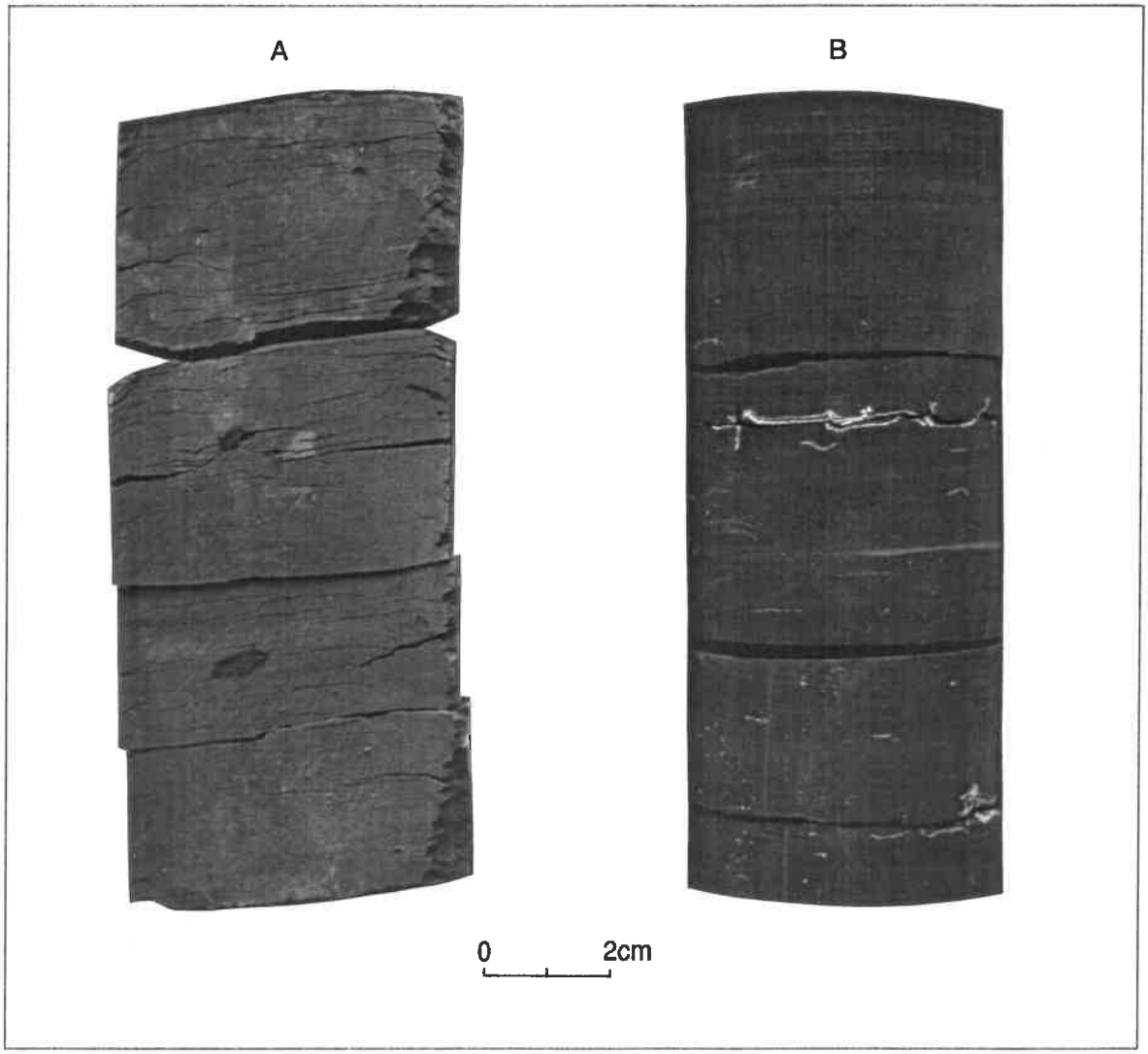

Figure 5.3 *Photograph of core 7533/03-U-01.*
A. Brownish grey claystone from Unit A.
B. Dark grey organic rich claystone from Unit B.

Some activity of unspecified bioturbation is observed in the lower part of the unit. Shell fragments occur scatteredly throughout the unit, but are most numerous in the darkest part. Numerous, more complete specimens of ammonites and bivalves have also been found.

Paleoenvironment

The lack of sediment coarser than clay, and absence of wave generated sedimentological structures, suggest an open shelf depositional environment. This interpretation is supported by the marine macrofossil assemblage. The low degree and absence of bioturbation together with the palynofacies discussion

below, indicate restricted bottom water conditions.

The depositional environment for this unit is therefore thought to be a dysoxic shelf. Kerogens in the lowermost 7 metres are characterized by rapid palynofacies oscillations showing large variations in marine and terrestrial components. This pattern of rapid shifts in kerogen content is indicative of large variations in depositional energies prior to the onset of organic rich claystone deposition.

Kerogens throughout the interval 64.75 - 48.64 m are characterized by total dominance of marine amorphous material. Marine microplankton, bisaccates, non-saccates, and the remaining terrestrial components make up only a very small fraction of the total kerogen content. This is characteristic for what many workers think is a poorly ventilated, marine depositional environment with anoxic bottom waters and relatively high organic productivity in surface water masses. Nevertheless a bottom fauna is present at numerous levels. Terrestrial input of organic material was also extensive, as shown by relatively large amounts of degraded plant material incorporated into the amorphous kerogen.

Unit C (48.38 - 45.07 m)

The laminated, dark grey, organic rich claystones are overlain by a basal 13 cm thick, greenish grey, mottled mudstone rich in shell fragments. The boundary is sharp. Above this bed, the unit consists of a distinctive greenish grey, nodular and fossiliferous marly limestone (Figure 5.4A). These skeletal grainstones and packstones (to wackestones) are sometimes intermixed with thin, green mudstones rich in shell fragments. Near the top of this unit the siliciclastic content increases slightly.

The nodular appearance may be a result of early diagenetic processes.

Bivalve fragments contribute to most of the macrofauna, the rest consists of ostracods, echinoderms including crinoids and bryozoans. Some micritized foraminifera are also present (Figure 5.4B).

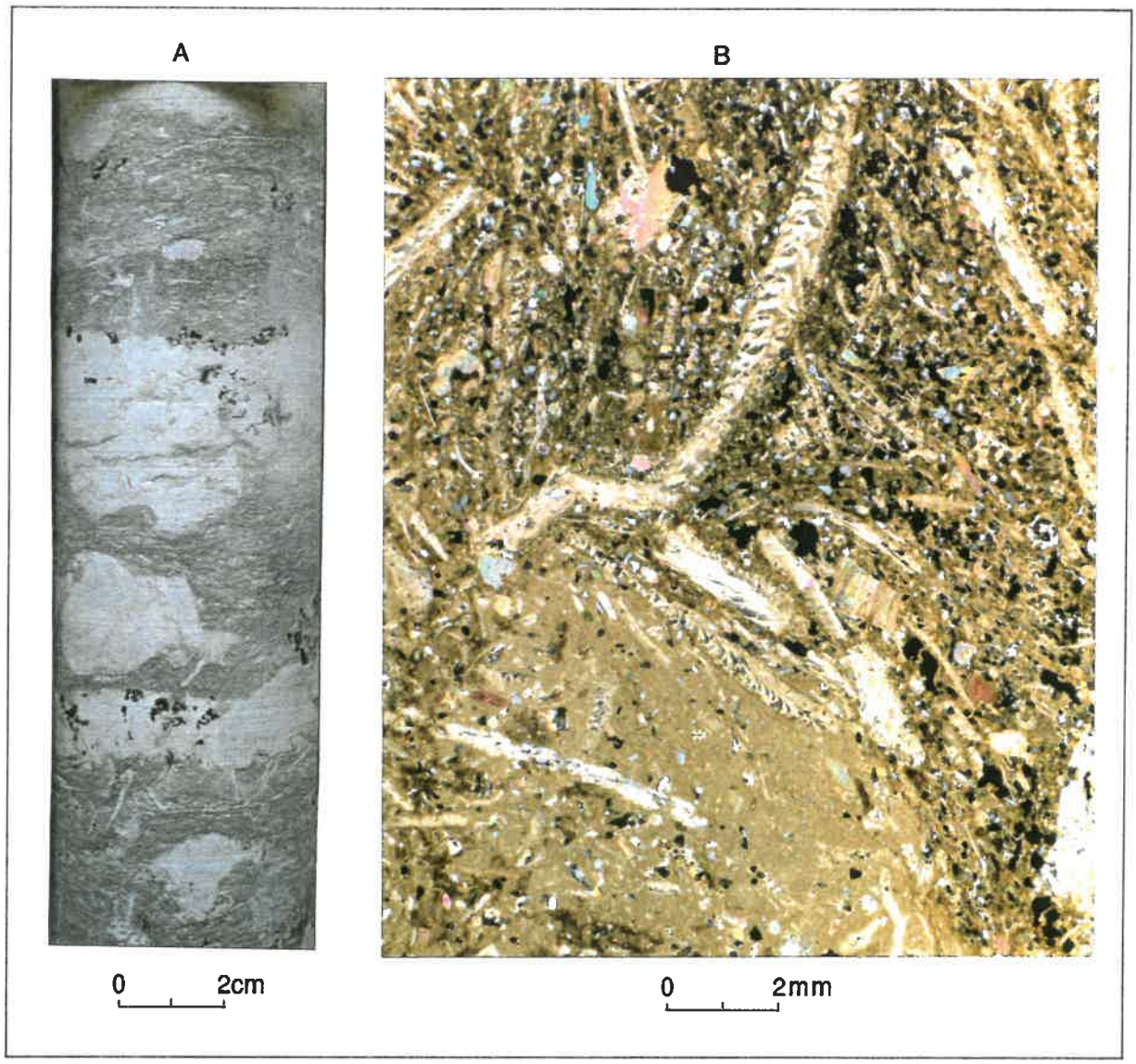

Figure 5.4 *Unit C of core 7533/03-U-01.*
A. Photograph of the nodular, marly limestone.
B. Thin section photograph showing frequent occurrence of Inoceramus debris.

Paleoenvironment

Unit C represents a condensed interval and there is a significant hiatus at the base of the unit. The relatively high diversity fossil assemblage, together with a largely devoid of terrigenous clastics, indicate an open marine shelf environment. The bioclastic grainstone intermixed with thin mudstone beds in the lower part of the unit, suggests shallow turbulent environment, interpreted to represent periodical storm deposits. The lack of reefs (seismic interpretation) provide the main evidence for an open shelf environment.

This nodular Valanginian marly limestone has a regional distribution (seen in

several wells and IKU-cores) and correlates to similar condensed intervals in the North Sea and the Barents Sea areas. A Valanginian calcareous nannofossil association with a comparable lithology is reported by Verdenius (1978) from Kong Karls Land. The unit may have been deposited at a very low sedimentation rate in a well oxygenated shelf setting.

Unit D

The boundary to the below Unit C is sharp with transition from packstone to greenish grey, sandy siltstone. The upper boundary of Unit D was not penetrated in this hole, but apparently only a few metres are missing (cfr. Section 5.2). Based on the presence of two different lithologies, Unit D is subdivided into two main lithofacies (lithofacies D1 and D2) which intermix throughout the unit.

Lithofacies D1

This facies consists of reddish brown and greyish green, sandy siltstones with variable amounts of fossil fragments (Figure 5.5). The boundaries between the two siltstones are sharp and probably caused by syndepositional/early diagenetic processes. The base and top of this facies are always greyish green (20-50 cm thick), so that the reddish brown siltstones in the middle are always surrounded by the greyish green rock.

The matrix supported shell debris shows an isotropic fabric. *Inoceramus* fragments are the main constituent, together with sporadic echinoderm debris.

The sand content in the sediment is in general 20 to 40 percent, and the grain size is generally very fine to fine with an angular to subangular texture.

The glauconite content is variable, but generally relatively high (Table 5.1). A few intraformational lithoclasts (0.1- 0.5x1-2cm), and occasional wood fragments are observed. Calcite cementation is moderate and generally has a patchy appearance.

No bioturbation is observed.

Mineralogy has been analysed by X-ray powder diffraction (Table 5.1) and on thin sections (Figure 5.5). A main purpose was to investigate whether any mineralogical changes exist between the reddish brown and the greenish grey sediment that could reflect two different source areas.

There are some minor mineralogical variations within both different coloured sediments (Figure 5.5), but none of them could be ascribed to different source areas.

Table 5.1 *Mineralogical whole rock compositions of samples from core 7533/03-U-01 (semi-quantitative wt%). No dolomite nor pyrite were recorded. (Tr - trace).*

Depth (m)	Sm	Mix	M/I/G	Chl	Kao	Qtz	Kfl	Pl	Cal	Sid	Pho
6.00	-	5	54	2	7	24	4	3	1	-	-
10.20	1	5	54	1	8	24	4	2	1	-	-
11.70	tr	6	45	1	13	25	3	5	2	-	-
13.05	-	-	18	1	8	23	2	3	4	41	-
13.30	-	-	1	1	2	50	7	17	22	-	-
26.00	-	-	1	-	3	79	8	4	5	-	-
26.70	-	9	36	1	13	20	2	7	4	8	-
27.30	-	12	40	1	10	23	1	8	5	-	-
30.00	-	-	-	tr	2	59	8	10	21	-	-
30.50	-	-	43	-	9	21	8	10	6	3	-
30.70	-	6	31	1	7	28	2	9	14	2	-
32.00	-	1	5	-	-	64	4	9	17	tr	-
32.90	-	-	-	tr	5	65	4	9	17	-	-
33.60	tr	8	37	tr	13	18	3	5	14	2	-
34.00	-	6	30	-	10	29	2	4	17	-	2
44.64	-	7	7	1	9	38	4	6	28	-	-
48.62	1	19	13	2	6	30	2	2	25	-	-

Lithofacies D2

Lithofacies D2 is subdivided into D2a (ripple laminated sandstones) and D2b (massive sandstones) (Figure 5.5).

Lithofacies D2a

Lithofacies D2a comprises light grey, very fine- to fine-grained subangular to rounded sandstones consisting of 30 cm to 1 m normally to inversely graded layers. Layer boundaries are occasionally erosive.

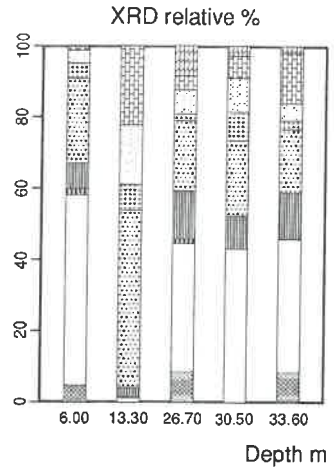

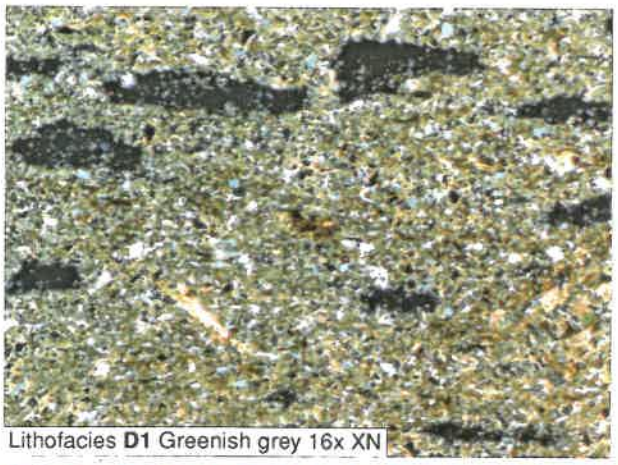
Lithofacies **D1** Greenish grey 16x XN

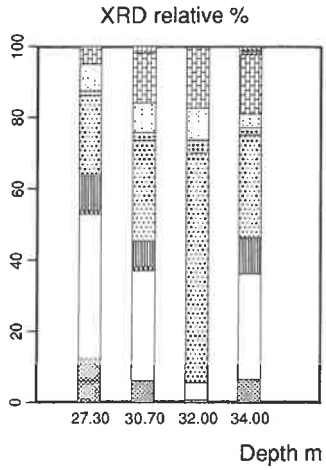

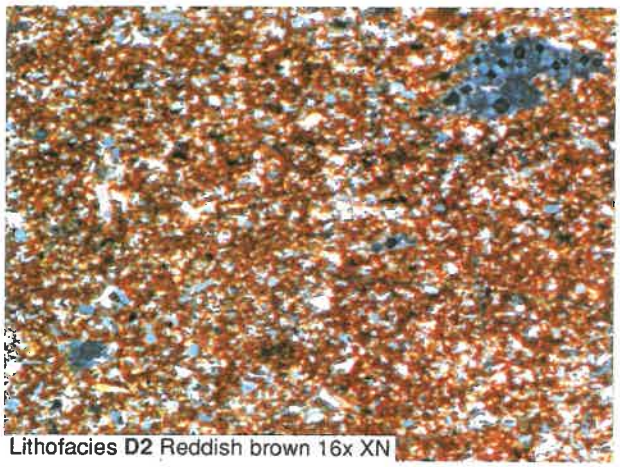
Lithofacies **D2** Reddish brown 16x XN

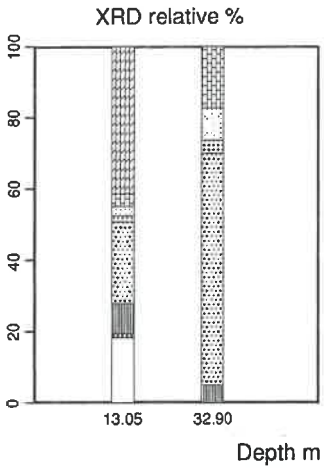


Lithofacies **D2a** 45x NL

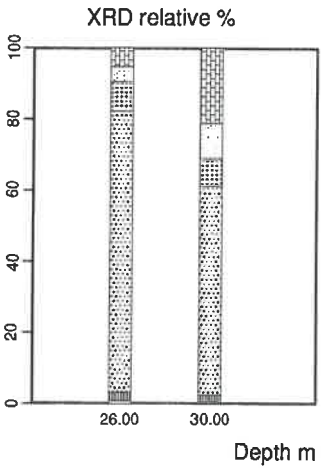


Lithofacies **D2b** 45x NL

Sedimentary structures are predominantly current generated. Unidirectional climbing ripples (Figure 5.8) and different dewatering structures dominate this facies. Small scale current ripples and sporadic vague plan parallel and tabular low-angle cross-stratification occur in some beds.

Scattered glauconites and wood fragments occur.

A few thin intervals, which are darker in colour due to mud admixture, show bioturbation and sometimes soft sedimentary deformation structures.

The degree of calcite cementation varies. Some intervals, often in contact with lithofacies D1, are quite strongly affected.

Lithofacies D2b

Lithofacies D2b consists of well sorted, light grey sandstones with abrupt lower boundaries. The subangular to rounded grains range in size from fine to medium sand.

The sandstones are predominantly massive, homogeneous, ungraded and generally coarser grained than the associated sandstones of lithofacies D2a. Nevertheless a few intervals with different low angle cross stratification (tangential contacts are observed) and planar parallel laminae occur.

Near the top of the unit a 4 cm thick, dark grey, silty claystone separates sandstone beds.

Some glauconite, wood fragments and siderite concretions are observed.

Lithofacies D2b is very porous (Figure 5.5). Calcite cementation is only occasionally observed near the top or base.

The mineralogical composition has been examined by use of thin sections and X-ray powder diffraction (Figure 5.5 and Table 5.1). Lithofacies D2a and D2b are both quartz dominated. The porosity has been slightly reduced by autigen syntaxial silica sement, growing in optical continuity with the quartz grain. The feldspar occurrence is minor, however, fresh and partly to fully dissolved feldspars occurs.

The mineralogical variation is minor, and can mainly be ascribed to different amount of illite/mica and carbonate cement.

Bioturbation is absent.

Paleoenvironment Unit D

Unit D reflects a bimodal association of rhytmically interchanging sediments. The rapid lithofacies alternation indicates derivation from two clearly different provenances, possibly entering the basin from slightly different directions.

Lithofacies D1

This texturally and mineralogically immature and poorly sorted sediment of lithofacies D1 indicates a depositional environment with a poor sorting mechanism. The reddish brown colour of the sediment may suggest a weathering product from a subaerial environment. A fully marine fauna and flora points to a submarine setting.

The fossil fragments may be derived from a shallow marine subsurface during erosion processes of bypassing continental sandy silt sediments. Alternatively, a relative fall in sea level may have caused exposure (red colour), and an "in situ" sediment was transported as mass flow systems out into (relatively) deeper waters.

There is no evidence of current activity or bioturbation. On the basis of isotropic fabric and lack of stratification and sedimentary structures, debris flow and mud flow systems activated from some kind of catastrophic event are most plausible for this sediment.

The immaturity of the sediment is evidence of rapid upheaval and erosion, consequently a short distance to the source terrain is likely. Nevertheless, a gradient is strictly necessary to induce avalanching, and a slope was probably most pronounced during a sea level lowstand or beginning of a transgression.

XRD-analyses (Figure 5.5) give no indications of different source areas for the two differently coloured siltstones, and texturally and mineralogically these are similar. The colour changes to greyish green near the top and bottom

of this lithofacies, may be as a result of late reducing processes near the sediment surface.

Lithofacies D2

Unidirectional climbing ripples in association with soft sedimentary deformational and dewatering structures, indicate rapid deposition of a liquefied sediment. This is supported by absent (lithofacies D2b) to scarce bioturbation (lithofacies D2a).

The homogeneous sediment and the unidirectional appearance of ripples throughout the unit support derivation from the same source.

The sandstones may have been emplaced by high density turbidity currents on depositional lobes fronting a prograding delta front. High frequency mass flow deposits show the importance of sediment remobilization and redeposition from shallow to deep water.

These high density turbidites were probably deposited in water depths well below storm wave base in what were normally muddy environments.

Biostratigraphic analyses show that much of the microplankton is reworked from Jurassic sediments (Section 5.4). This is in good agreement with the assumption that the unit includes turbidites and gravity flow deposits.

For further discussion, see Section 6.2.

Glaciotectonic influence (see Section 3.3) has been observed down to 15.6 m. The lowermost zone is 30 cm thick. Except for glacially deformed sandstone at approximately 8 metres below seabed, all deformed zones are in siltstone. The sediment above the defined base of Quaternary at 1.8 m is classified as a glacitectonite.

5.4 Biostratigraphy

The Jurassic part of core 7533/03-U-01 (120.55 - 48.38 m) has been analysed for ammonites (Figure 5.6) and palynomorphs (Figure 5.7). The Cretaceous part of the core (48.38 - 1.8 m) has been analysed for foraminifera, palynomorphs (Figure 5.7) and calcareous nannoplankton. Arenaceous species are dominant

(95-99%) in the foraminifera assemblages except in a sample from 46.15 m. Selected specimens are illustrated (Figures 5.8 and 5.9).

A latest Boreal Bajocian - early Bathonian age is suggested for the interval 120.55 - 115.67 based on the ammonites *Cranocephalites* cf. *pompeckji* at 117.24 m, and *Arctocephalites* at 115.67 m together with occurrence of the dinoflagellate cyst *Sirmiodinium grossi*.

The overlying strata up to 97.23 m are assigned a Bathonian - early Callovian age. Ammonites between 99.42 m and 90.0 m point to a pre Late Callovian age, while the Upper Callovian seems to have been reached at 84.13 m continuing at least up to 75.22 m. A latest Early Oxfordian ammonite has been found at 70.99 m. An earliest Middle Oxfordian ammonite fauna is recorded between 70.85 m and 68.56 m.

A Middle Oxfordian age is favoured up to 66.23 m. If present, the Upper Oxfordian substage is located somewhere between 66.23 m and 63.28 m.

An Early Kimmeridgian ammonite is found at 63.28 m, and the Lower Kimmeridgian can be extended up to 61.41 m on ammonite evidence. Late Kimmeridgian ammonites appear at 59.98 m and ammonites from the middle part of this substage have been found up to 9 cm below the top of the black shale.

The limestone interval is assigned a Valanginian age based on combined foraminifera and calcareous nannoplankton evidence, whereas foraminifera and dinoflagellate cysts are the stratigraphically significant fossil groups in the Hauterivian sandy beds above. Middle Hauterivian or younger strata have been reached at 37.90 m, and the uppermost part of the core may be as young as early Barremian.

Unit A (120.55 m (TD) - 71.52 m), latest Boreal Bajocian - Callovian

75.22 - 71.52 m:	Upper Callovian - Lower Oxfordian
84.13 - 75.22 m:	Upper Callovian
97.23 - 84.13 m:	Callovian
115.67 - 97.23 m:	Bathonian - lower Callovian
120.55 - 115.67 m:	(uppermost Boreal Bajocian) - lower Bathonian

The lowermost ammonite in the core, from 117.24 m, is a specimen determined as *Cranocephalites* cf. *pompeckji* indicative of the uppermost Boreal Bajocian in the scheme of Callomon (1985, text-fig. 3). But due to extreme provincialism in Aalenian - Lower Callovian ammonite faunas, correlation of the Boreal *Cranocephalites* faunas is problematic, and Poulton (1987) suggested a Lower Boreal Bathonian age for these.

A representative of the ammonite genus *Arctocephalites* occurs at 115.67 m. The age of this is also debatable, opinions ranging from Lower to Middle Bathonian.

Poorly preserved ammonites are present in the interval 99.42-90.00 m with *Kepplerites (?Toricellites)* sp. at 99.42 m, *Pseudocadoceras* sensu lato including *Costacadoceras* at 94.60 m and *?Pseudocadoceras* sensu lato at 90.00 m. These records indicate a Middle Bathonian - (?Early) Callovian age for the beds in question.

Although the lower part of this interval contains relatively diverse dinoflagellate cyst assemblages dominated by *Parvocysta bjaerkei* and *Escharisphaeridia* spp., evidence for precise age assignation has not been found. *Sirmiodinium grossii* occurs consistently suggesting an age no older than Bathonian at the base of the core according to published information from West Europe. But *S. grossii* is a long-ranging species, and Bathonian markers have not been found. Distinguishing between Bathonian and Callovian strata on the basis of dinoflagellate cysts seems to be difficult in the area, but the appearance of *Chytroeisphaeridia cerastes* at 97.23 m may favour a Callovian age at least from this level. The first observed specimens of *Liesbergia scarburghensis* at 84.13 m point to a Late Callovian age for these beds. This is supported by acme occurrences of *L. scarburghensis* and *Mendicodinium groenlandicum* at 77.15 m in kerogens dominated by dinoflagellate cysts. Blooms of *L. scarburghensis* are also known from the Lower Oxfordian.

A specimen of the Late Callovian ammonite *Longaeviceras* cf. *longaevum* has been recorded at 75.22 m.

IKU SINTEF GRUPPEN

Unit B (71.52 - 48.38 m), Late Callovian - Kimmeridgian sensu gallico

59.98 - 48.38 m:	Kimmeridigan sensu gallico
63.28 - 61.41 m:	Lower Kimmeridgian sensu gallico
66.23 - 63.28 m:	mainly Upper Oxfordian?
70.85 - 66.23 m:	Middle Oxfordian
71.52 - 70.99 m:	(Upper Callovian) - Lower Oxfordian

The Lower Oxfordian is thin since the upper part of the *C. cordatum* Zone (*C. cordatum* Subzone) is located at 70.99 m due to the presence of a specimen of *Cardioceras* (*Cardioceras*) cf. *cordatum* at this level.

The ammonites *Cardioceras* (*Plasmatoceras*) *tenuistriatum* and *C.* (*P.*) *tenuicostatum* occur in the interval 70.85 - 70.37 m indicative of the lowermost Middle Oxfordian *C. densiplicatum* ammonite Zone (Sykes & Callomon 1979). Late forms of *Cardioceras* (*Cardioceras*) that have transitional features to the subgenus *Maltoniceras* are present at 68.88 m and 68.56 m. They are still indicative of the *C. densiplicatum* Zone and are the youngest Oxfordian ammonites found in the core.

The uppermost record of the dinoflagellate cyst *Liesbergia scarburhensis* at 66.23 m is evidence for extending the Middle Oxfordian interval at least up to this level. Some other last occurrences have also been noted in these strata or in the uppermost part of the unit below: *Stephanelytron redcliffense* (72.37 m), *Nannoceratopsis pellucida* (72.17 m), *Chytroeisphaeridia cerastes* (70.03 m), *Scriniodinium galeritum* (66.23 m), and *Scriniodinium crystallinum* (64.75 m). Most of these taxa range up into the lowermost Kimmeridgian. In these strata sieved kerogens show an upward decrease in marine microplankton and an increase in marine amorphous material. The dinoflagellate cyst assemblages are dominated by *Sirmiodinium grossii* and *Rhynchodiniopsis cladophora*.

We have no paleontological data showing that the Upper Oxfordian is represented in the core. Obvious sedimentological evidence for break in sedimentation is not observed, but rapid oscillations take place in kerogen content in these beds. Most likely the substage is represented, but it is less than 2.95 m thick since poorly preserved ammonites of the family Aulacostephanidae belonging to the genus *Rasenia* or *Pictonia* (but not to *Ringsteadia*), indicative of the Lower Kimmeridgian sensu gallico occur at 63.28 m.

All the younger ammonites found between 63.28 m and 48.47 m are indicative of the Kimmeridgian sensu gallico. An older assemblage represents *Amoeboceras* (*Amoebites*) ex gr. *A. subkitchini* from 62.66 m and *A. subkitchini* (Birkelund & Callomon 1985, Wierzbowski 1989), which generally correspond to lower and middle parts of the *R. cymodoce* Zone in the Subboreal subdivision of the stage. It is in good agreement with occurrence at 61.60 m and 61.41 m of *Rasenia* ex gr. *R. evoluta* pointing to the upper part of the *R. cymodoce* Zone.

The profuse occurrence of ammonites of the genus *Xenostephanus* between 59.98 m and 58.65 m indicates generally the *A. mutabilis* Zone of the Subboreal subdivision of the Kimmeridgian (Birkelund et al. 1983, Mesezhnikov 1984, Wierzbowski 1989). Then, there appear younger assemblages composed of *Amoeboceras* (*Amoebites*) *elegans* and *Amoeboceras* (*Hoplocardioceras*) *decipiens* between 57.66 m and 48.47 m. The assemblage generally represents the *A. elegans* - *A. decipiens* horizon which may be correlated with some parts of the *A. eudoxus* Zone of the Subboreal subdivision (Wierzbowski 1989, Wierzbowski & Århus 1990).

The dinoflagellate cyst recovery from this Kimmeridgian part of the succession does not add much stratigraphic information. *Sirmiodinium grossii* dominates assemblages in the lower part of the stage, whereas the upper part shows influxes of *Cribroperidinium* spp. at 53.95 m, spheromorph clusters and abundant *Acanthaulax* sp. at 50.69 m, and *Pterospermella* spp. and leiospheres at 48.64 m. *Gonyaulacysta jurassica* occurs to the top of the unit, consistent with evidence from other Barents Sea cores and Spitsbergen where also *Cribroperidinium* spp. and *Acanthaulax* sp. appear and *Tubotuberella apatela* reappears in the upper or uppermost part of the Kimmeridgian sensu gallico.

Unit C (48.38 - 45.07 m), mainly Valanginian

Calcareous nannoplankton has been recorded in some marl samples from this thin interval. Biostratigraphic significant taxa have only been found in a sample from 47.18 m, that contains a rich, but low diversity nannoflora dominated by *Ellipsagelosphaera britannica*. *Crucibiscutum salebrosum* is common. The co-occurrence of *Rucinolithus* (8 rays), *Micrantholithus brevis* and of calcite wedges (*Triquetrorhabdulus? shetlandensis* Perch-Nielsen 1988) is suggestive of the Valanginian. In our experience *Rucinolithus* (8 rays) occurs only in the Lower Valanginian. The flora in the other samples is virtually restricted to the long-ranging species *Ellipsagelosphaera britannica* which also has a wide environmental tolerance.

Several foraminifera species used as markers in the North Sea (King et al. 1989), Haltenbanken area and the Barents Sea (internal reports) occur in the section. As the distribution of many of these species is supposed to be environmentally controlled, the stratigraphic range given may vary slightly in different regions and publications.

The foraminifera fauna in the lower part of the unit is characterized by abundance of *Recurvoides*, *Trochammina*, *Textularia*, *Reophax* cf. *minuta* and *Bigenerina gracilis*.

A "carbonate foraminiferal biofacies" occurs in this unit, with abundance of *Trocholina infragranulata*, *Trocholina* spp., *Patellina*, *Spirillina* and *Marssonella subtrochus* in the upper part of the interval. *T. infragranulata* is originally described from the Hauterivian (Noth 1951), but is used as a Valanginian marker in the North Sea (King et al. 1989).

The fauna in the limestone interval needs further elaboration. This would probably result in a more refined biostratigraphic resolution than was possible for this study. A middle to outer shelf facies is indicated, based on the assemblages from the upper part of the unit, if in situ.

Unit D (45.07 - 1.8 m), Hauterivian - (early Barremian)

Age diagnostic species of dinoflagellate cysts are few in the lower part of the unit, which is dominated by the *Oligosphaeridium complex* group and *Sirmiodinium grossii*. *Rhynchodiniopsis aptiana* is recorded from 44.53 m and upwards. This species occurs in the upper part of the Valanginian and lower part of the Hauterivian in Spitsbergen (middle part of the Rurikfjellet Formation), but its absence in the upper part of the Rurikfjellet Formation is probably due to the more marginal marine facies. *R. aptiana* is well known from the Barremian of western Europe as *Gonyaulacysta cladophora* sensu Duxbury, *Gonyaulacysta/Rhynchodiniopsis fimbriata* or *Gonyaulacysta anglese*. The Valanginian of Spitsbergen is relatively easily recognized on the basis of the occurrence of a number of characteristic species. These are missing in the present core and thus a Hauterivian age is most likely from the base of the unit.

Chlamydophorella trabeculosa appears at 37.90 m indicating that middle Hauterivian or younger strata have been reached. *Muderongia simplex* is present in the same sample and occurs quite consistently up to 12.46 m. It is disputed if this species ranges above the Hauterivian.

Last occurrences of *Aprobolocysta eilema*, *Oligosphaeridium abaculum* and *Nelchinopsis kostromiensis* have been noted at 9.57 m, 6.05 m and 3.25 m, respectively. *A. eilema* and *N. kostromiensis* were originally described from the Hauterivian, *O. abaculum* from the Barremian. The ranges of *N. kostromiensis* and *Pseudoceratium anaphrissum* are slightly overlapping in the Barents Sea. Although *A. anaphrissa* has only been recorded in the Quaternary rubble at 0.63 m, it cannot be excluded that at least parts of the present unit may be as young as early Barremian in age.

The interval between 45 m and 30 m contains foraminiferal zonal markers used in the North Sea (King et al. 1989). Abundant specimens of *Falsogaudryinella moesiana* and *Marssonella kummi* indicate a Hauterivian age, but are also reported to occur in older and younger strata. The range at this latitude may be somewhat different from the North Sea area. Compared to the strata above a less restricted environment is expected, a deep-water "outer sublittoral-upper bathyal" biofacies. Calcareous foraminifera occur sporadically in the zone.

The foraminiferal assemblages from the beds above about 30 m are characterized by long-ranging species with ecological rather than biostratigraphic significance. These foraminiferal assemblages, dominated by noncalcareous agglutinating foraminifera, are described as "restricted basin" biofacies (King et al. 1989). *Haplophragmium aequale* indicates a late Hauterivian - Barremian age. *Rhabdammina*, *Ammodiscus*, *Glomospira*, *Haplophragmoides*, *Trochammina*, *Textularia* and *Verneuilinoides* are the dominant genera. These arenaceous assemblages have a high resistance for unfavourable conditions (salinity/pH changes, reducing bottom conditions and high turbidity).

A considerable amount of Upper Callovian-Lower Oxfordian reworked palynomorphs is present in this Hauterivian-lower Barremian succession. Samples at 44.53 m, 27.65 m, 6.05 m and 3.25 m contain such elements. At several other levels reworked dinoflagellate cysts and foraminifera of taxa with longer Jurassic ranges occur.

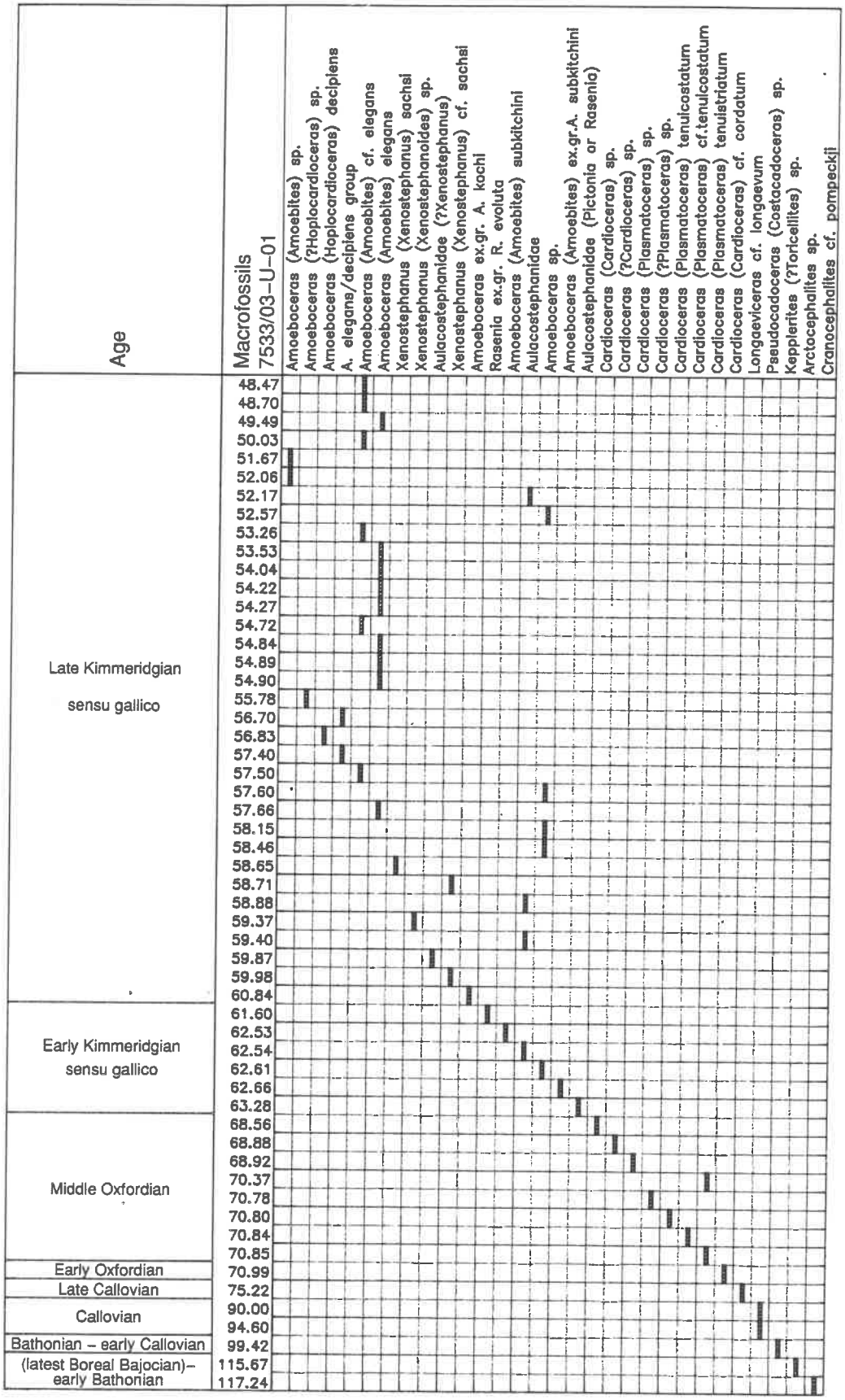

Figure 5.6 *Range-chart of macrofossils recorded in core 7533/03-U-01 sorted according to earliest occurrence.*

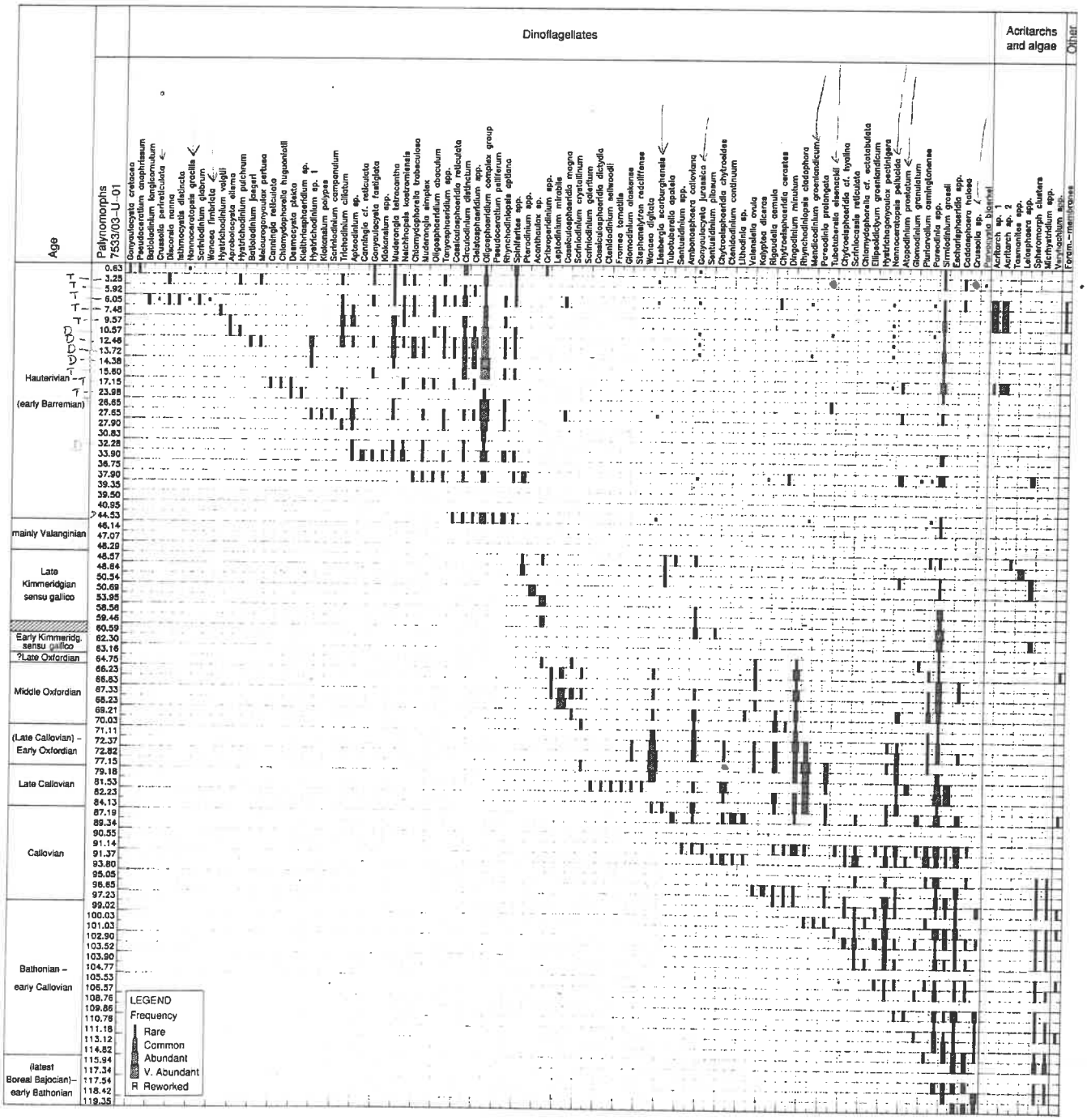

Figure 5.7 *Range-chart of palynomorphs recorded in core 7533/03-U-01 sorted according to earliest occurrence.*

Figure 5.8 *Selected acritarchs and dinoflagellate cysts from core 7533/03-U-01. Taxon name and author are followed by sample depth and reference to England Finder.*

1. *Acritarch* sp. 1
   Sample 6.05 m, U22/2
2-4. *Acritarch* sp. 1
   Sample 7.48 m, R21/2
   2: high focus
   3: focused in section, showing flange along the perimeter.
   4: low focus showing round pylome.
5. *Acritarch* sp. 1
   Sample 7.48 m, U36/1
   Strongly ornamented morphotype with extended peripheral flange.
6,7. *Acritarch* sp. 2
   Sample 7.48 m
   6: high focus showing smooth wall.
   7: low focus showing round pylome and rupture in vesicle wall.
8,9. *Aprobolocysta eilema* Duxbury 1977
   Sample 9.57 m, T14/3
   8: high focus showing apical archeopyle margin and granular periphragm.
   9: low focus showing lateral and antapical cavation.
10. *Oligosphaeridium abaculum* Davey 1979a
   Sample 6.05 m, 022/2
   High focus showing distinct paratabulation and granular cyst wall.
11. *Sirmidinium grossii* Alberti 1961
   Sample 6.05 m, G24/0
12. *Chlamydophorella trabeculosa* (Gocht) Davey 1978
   Sample 13.72 m, T37/1
13. *Atopodinium prostatum* Drugg 1978
   Sample 105.53 m, b:R23/3
14. *Parvocysta bjaerkei* Smelror 1987
   Sample 99.02 m, b:T19/1
15. *Chytroeisphaeridia cerastes* Davey 1979
   Sample 91.14 m, a:L16/2

Figure 5.9 *Selected dinoflagellate cysts from core 7533/03-U-01. Taxon name and author are followed by sample depth and reference to England Finder.*

1. *Liesbergia scarburghensis* (Sarjeant) Berger 1986
   Sample 72.37 m, b:P48/3
2. *Tubotuberella apatella* (Cookson & Eisenack) Ioannides et al. 1977
   Sample 50.54 m, b:X14/2
3. *Kalyptea disceras* Cookson & Eisenack 1960
   Sample 68.23 m, b:L44/4
4. *Scriniodinium crystallinum* (Deflandre) Klement 1960
   Sample 67.33 m, a:039/2
5. *Nannoceratopsis pellucida* Deflandre 1938a
   Sample 77.15 m, b:M45/1
6. *Mendicodinium groenlandicum* (Pocock & Sarjeant) Davey 1979c
   Sample 77.15 m, b:040/3
7,8. *Stephanelytron redcliffensis* Sarjeant 1961a
   7: Sample 72.37 m, a:T19/2
   8: Sample 72.82 m, b:E51/2

IKU SINTEF GRUPPEN

Core 7533/03-U-01

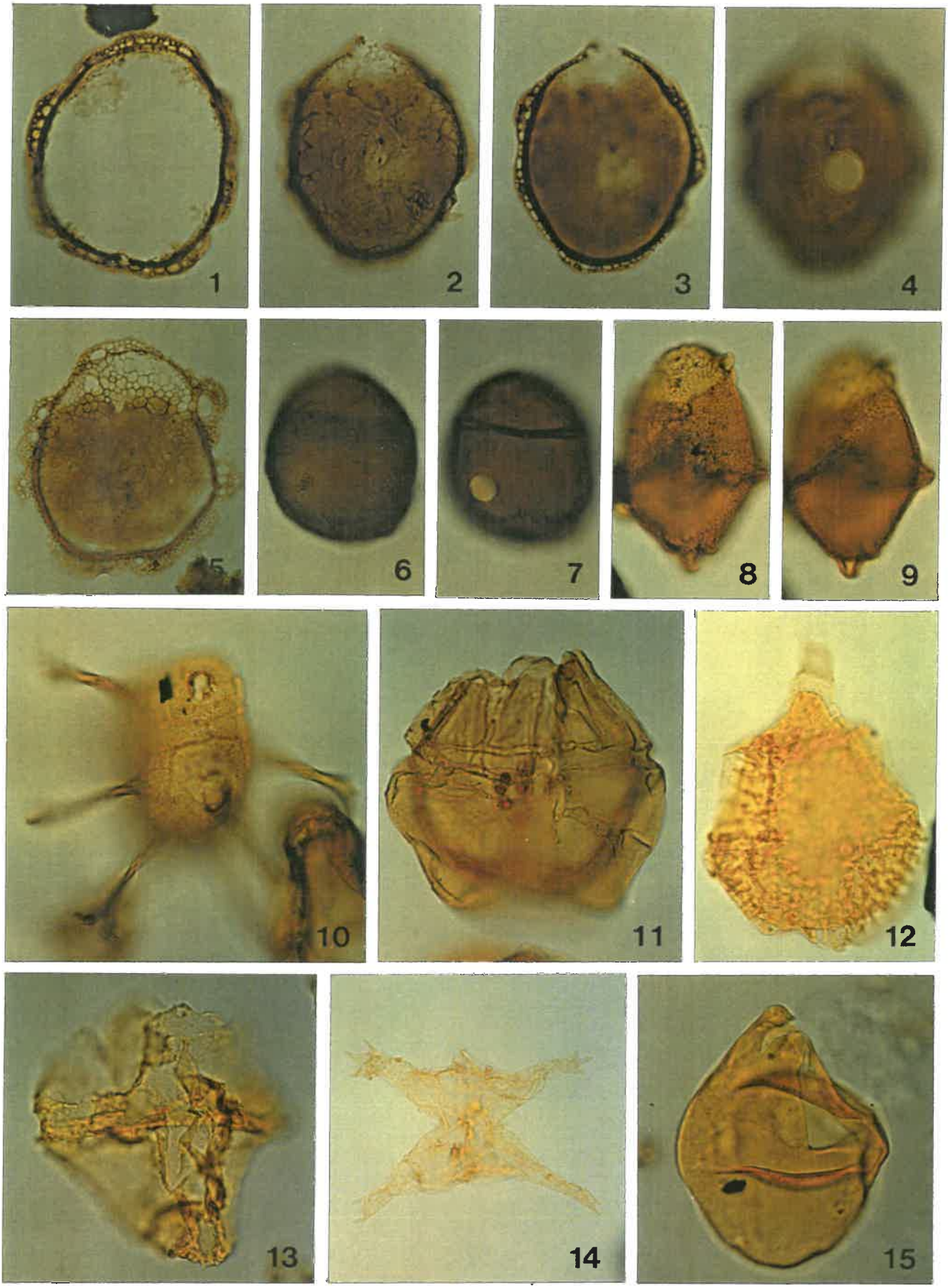

Figure 5.8

Core 7533/03–U–01

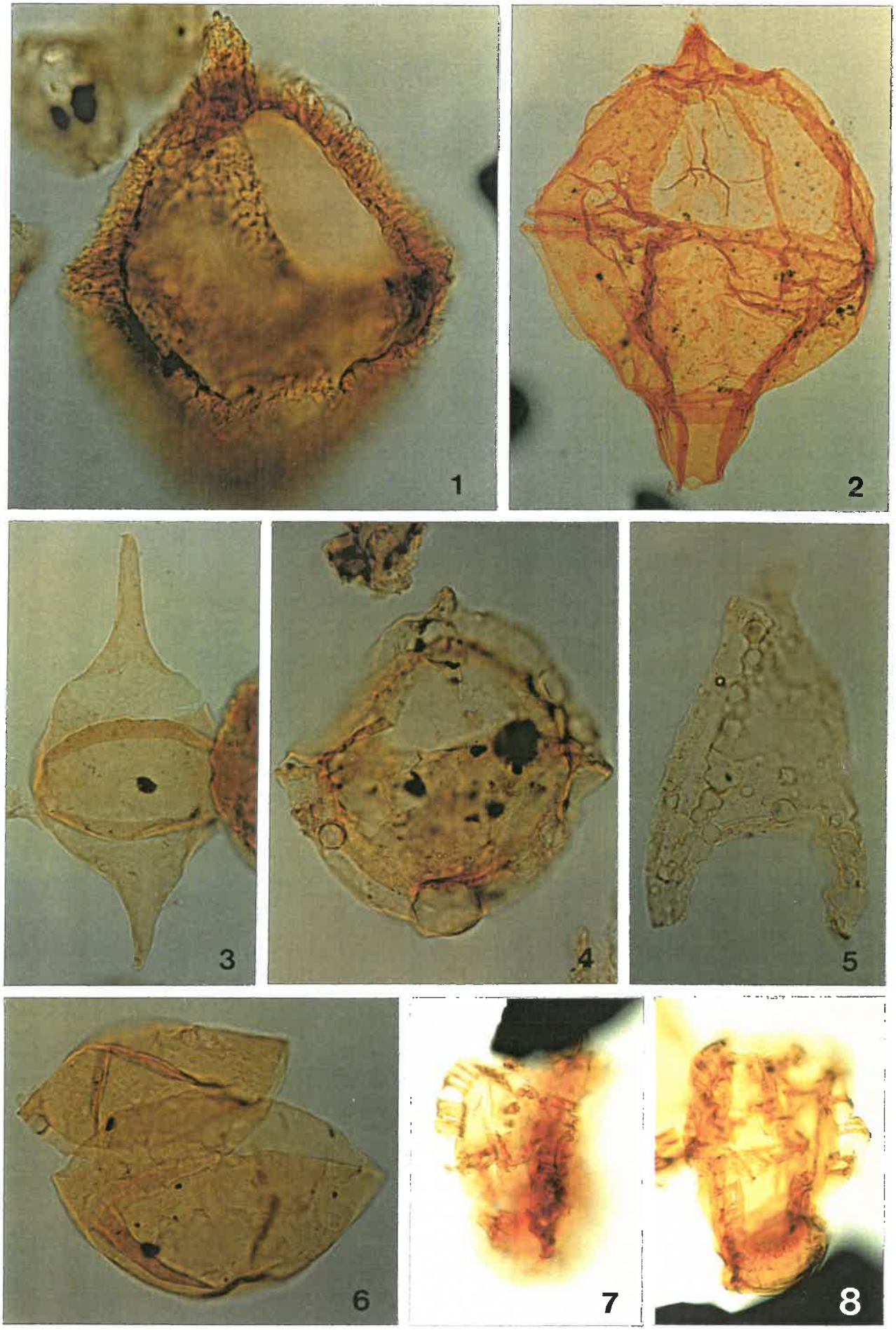

Figure 5.9

5.5 Organic Geochemistry

Unit A (120.55 m (TD) - 71.52 m)

A total of fifteen canned samples was collected from this unit, which comprises the lower half of the core. In general, methane is the main hydrocarbon present in the headspace and occluded gas fractions (Figure 5.10). This is reflected in the generally low composite gas wetness values of less than 10%, although if the occluded gas fraction is considered separately, gas wetnesses of up to 75% occur. This contrast reflects the greater mobility and preferential loss of methane from the canned core chips during storage.

The concentration of C_{5+} hydrocarbons is low and is primarily restricted to the occluded gas fraction, reflecting the lower mobility of these compounds relative to methane. The iC_4/nC_4 ratio of the headspace and occluded gas fractions shows an increase with depth away from the boundary with the overlying Upper Jurassic shales (Figure 5.10). In general, the iC4/nC4 ratios observed in this unit (<0.8) are lower than those in the overlying organic-rich shales (typically 1 and greater). This is surprising since it might be expected that the lowest values would be associated with hydrocarbon-prone organic matter. A possible explanation may lie in expulsion of early gas from the organic-rich shales down into Unit A, the most mature gases occurring adjacent to the boundary between the two units. Alternatively, the gas in Unit A may be derived from a different source to that occurring in Unit B.

It is interesting to note that the composition of the headspace/occluded gas in the lowermost sample of Unit B is more similar to that of the samples from Unit A, than that of the majority of the samples from Unit B. This may reflect the gradational nature of the boundary between these two units.

The $\delta^{13}C$ composition of the methane and ethane from two samples at 101.88 m and 82.92 m is similar to that normally associated with mature petroleum gas (Figure 5.11). A relative enrichment in the deuterium content of the methane from these samples is difficult to fully reconcile with the ^{13}C composition of the methane, and could reflect either a contribution from another source, or evidence of fractionation.

Data from a total of fifty-two samples indicate that the total organic carbon (TOC) content of the rocks in Unit A is relatively constant, with values of between 0.5 wt% and 1 wt% for the most part (Figure 5.12). Slightly more

organic-rich layers occur sporadically, e.g. 96.20-95.65 m, 82.92 m, but only the uppermost of these represents an appreciable increase in TOC content. Rock-Eval data (Figures 5.12 and 5.13) suggest that the kerogen in the unit has no appreciable potential for the generation of hydrocarbons, and can be characterized as type III to type III/IV kerogen.

The low maturation level of the kerogen is indicated by typical Tmax values of between 424°C and 434°C. Lower Tmax values of less than 410°C occur at 113.60 m and 98.73 m, where they are associated with relatively inert kerogen which yields almost nothing in the way of pyrolysate, i.e. very low S_2 peak values leading to inaccurate determination of Tmax. There is no evidence for the occurrence of appreciable amounts of non-indigenous hydrocarbons in these rocks.

Unit B (71.52 - 48.38 m)

The hydrocarbon composition of the headspace and occluded gas fractions was characterized for seven samples from the dark-coloured shales which comprise Unit B. These shales were found to have very high contents of gaseous hydrocarbons, particularly methane, as was suggested by visible evidence of gas escape when the core was collected. Gas wetness values are typically less than 2% for the combined headspace/occluded gas fractions, and are only slightly higher when the occluded gas fraction is considered separately.

There is no obvious trend in the composition or amount of gas present in the black shales themselves, although the lowermost sample from this unit, as was mentioned previously, is more similar to the samples from the underlying unit than it is to the majority of the samples from Unit B. The iC_4/nC_4 ratios obtained from these samples are mostly very high, and are consistent with thermal immaturity.

Isotopic data from two of the samples clearly suggest that the adsorbed gas collected from two samples from this unit contains contributions from both petrogenic and biogenic sources. This may explain the high methane content and very high iC_4/nC_4 ratios observed from these samples, but stands in marked contrast to the composition of the gases from the underlying organic-lean unit.

TOC and Rock-Eval data divide this unit into three intervals: a lower interval (ca 71.52-68.5 m) characterized by TOC contents of ca 2 wt% comprised of type

IV kerogen; a middle transitional interval (ca 68.5-63.5 m) with variable TOC contents of between 2 wt% and 15 wt% and hydrogen indices typical of type IV and type II/III kerogen; and an upper interval (63.5-48.38 m) characterized by high TOC contents of 10-20 wt% and hydrogen indices typical of type II to type II/III kerogen.

This sub-division of Unit B is supported by the spectral gamma data from which a lower "cold" (ca 71.52-64 m) and an upper "hot" (ca 64-48.38 m) interval can be recognized. There is no clear lithological expression of these intervals, although the lower and middle intervals tend to contain a number of lighter coloured interbeds. Horizontal velocity data show a slight decrease in the organic-rich interval, followed by a sharp increase into the calcareous rocks of the overlying unit.

Tmax values of less than 420°C in most of the organic-rich samples suggest that the kerogen in these samples is thermally immature. An increase in Tmax value to ca 430°C was observed in the previously defined lower and middle intervals of this unit, where they are associated with less hydrogen-rich kerogen types. This association between Tmax and kerogen type is widely recognized (Espitalie et al. 1986).

The high petroleum potential values and their associated hydrogen indices are similar to those reported from the Hekkingen Formation of the Tromsø and Nordkapp Basins in earlier IKU shallow drilling reports. The high values suggest that these organic-rich shales represent potentially prolific oil source rocks with increased thermal maturity.

Unit C (48.38 - 45.07 m)

One canned sample was collected from this thin calcareous unit which unconformably overlies the black shales of Unit B. Headspace and occluded gas concentrations are markedly reduced from those observed in the underlying unit, but are similar in the predominance of methane as the most abundant gaseous hydrocarbon.

The carbon isotope composition of adsorbed methane and ethane in this sample is similar to that described from Unit A, but is significantly heavier than that described from Unit B. These similarities and differences are also preserved in the deuterium composition of the methane. These observations are somewhat unexpected since, with the recognition of a possible biogenic

contribution to the gas of Unit B, it would be only reasonable to expect an increased biogenic contribution in the shallower rocks of Unit C.

Again a possible explanation is that the gas in this unit represents fractionated material which was originally produced in Unit B, but which has escaped biodegradation, possibly due to the exclusion of ground water due to low porosity or permeability. A number of sharp spikes in the horizontal velocity log would support the presence of a number of well-cemented intervals in this unit.

The three samples analysed from this unit for TOC content were all found to be poor in organic matter, with TOC contents typically less than 0.3 wt%. Rock-Eval data from this unit suggest that the kerogen is largely inert, yielding almost no pyrolyseable material on analysis. As a result, reliable Tmax data could not be obtained from these samples.

Unit D (45.07 - 1.8 m)

Analysis of the headspace and cuttings gas in eight canned samples from this unit indicated very low concentrations of hydrocarbon compounds, of which methane was the most abundant. The low concentrations present make the gas wetness and iC_4/nC_4 data largely meaningless. The total absence of gaseous hydrocarbons from most of the samples from Unit D is unusual and may reflect loss of gas during sample collection and storage. If a rock is sufficiently porous, gas escape may occur extremely rapidly on arrival on deck. Carbon and deuterium isotope data from one sample at the base of this unit indicate a composition similar to that described from the underlying calcareous unit and Unit A, i.e. a relatively mature, petrogenic composition. Hydrocarbon concentrations in the other samples from this unit were too low to permit accurate analysis of the isotopic composition.

The thirteen rock samples analysed from this unit are characterized by low TOC contents of less than 0.5 wt%. Rock-Eval data from these samples indicate that the kerogen is almost wholly inert with respect to hydrocarbon evolution, and hydrogen indices are typically less than 30 mg/gTOC. No reliable Tmax data were obtained from these samples as a result of the nearly inert nature of the kerogen.

In conclusion, the succession penetrated by core 7533/03-U-01 can be divided into an extremely organic-lean upper half and a more organic-rich lower half. Of the more-organic-rich lower half, only the upper 20 m (Unit B) have ~~any~~ some significant source potential, although increased thermal maturation will be required to realize this potential. The extremely organic-rich interval comprising Unit B apparently represents a condensed equivalent of the Hekkingen Formation described from the Tromsø and Nordkapp Basins, and appears to be more akin to the Alge Member of this formation in terms of its organic geochemistry. No clear evidence of oil shows was observed, although high gas concentrations are associated with these black shales. This association is not inconsistent with the low thermal maturity of the kerogen.

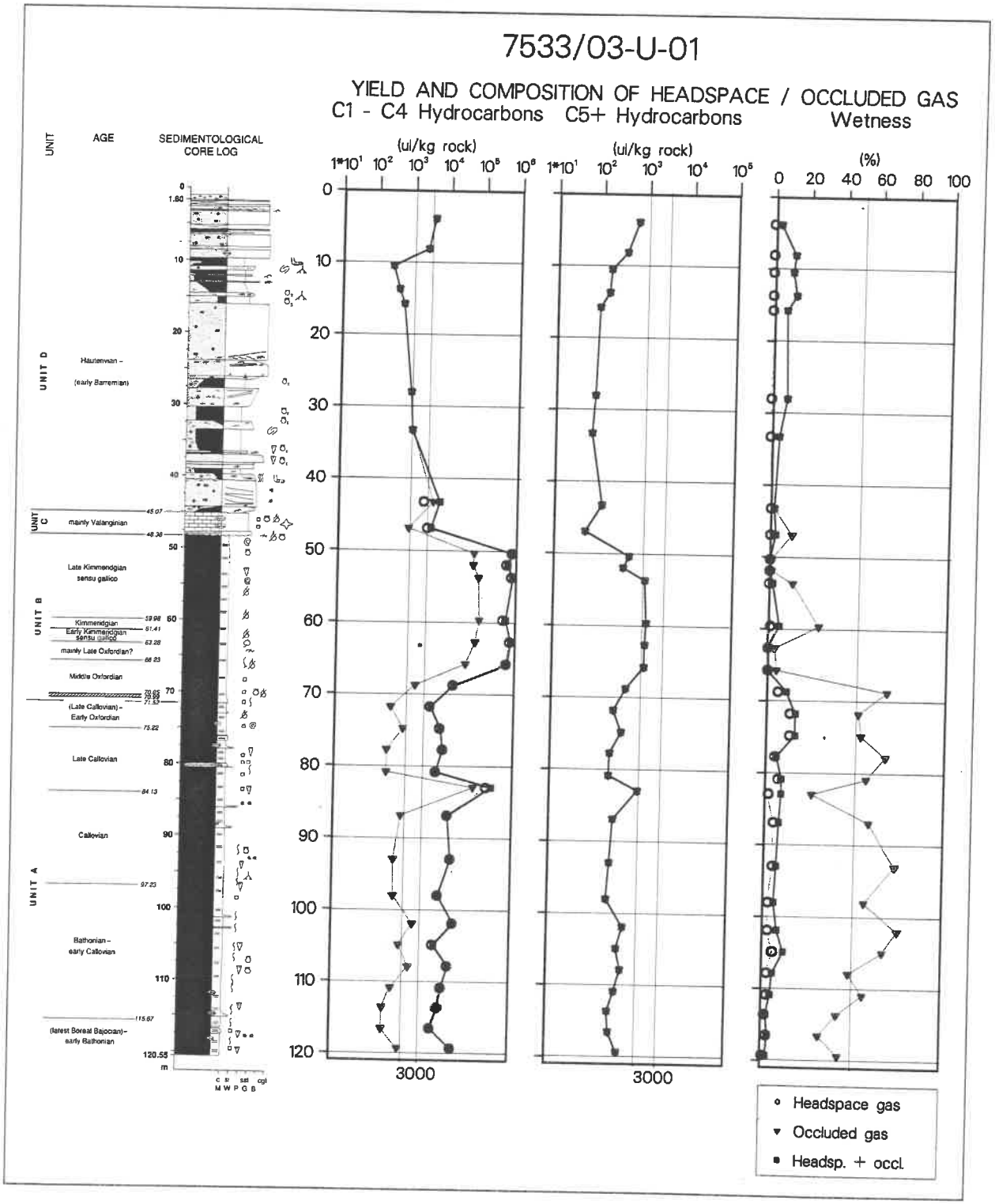

Figure 5.10 Yield and composition of headspace/occluded gas in core 7533/03-U-01.

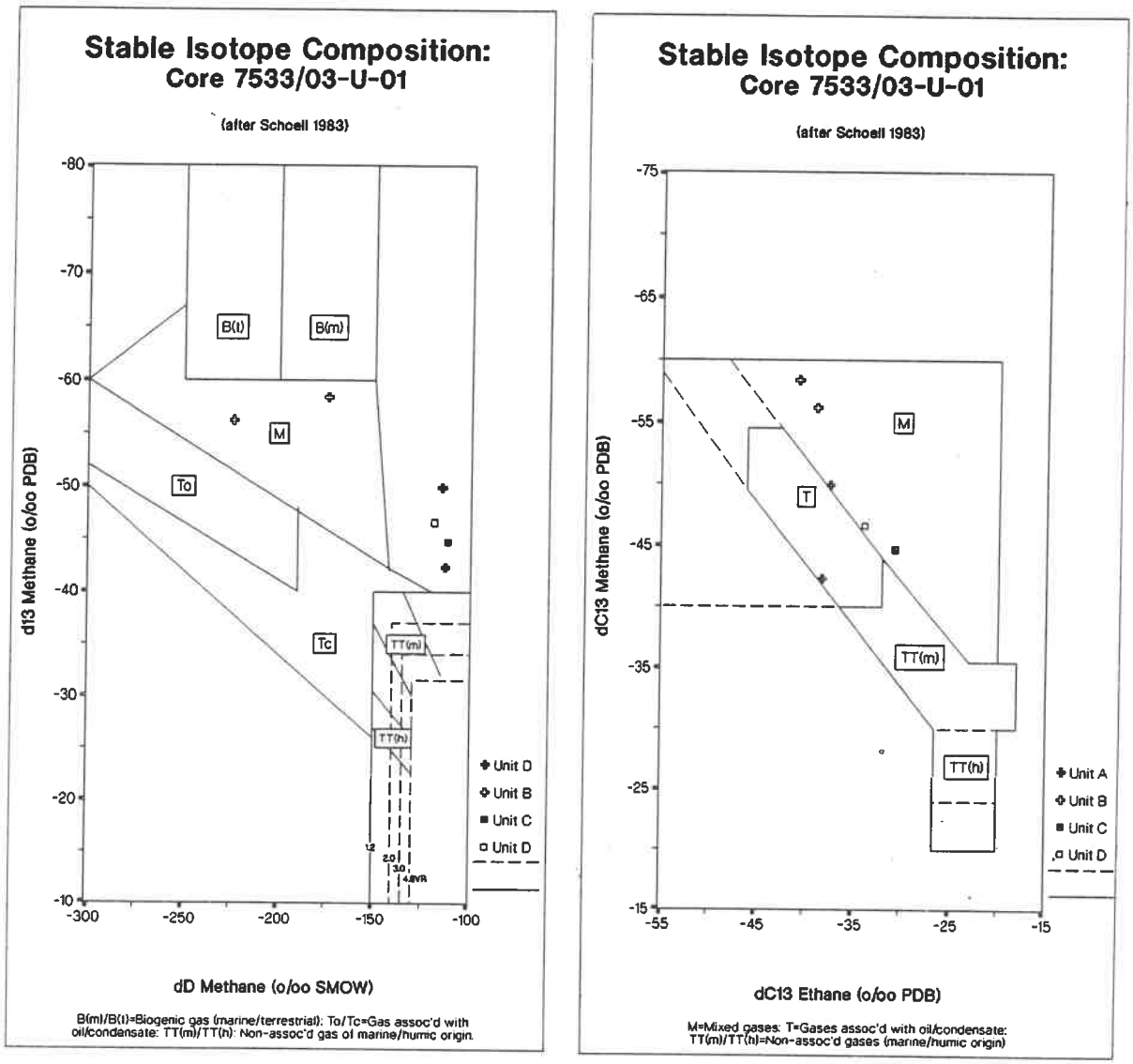

Figure 5.11 *Summary diagrams of stable carbon and deuterium isotope composition of adsorbed methane and ethane in core 7533/03-U-01.*

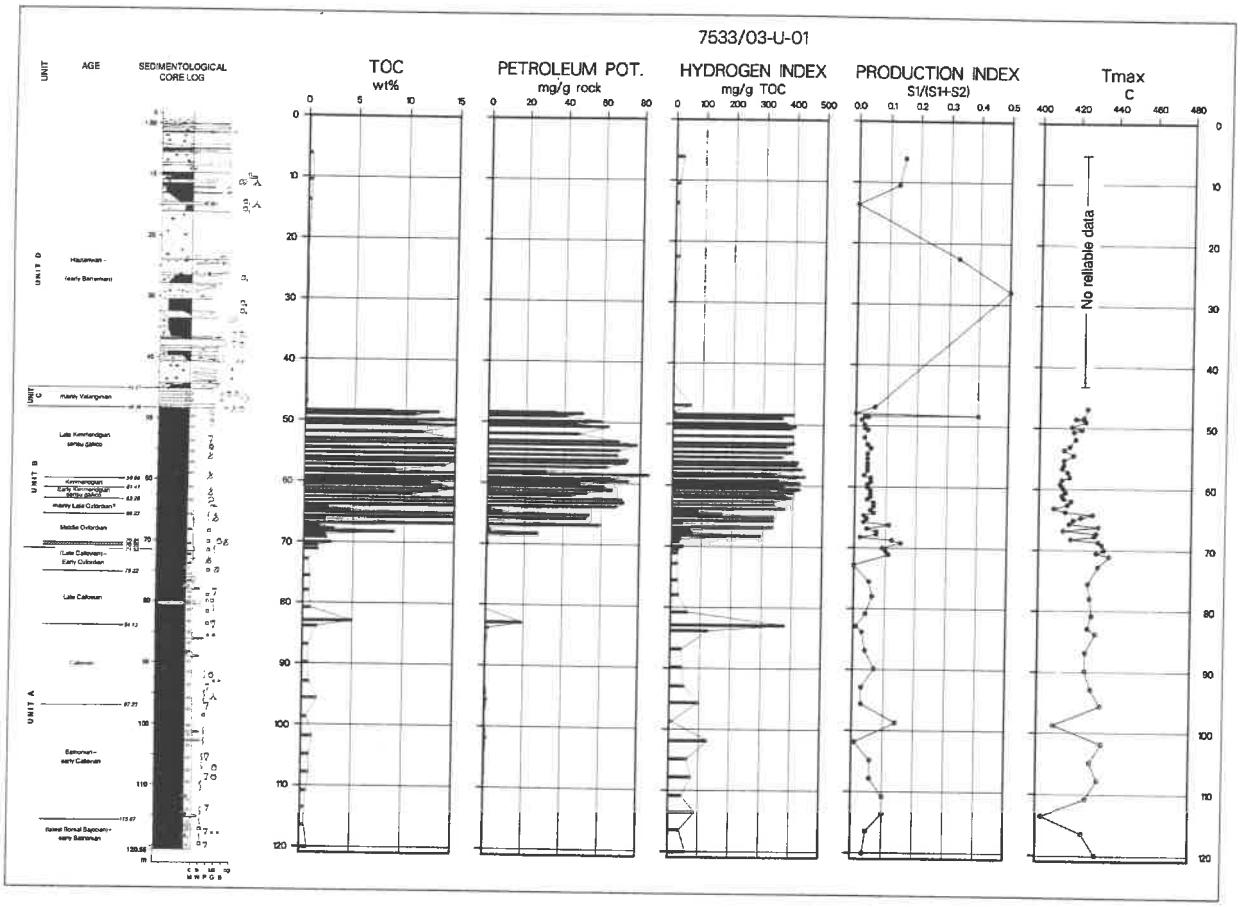

Figure 5.12 *Total organic carbon content and data from Rock-Eval data from core 7533/03-U-01.*

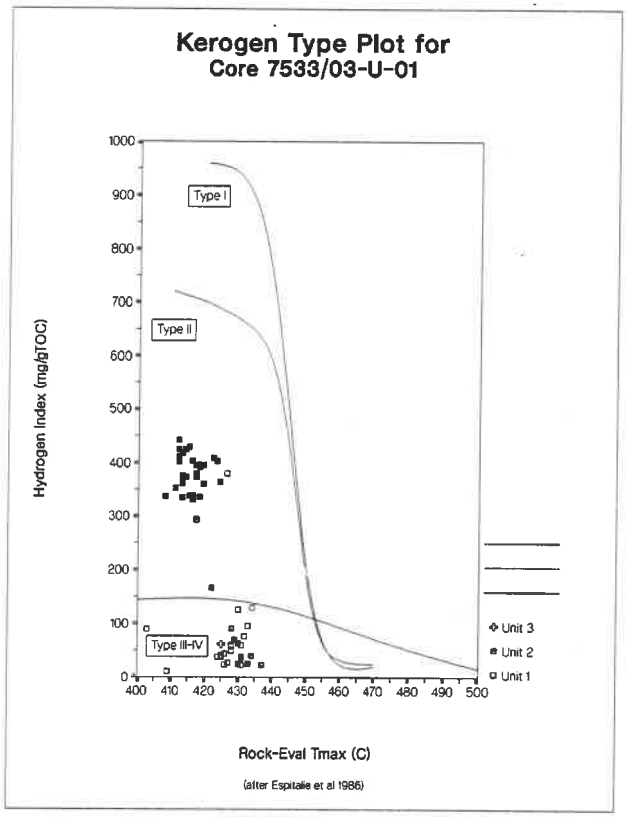

Figure 5.13 *Kerogen type/maturation summary plot for core 7533/03-U-01.*

6. DISCUSSION

6.1 Structural framework

The main structural elements in the southwestern part of the Barents Sea were described and given formal names in Gabrielsen et al. (1990). In the northern areas, informal names are in use due to less data coverage.

The area covered by the subcrop map (Figure 6.1) is part of a large platform area which was established in the Arctic in the Permian, and which was stable through the Triassic period. The platform can be divided into four structural elements in the area of the shallow wells (Figure 2.1).

Core 7532/02-U-01 is situated on the Sentralbanken high, which is an elevated part of the platform area, and where post-Triassic rocks were eroded completely in the Tertiary and Quaternary. Its structural elevation is mainly due to post-Cretaceous tectonic movement. Seismic and gravity data indicate that the Sentralbanken high did not exist as a high in pre-Jurassic time (Gabrielsen et al. 1990).

Core 7427/03-U-01 was drilled on the eastern part of the Gardarbanken high, which is interpreted to have an origin as a high prior to the Permian (Gabrielsen et al. 1990). However, in the core-hole area and in the eastern parts of the high, stable platform conditions apparently prevailed throughout the Triassic.

Core 7533/03-U-01 is located at the boundary between the Sentralbanken high and the Olga basin, in an area where Jurassic and Cretaceous rocks are preserved. The Sentralbanken high, Olga basin and Kong Karl platform are all characterized by compressional structures (reverse faults, anticlines), while such structures are not observed on the Gardarbanken high.

The most important structural set is a set of anticlines trending NNE-SSW. The anticlines typically are asymmetrical, with a relief of 100 - 500 ms at the Triassic level. Their lengths vary from a few kms up to several tens of kms. Profiles across the larger anticlines indicate that the Permian to Lower Triassic levels are deformed by reverse faults, while the Middle Triassic to Cretaceous levels are deformed mainly by folding. In some anticlines, the crest is modified by normal faults. Our seismic study indicates no thinning or thickening related to the anticlines in the Triassic section, and the anticline formation is thought to postdate the Triassic.

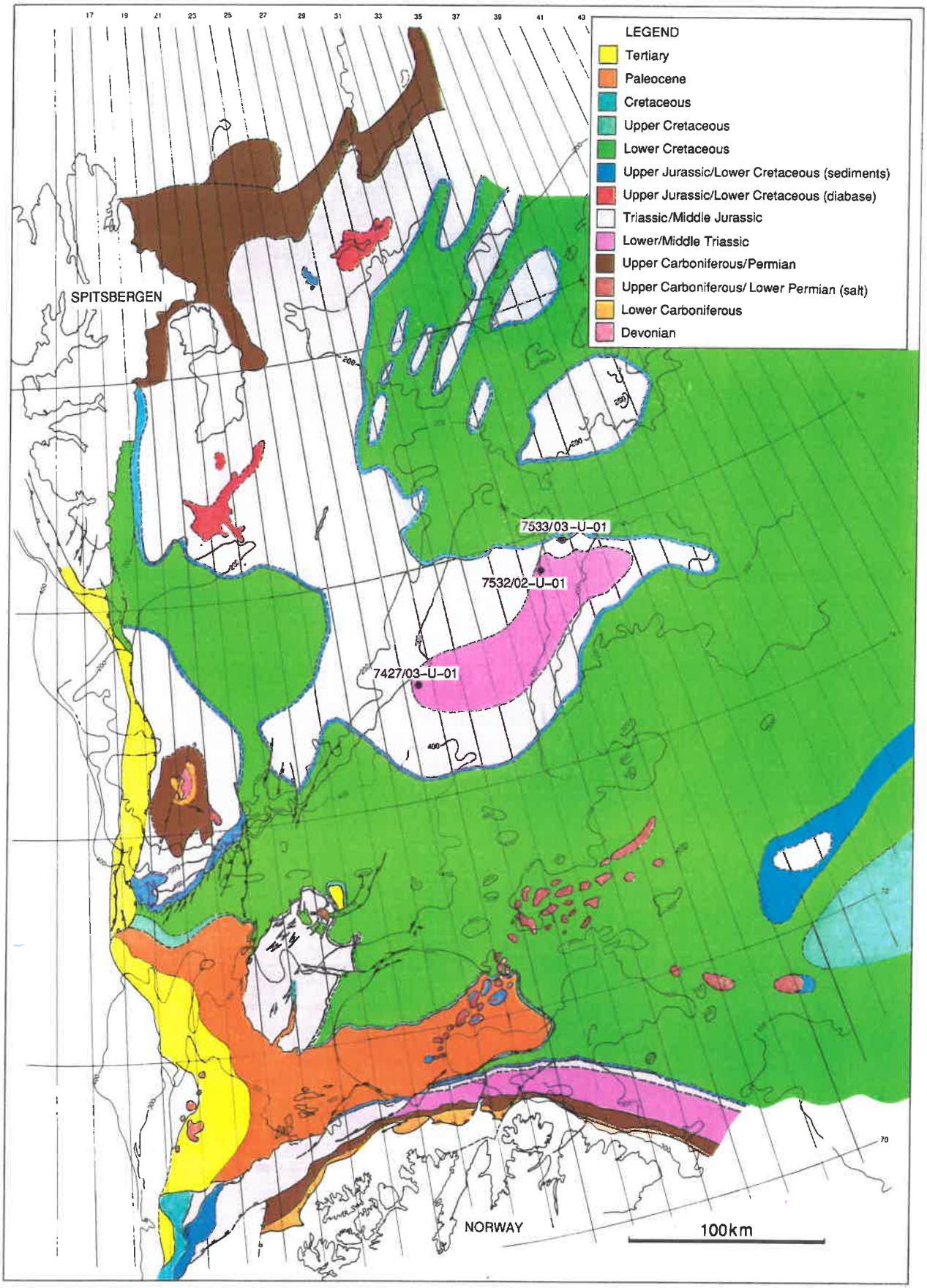

Figure 6.1 *Map of Hopendjupet area showing subcrop of the main reflectors towards the base of Quaternary. Based on interpretation by NPD (From Sigmond in prep.).*

The second structural set is made up of normal faults trending NW-SE. Their throws are in the order of 10-100 ms, and their lengths normally do not exceed 5 km. Because of the regional data coverage, these faults are normally observed only on one seismic line, and in most areas they were not drawn on the map. The faults seem to postdate the Triassic succession.

To conclude, the structural geology of the area indicates stable conditions throughout the Triassic Period. The major anticlines apparently did not grow until late Jurassic or early Cretaceous times (see below). It could, however, be noted that salt movement took place in the Anisian in the salt basins to the south. This affected, smaller areas and resulted only in extensive thicknesses of the Triassic succession within these salt-induced synclines. Thus, there is little evidence of tectonic movements which could cause rapid changes in the Middle Triassic paleogeography or depositional conditions.

The anticlines and normal faults in general affect all of the sedimentary section preserved, including the Lower Cretaceous. It is thought that the main deformation of the platform could be correlated with the Tertiary (Eocene) deformation of Svalbard, although a Late Cretaceous date cannot be excluded from the data since no Tertiary rocks are preserved.

6.2 Middle Triassic

The lithology and distribution of the Middle Triassic succession in the southwestern Barents Sea are fairly well known from seismics, wells and shallow cores. The formal lithostratigraphy defined for the Triassic of the Barents Sea area is based on well data from the Hammerfest Basin and surrounding areas (Worsley et al. 1988). The Ingøydjupet Group comprises the Griesbachian to Norian succession and is divided into the Havert, Klappmyss, Kobbe and Snadd Formations (Figure 6.2). The Middle Triassic comprises the Anisian Kobbe Formation and the Snadd Formation of Ladinian to Norian age.

During the Middle Triassic the majority of the Barents shelf represented a shallow marine to deltaic depositional environment, with continental deposits accumulated in the eastern Barents Sea and in the Timan Pechora area (Figure 6.3). East and southeast of Spitsbergen, anoxic to dysoxic bottom conditions occurred throughout most of Anisian and Ladinian (Leith et al. in press). This is seen both in central and eastern Spitsbergen (Mørk et al. 1982, Steel & Worsley 1984) as well as in the Svalis Dome area (Mørk et al. 1989). To the

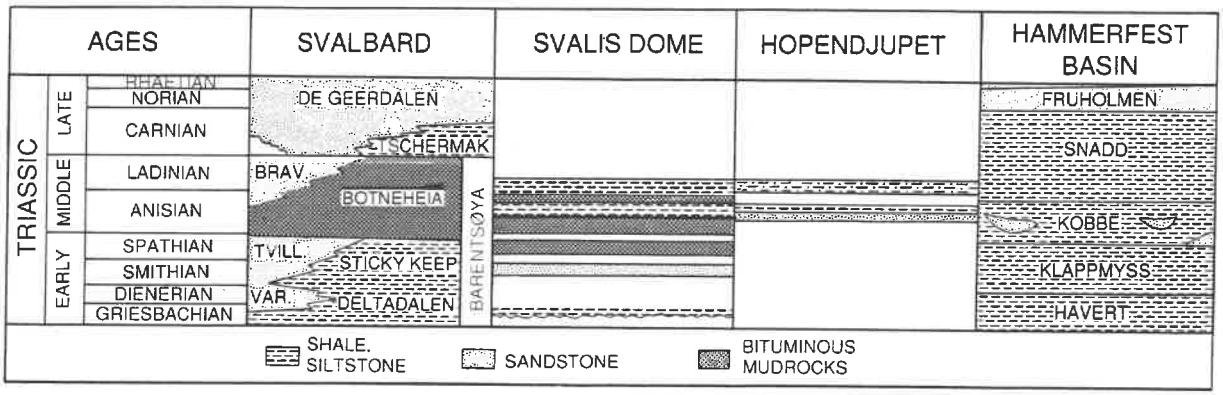

Figure 6.2 *Lithostratigraphic correlation scheme of Svalbard, Hammerfest Basin, Hopendjupet and the Svalis Dome (from Mørk et al. 1989, Worsley et al. 1988, and this study).*

west and south the American/Greenland continent and the Baltic Platform made a barrier only breached during brief transgressions probably reaching the Mid-Norwegian shelf (Jacobsen & Van Veen 1984) and East Greenland in Ladinian times (Clemmensen 1980). In Svalbard, a western source shed clastics along the margin seen in part of the Bravaisberget Formation (Mørk et al. 1982). More shallow to deep shelf deposits are seen in parts of the Bravaisberget and throughout the Barentsøya Formations during the Anisian and Ladinian times (Mørk et al. 1982). On the Barents Shelf, a general west/northwestwards progradation of the shelf edge is seen (Rønnevik et al. 1982).

Drilling of the two core-holes penetrating the Middle Triassic aimed at:

1) Obtaining stratigraphic control.

2) Investigating the hydrocarbon potential.

3) Obtaining tie to seismic interpretation.

More specifically, the location of well 7427/03-U-01 was selected to test a Middle Triassic section in the clinoform area to study the potential of source rocks, while the location of well 7532/02-U-01 was selected to penetrate Middle Triassic rocks as old as possible. Seismic interpretation indicates that older Triassic rocks subcrop farther east, but correlation is more difficult due to their more proximal position related to the source area.

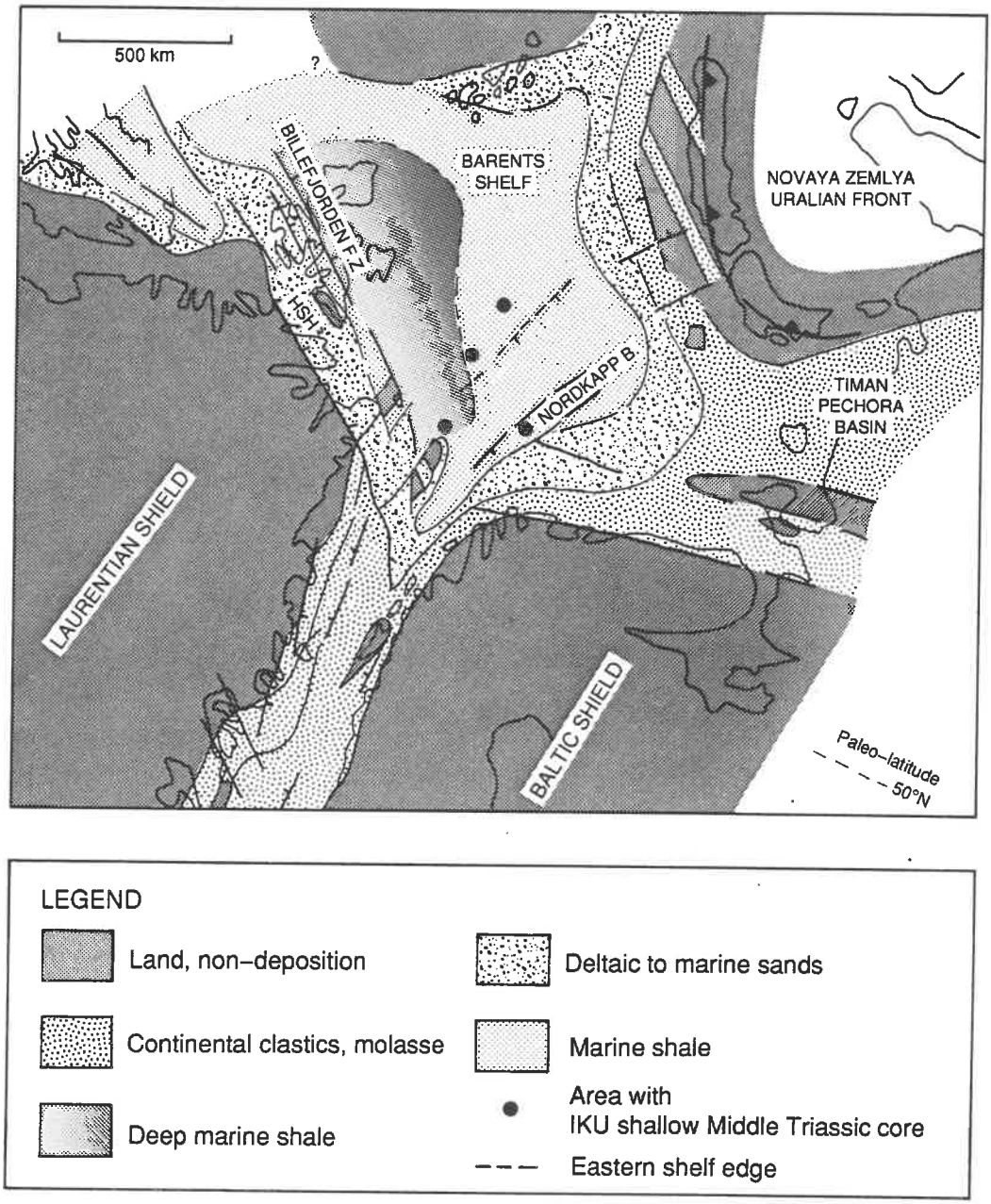

Figure 6.3 *Paleogeographic reconstruction of the Middle Triassic (Anisian) (modified from Doré in press).*

Description of reflectors and seismic units

Seismically, the Triassic in the Hopendjupet area can be divided into four main sequences (Figures 6.4 and 6.5) which have been correlated regionally in the Barents Sea. These sequences are,

Sequence I - Base of Triassic to Base of Smithian
Sequence II - Base of Smithian to Base of Anisian
Sequence III - Base of Anisian to Top of Anisian
Sequence IV - Top of Anisian to Middle Jurassic

The definition of sequence boundaries is based on regionally mappable downlap and/or onlap. The mapping was carried out using seismic data from the surveys listed in Table 6.1, which give a regional 10x10 km grid of good quality data.

The ages of the sequences refer to datings in the deep wells in the southwestern Barents Sea, and they must be regarded as approximate due to uncertainties in dating and the long distance of seismic correlation.

Cores 7532/02-U-01 and 7427/03-U-01 were drilled in the upper part of sequence III and in the lower part of sequence IV, respectively. To interpret the paleogeography, a description of seismic sequence III is useful.

Table 6.1 Seismic surveys used for regional interpretation.

NPD SB 87	Conventional (+sparker)	Sentralbanken high
NPD SBSW 87	Conventional	Sentralbanken high
NPD SENT 86	Conventional	Sentralbanken high
NPD STOB 89	Conventional + shallow digital	Olga basin
NPD NOLO 85	Conventional	South of 74°30'N
GLR3 87	Conventional	Svalis Dome area
NPRI 87	Sparker	Olga basin

Seismic sequence III (Anisian)

The sequence is bounded below by a reflector which is characterized by downlap to the west and onlap in the central part (Figure 6.4). East of 32°-33°E, the base of the sequence is poorly defined because the reflections are weak and parallel. The sequence is bounded above by a reflector characterized by onlap and toplap to the west shown in Figure 6.4 and in the dotted area in Figure 6.6. East of the dotted area, the reflectors are parallel, but commonly discontinuous and weak.

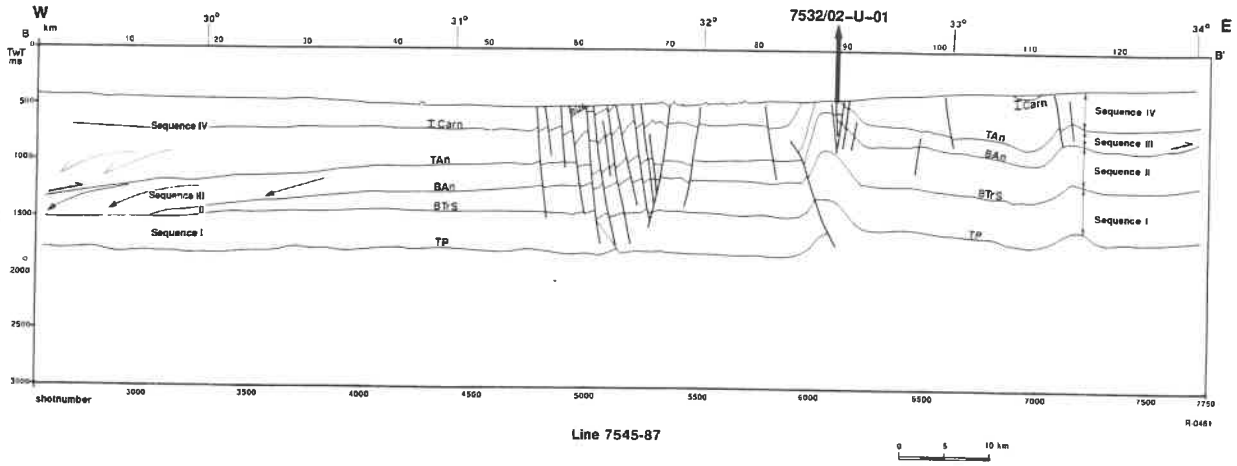

Figure 6.4 *Structural cross-section in Hopendjupet. Arrows show downlapping clinoforms. Half arrows indicate onlap. Location is shown in Figure 6.7.*
Legend to section: TP - Top of Permian, BTrS - Base of Smithian, BAn - Base of Anisian, TAn - Top of Anisian, ICarn - Intra Carnian, MJ - Middle Jurassic, IUC - Intra Upper Cretaceous, BT - Base of Tertiary.

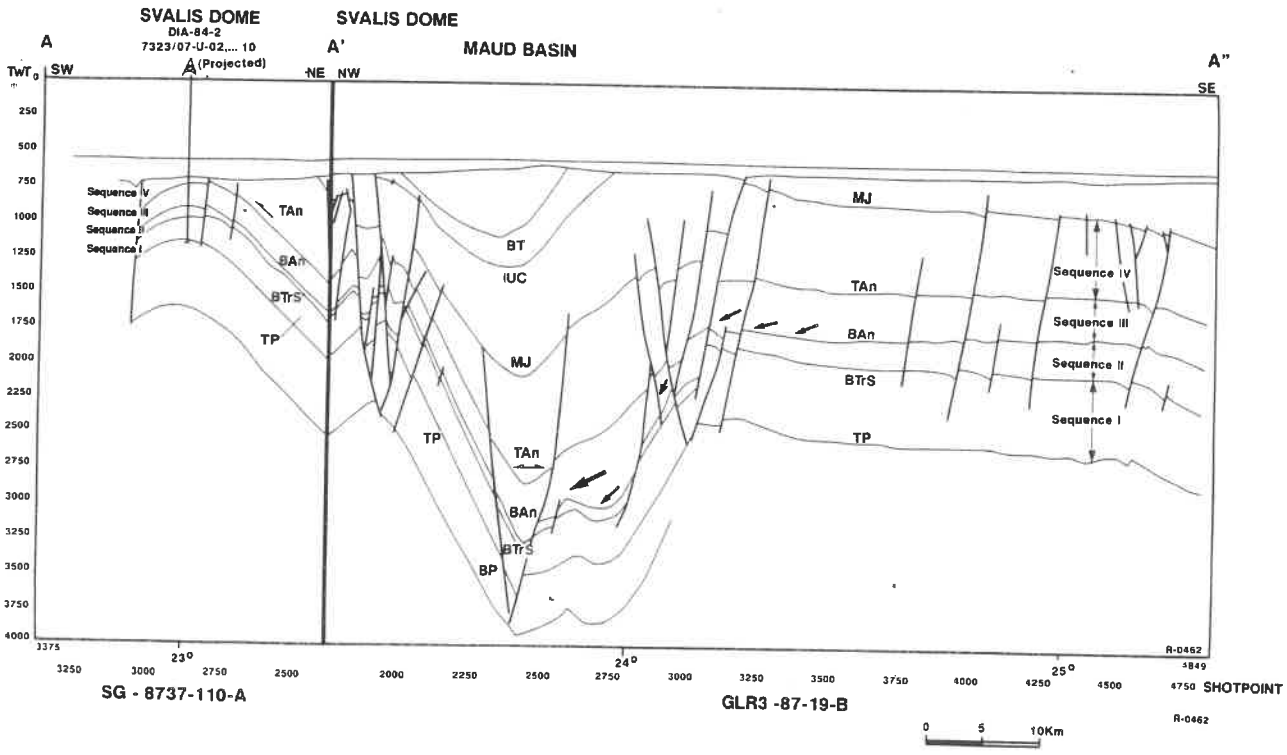

Figure 6.5 *Structural cross-section in the Svalis Dome area. Arrows show downlapping clinoforms. Half arrows indicate onlap. Location is shown in Figure 6.7.*
Legend to section: BP - Base of Permian, TP - Top of Permian, BTrS - Base of Smithian, BAn - Base of Anisian, TAn - Top of Anisian, ICarn - Intra Carnian, MJ - Middle Jurassic, IUC - Intra Upper Cretaceous, BT - Base of Tertiary.

Note that the section has a dogleg shape, so that the Svalis Dome appears twice.

As shown in Figures 6.4 and 6.5, the sequence onlaps sequence II to the east and downlaps to the west. The maximum thickness of approximately 300 ms is attained in the central parts of the Hopendjupet area between 27°- 28°E and 32°-33°E. Internally, the sequence is characterized by very well developed clinoforms to the west (dotted area in Figure 6.7). These clinoforms are onlapped by the overlying sequence IV. At the base of this Ladinian to Jurassic sequence, progradation from the east can locally be observed.

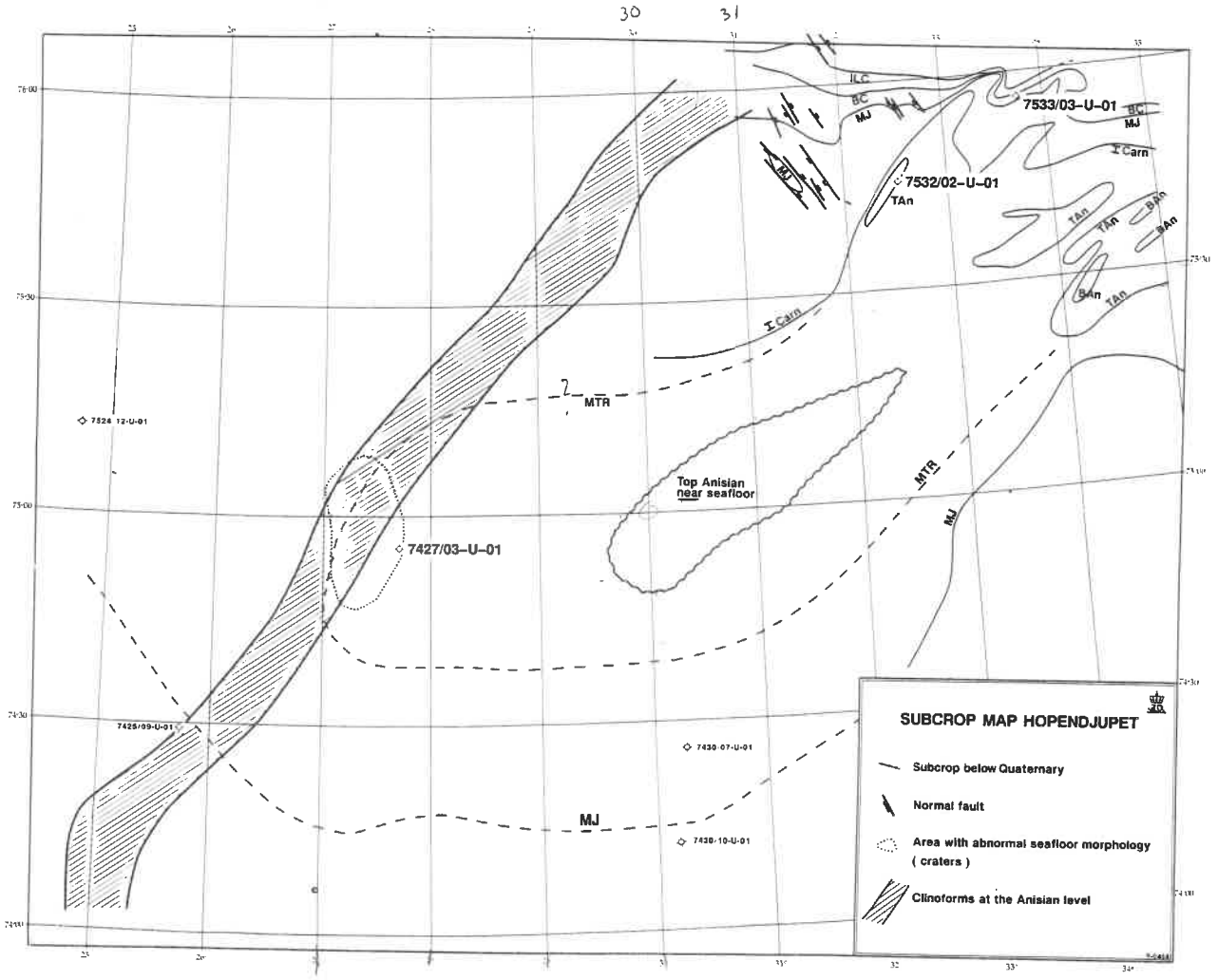

Figure 6.6 *Map of the Hopendjupet area showing subcrop of the main reflectors towards the base of Quaternary. The Anisian clinoforms are partly overlain by younger Triassic sediments.*

Legend to abbreviations: ILC - Intra Lower Cretaceous, BC - Base of Cretaceous, MJ - Middle Jurassic, ICarn - Intra Carnian, TAn - Top of Anisian, BAn - Base of Anisian, MTR - approximate position of the top of Middle Triassic.

The dashed lines are based on the subcrop map of Sigmond (in prep.).

There is a change in geometry of the prograding part of the Anisian sequence at approximately 73°55'N. To the north, the clinoforms are more tabular and steep, and the onlap of the overlying sequence is in general well defined. The clinoforms, which are thought to represent progressive stages of shelf progradation, typically have a horizontal extension of 10-15 km and a height difference of 150-200 ms (more than 300 metres). To the south, the clinoforms are more sigmoidal, with less vertical relief, and two onlap surfaces can be defined. The uppermost onlap surface corresponds to the top of sequence III, the lowermost surface possibly corresponds to an intra Anisian level. This difference is illustrated by Figures 6.4 and 6.5. Also to the south, the thinning of the section is more gradual, and progradation can be observed west of the main progradational area indicated in the map (Figure 6.7).

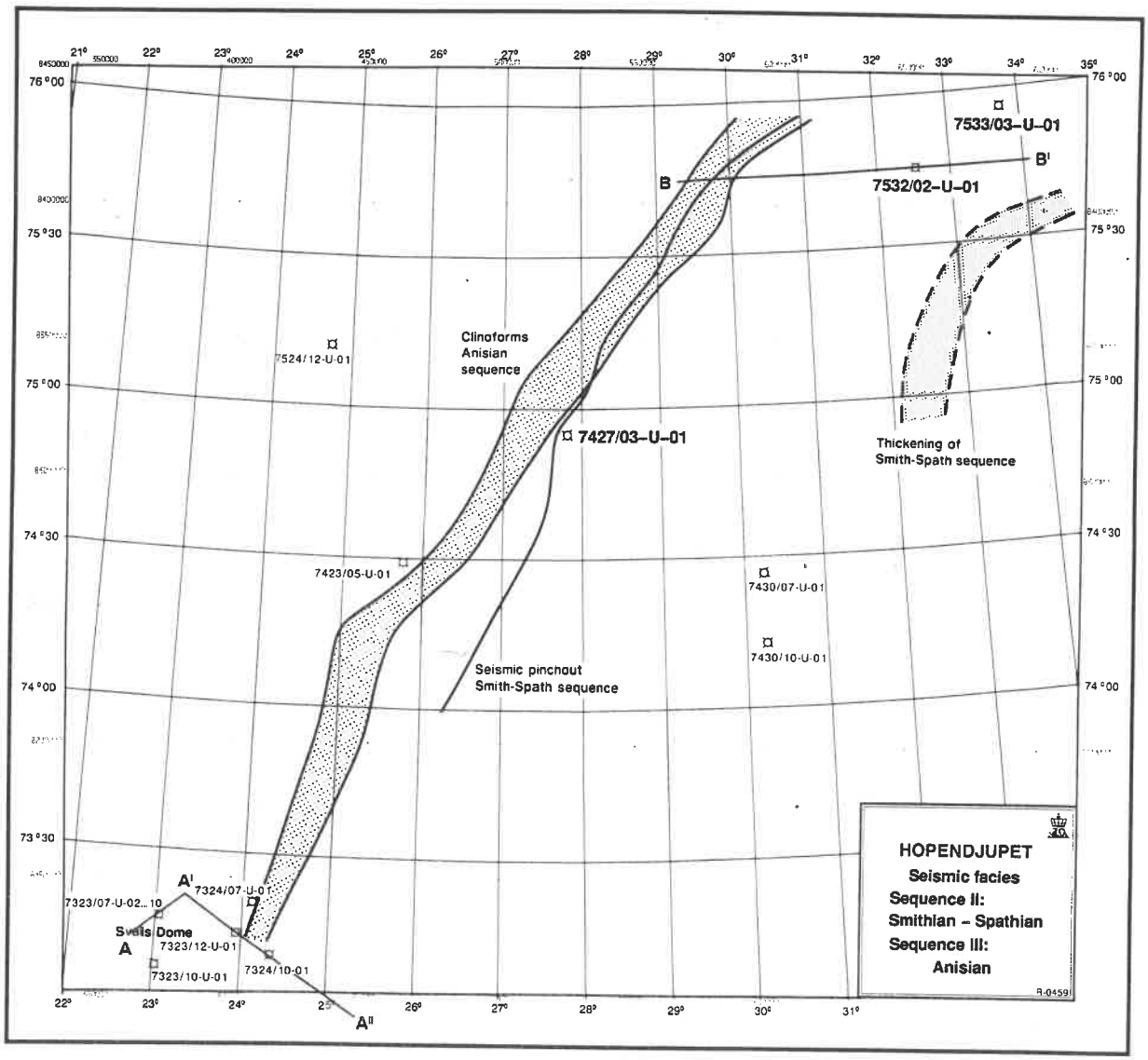

Figure 6.7 *Sketch map showing distribution of seismic facies of sequences II (Smithian-Spathian) and III (Anisian) in the Hopendjupet area. The location of the profiles AA'A" and BB' is shown, as well as position of the shallow drillings (e.g. 7430/10-U-01) and the deep well 7324/10-1.*

More geological data are needed to explain the change in geometry of the clinoforms at about 74°N. It could be suggested that this change is related to a different paleogeography, e.g. deeper water to the north prior to deposition.

The Anisian sequence subcrops below the Quaternary along the crests of the major anticlines of the Sentralbanken high. In a large area in the deeper part of Hopendjupet, the top of the sequence is found at less than 100 ms from the sea floor, but covered by younger sedimentary rocks (Figure 6.4). The base of the sequence subcrops at a few locations in the easternmost part of the study area (Figure 6.6).

Correlations

In the area north of 73°N only two exploration wells (7321/8-1 and 7324/10-1) have been drilled through the Middle Triassic section. In addition, data from 11 shallow cores drilled in the Triassic succession at the Svalis Dome are available. Seven of these penetrated the Middle Triassic succession.

A regional seismic grid was interpreted in order to correlate the Hopendjupet shallow drillings with the Middle Triassic sections in the Svalis Dome and the deep wells 7324/10-1 in the Maud Basin and well 7226/11-1 further south. The objectives of the interpretation were:

- To produce a subcrop map (Figure 6.6) and to obtain structural control.
- To correlate the main Triassic sequences internally between the Hopendjupet wells to obtain stratigraphic control.
- To characterize and correlate the main seismic sequences and compare with the well data.

The base of seismic sequence III was not drilled in Hopendjupet. Its lower boundary has been correlated seismically to the deep well 7226/11-1, and is thought to correspond to the lowermost Anisian or the uppermost Spathian. At the Svalis Dome, the Spathian - Anisian boundary was penetrated by the shallow core 7323/07-U-04 (Vigran et al. 1986, IKU Shallow Drilling 1986, Mangerud & Rømuld in press). Based on ammonite evidence it appeared, however, that a hiatus spanning the earliest Anisian might be present at this

locality. The seismic tie from the Svalis Dome is difficult due to the thinning of the sequence towards the west (Figure 6.5).

In core 7532/02-U-01, the reflector interpreted as the top of seismic sequence III subcrops close to the site. The difference in elevation up to the reflector, measured vertically, is approximately 30 ms (45-50 metres). A further age assignment than a general Anisian age cannot be given from the recorded fossils, but based on negative evidence a middle to late Anisian age is suggested.

In core 7427/03-U-01, the reflector interpreted as the top of sequence III, is found at approximately 595 ms below sea level, corresponding to approximately 115 ms below the Quaternary. Based on seismic and biostratigraphic evidence this cored part of seismic sequence IV is dated as early Ladinian.

The top of seismic sequence III is interpreted to represent the late Anisian, based on its localization approximately 90 metres below the Ladinian section in core 7427/03-U-01 and approximately 45 metres above the Anisian section in core 7532/02-U-01. It can also be correlated to the late Anisian beds at the Svalis Dome. Here the "Top Anisian reflector" seems to be intra latest Anisian (Vigran et al. 1988, IKU report, Follow-up study Dia-Structure). In Spitsbergen, the Anisian-Ladinian boundary is found in the upper part of the Botneheia Member (Mørk et al. 1989), while the same boundary is situated between the Kobbe and Snadd Formations in the Hammerfest Basin (Worsley et al. 1988).

The lithology seen in the Ladinian core 7427/03-U-01, closely resembles the description of the Tschermakfjellet Formation in Spitsbergen defined by Buchan et al. (1965). This formation consists of dark grey, silty shale grading locally to shaly siltstone and very fine-grained sandstone with small reddish weathered, siderite nodules (Buchan et al. 1965, Mørk et al. 1982). The unit is now regarded as Carnian (Mørk et al. 1989, Mørk et al. in press). Besides in outcrops in central Spitsbergen, it is recognized on Edgeøya, Barentsøya and Sørkapp Land and a parallel development also occurs on Bjørnøya, where it, however, is assigned a Late Ladinian age (Mørk et al. 1990). The silty to sandy layers in the upper part of core 7427/03-U-01, might represent a transition to the De Geerdalen Formation equivalents. Buchan et al. (1965) described this formation as consisting of recurrent coarsening upward units, grading from shale to sandstone, which could correspond to the increasing silt-content in the uppermost part.

Based on the apparent similar lithological development in the late Anisian-Ladinian in Hopendjupet and the Ladinian-Carnian in Spitsbergen, we suggest that this development started in the eastern/northeastern Barents Sea and gradually moved westwards into the Spitsbergen area. A similar development in the late Ladinian on Bjørnøya reported by Mørk et al. (1990) is in agreement with this.

Paleogeography

The Anisian core 7532/02-U-01 is from the geometry of seismic sequence III, suggested to represent a shelf prograding from the east-southeast (Figure 6.7). The deposits of the sequence onlap the shelf topography created by seismic sequence II, and created a NNE-SSW trending Anisian shelf edge (Figure 6.7).

The general depositional environment seen from seismics and well data at Hopendjupet and the Svalis Dome places the paleo-shelf edge some place between the two Triassic Hopendjupet core-holes and the Svalis Dome (Figures 6.3 and 6.7). At the Svalis Dome, a general regressive trend throughout the Anisian (Figure 6.8) is seen from cores 7323/07-U-04, -01, -07 and -09, with deposition in dysoxic offshore setting during the late Spathian to earliest Anisian, and with a sudden relative sea level fall seen in the middle Anisian (core 7323/07-U-01). Throughout the late Anisian a general regressive trend is traced, with an important transgression occurring in latest Anisian (middle part of core 7323/07-U-09). The reflector penetrated at the base of the shale-unit in this Anisian core-hole, was correlated to the "Top Anisian reflector" (Vigran et al. 1986, IKU Shallow Drilling 1986), marking the onset of the rapid transgression taking place in the latest Anisian. This most probably correlates with the late Anisian - early Ladinian transgression recognized by Mørk et al. (1989) in the Sverdrup Basin, in one area on Spitsbergen and on Bjørnøya. They pointed at the fact that the simultaneous nature of this transgression has not been able to prove, although it is traceable throughout most of the Arctic.

The sediments recorded in the Anisian core 7532/02-U-01 in Hopendjupet reflect deposition in a nearshore delta front environment. The predominating terrestrial organic matter reflects, together with seismic data, drainage of a land area to the southeast. Marginal marine sediments were deposited both on Franz Josef Land (Ulmishek 1985, Gramberg 1988, Mørk et al. in press) and on western Spitsbergen (Mørk et al. 1982) during the Anisian. On Edgeøya and

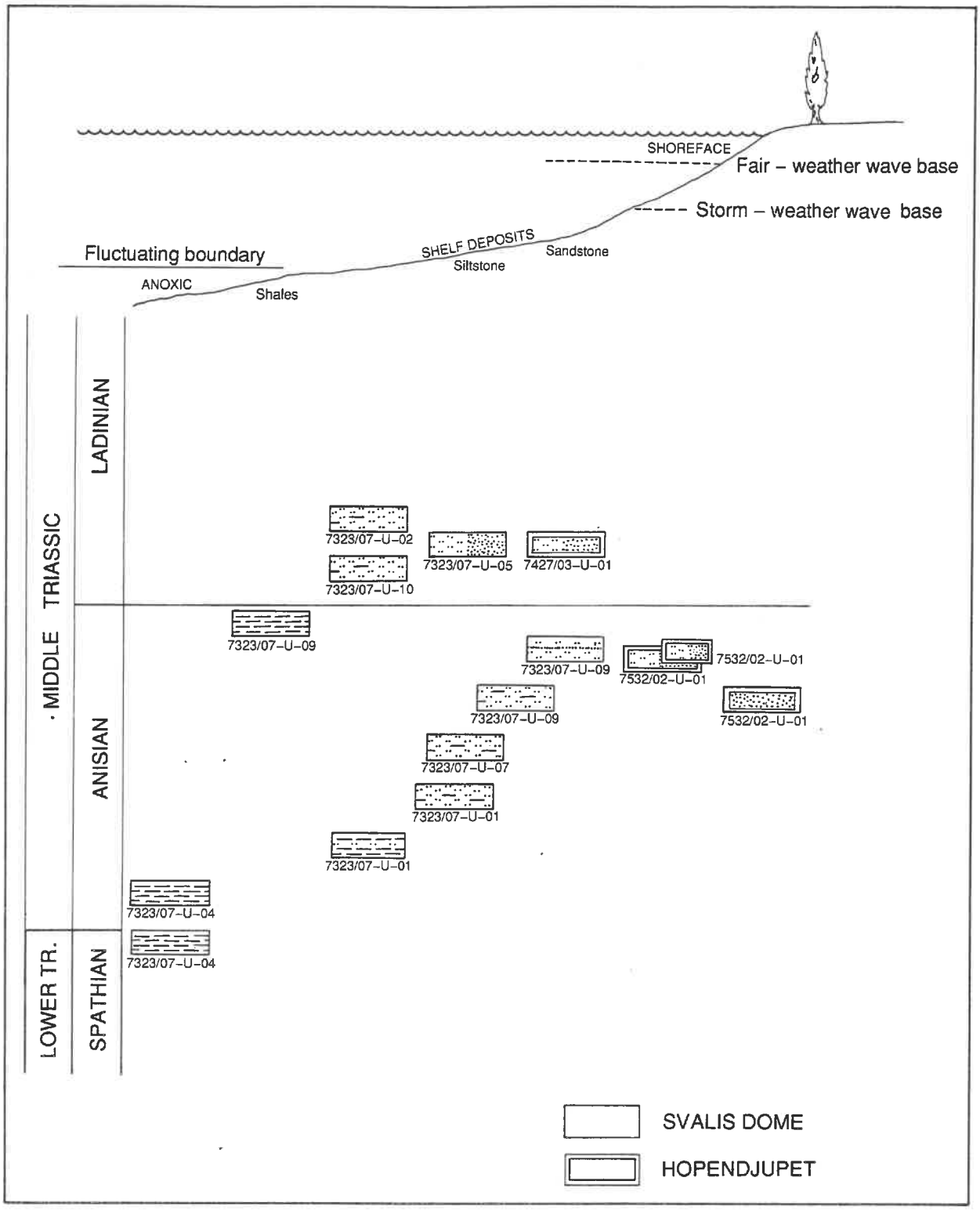

Figure 6.8 *A schematic profile showing the cores from the Svalis Dome and Hopendjupet arranged in chronological order, and placed within interpreted depositional environment. The positions of the cores are based on concluded chronostratigraphic ages. Vertical scale does not reflect the thickness-variation.*

Barentsøya, more deep marine settings occurred. We therefore postulate that the shelf edge situated west of Hopendjupet turned northwest, in the area

between the postulated land area north/northeast of Franz Josef Land and the northeastern margin of the North-America/Greenland plate as indicated on the paleogeographic map (Figure 6.3).

Seismic interpretation indicates that a general change in the conditions of deposition took place in the latest Anisian/earliest Ladinian. Such a change is suggested by two observations: Firstly, the onlap on the Anisian shelf edge and secondly, a different geometry of the Ladinian-Jurassic sequence IV where regional progradation has not been observed. Rather, this uppermost sequence seems to infill the post-Anisian topography. However, the seismics is not conclusive, as clinoforms occur in some seismic lines at the base of sequence IV. The change in depositional conditions could be related to a change in sea level (regression, and/or to a change in the source area for sediments).

The Ladinian core-hole 7427/03-U-01 is geographically situated at the eastern boundary of the zone of clinoforms in seismic sequence III, but contained sediments belonging to sequence IV, which here overlie sequence III. It is also located slightly to the east of the pinch-out of sequence II. The well penetrated the lowermost part of sequence IV, which farther to the west onlaps the Anisian shelf edge, and which shows progradation in the area of onlap.

The core penetrated Ladinian shales and siltstones with organic material of predominantly terrestrial origin. A lower shoreface to upper offshore environment was interpreted both from sedimentological and palynofacies data. Several coarsening upwards cycles and rapid changes in palynofacies most probably reflect an environment where the delta front switched. Similar development could also be caused by rapidly oscillating sea level. The core shows that relatively deep marine conditions existed during the early Ladinian, and that the source-area still was located to the southeast. The core is interpreted to be located landward of the shelf edge. The sea level was probably lower than in the late Anisian, when an important transgression is interpreted from core 7323/07-U-09 at the Svalis Dome to the southwest. On the Svalis Dome, the three early Ladinian cores (7323/07-U-02, -05 and -10) reflect a distal marine offshore setting. The data from the Svalis Dome show a regressive trend during the early Ladinian with a relative sea level rise somewhat higher up in the Ladinian section (7323/07-U-02). A regressive trend in the earliest Ladinian is also documented from Bjørnøya and Spitsbergen (Mørk et al. 1989).

Triassic Hydrocarbons: Character and possible origins

Streaming oil-shows were a feature of siltstone and fine-grained sandstone intervals in the central part of core 7427/03-U-01. Interbedded claystone layers appear to contain only very minor concentrations of related liquid hydrocarbons, and may therefore be considered as representing rather effective permeability barriers. The recovered oil shows no evidence of biodegradation on preliminary examination, and is characterized by a typically oil-like, mature, n-alkane envelope.

The relatively equal height of the pristane and nC_{17} peaks observed in the saturated hydrocarbon gas chromatograms of these oils differs from the low pristane/nC_{17} ratios normally associated with mature oils. Artificial oils generated from samples of the Hekkingen Formation from the Tromsø and Nordkapp Basins, and from middle Anisian-age shales at the Svalis Dome are characterized by low pristane/nC_{17} ratios, as is normal in most mature Norwegian oils. However, artificial oil generated from Upper Spathian to Lower Anisian-age shales at the Svalis Dome (7323/07-U-04) has a similar pristane/nC_{17} ratio to that in the Hopendjupet oil-stain. Obviously, this is a rather tenuous connection, and more detailed characterization is required before a more definite correlation can be assigned.

Gas isotope and Rock-Eval data from the Anisian-age, lower sandstone interval in core 7532/02-U-01 suggest the presence of more subtle oil-staining in this core as well. The gas isotope data are similar to those associated with the staining in core 7427/03-U-01, and are different from that associated with the Upper Jurassic shales in core 7533/03-U-01. More detailed analysis of this interval will be required if the extent and origin of this staining is to be properly substantiated.

It is quite clear from the available organic geochemical data that the kerogen in the claystones sampled by core 7427/03-U-01 are unlikely to have generated the oil which is present in this core. At best, these mudrocks may represent a more proximal equivalent of the organic-rich black shales of the Barentsøya Formation of Eastern Svalbard. The existence of a more basinal source rock down-dip of the core location must therefore be postulated.

Anisian source rocks as suggested above are predicted to occur in the clinoform zone and westwards. The general dip of the clinoforms could facilitate migration towards the core-hole position. The Upper Spathian was penetrated at the Svalis Dome (7323/07-U-04) which represented an anoxic

offshore environment. According to the seismic interpretation, the Spathian section should be at a comparable distal position in the two areas. Thus, the Ladinian core 7427/03-U-01 seems to be vertically underlain by Spathian distal shales, which could have a source rock potential comparable to the Svalis Dome. The paleogeographical model suggests that Spathian and Early Anisian source rocks, comparable to those at the Svalis Dome could be a feasible source for the oil encountered in the core. Regarding earlier predictions (i.e. Leith et al. in press), this represents new and important data.

The relatively high maturity of the kerogen in the cored succession suggests that a significant uplift event has occurred, although the point in time at which this occurred is open to debate. Certainly the uplift experienced by the succession in core 7427/03-U-01 is significantly greater than that experienced by the other two cores collected during this study.

The apparent efficiency of the permeability barriers formed by the interbedded shales would tend to argue against vertical migration as a source for the oil staining, at least in a local sense. Lateral migration from a more basinal source rock seems more likely. Although the maturity of the cored rocks is sufficient to have permitted hydrocarbon generation, the uplift experienced by the rocks in this area would tend to suggest that hydrocarbon generation is now largely inactive. Since the deepest parts of the adjacent basin are only 1.5 km deeper at best, a similar situation is likely to hold there also.

Another explanation can be put forward based on the spillage of hydrocarbons from previously-filled reservoirs during the latest uplift event, as has been suggested for the Snøhvit Field (Skarpnes 1989). This would provide a source of mature oil which is currently being redistributed in accordance with the altered geometry of the basin. The fractionation which would accompany such an event could be considered consistent with the slightly abnormal isotopic composition of the associated gases, and might help explain the mobility of the oil (e.g. Thompson 1987).

The sandy intervals of core 7427/03-U-01 had a high content of undegraded oil believed to have migrated from deeper strata. The high hydrocarbon content of the oil and its undegraded nature can only be explained in two ways; either seabed temperatures have been sufficiently low to inhibit microbial activity, or the core has penetrated an active migration conduit.

The undegraded nature of the oil and the ease with which it flowed from the rock suggests that the core has sampled part of an active oil-seep system.

The crater area at site 7427/03-U-01

Drill site 7427/03-U-01 was located in a 10 m deep local depression in Triassic bedrock. Similar depressions occur in an area that appears to be restricted to the area where the clinoforms of the Anisian seismic sequence III intersects with the East-West trending anticline at the Triassic level which defines the Sentralbanken high (dotted area in Figure 6.5). The drill site was localized in the eastern part of this area. The depressions are visible on both analog and conventional seismic lines, and a smaller area has been mapped in detail by the Norwegian Polar Research Institute (Solheim et al. 1988) using side-scan sonar and multibeam echosounder. The features proved to be a series of steep-walled, crater-like depressions (Figure 6.9).

Solheim et al. (1990) discussed various processes for the foundation of the depressions, of which two are more likely than the other: gas blow-out from decomposed gas hydrates and glaciotectonic.

Core 7427/03-U-01 was drilled within one of the depressions in an attempt to approach the solution of how the depression was formed and whether the formation mechanism was related to existence of hydrocarbons in the area. As mentioned in Section 4.2, the basal till that generally occurs in the area, was absent in the depression and only soft, Upper Pleistocene/-Holocene clay was found. This implies that the depression was formed in Late Pleistocene or Holocene time, i.e. after or at the very end of the last glaciation of the area (Hald et al. 1990). It is also in agreement with a rapid retreat of the glacier, leaving only minor deposition of glacial sediments (Solheim et al. 1990). A 12 m high rim was observed on the NE side of the depression (Figure 6.9).

At drill site 7524/12-U-01, IKU measured an average seabed temperature of -0.5°C (Sættem 1988). We may therefore suggest that the temperature at the seabed at site 7427/03-U-01 could have been close to 0°C, at least since the Late Pleistocene. This would be consistent with an inhibition of microbial activity suggested above and the low degradation of the observed hydrocarbons in the core. It would neither exclude active migration of hydrocarbons from deeper strata. Active migration and the suggested low temperatures support Solheim et al.'s (1990) theory that gas hydrates may have existed in the area, and that sudden dissolution of gas hydrates may have formed the

craters. The location is close to the theoretically stable area of gas hydrate (Løvø et al. 1990).

As mentioned in Section 4.3, evidence of glaciotectonic influence has been found down to at least 16.3 m in core 7427/03-U-01. High glaciotectonic activity is documented elsewhere in the Barents Sea (Sættem 1990, in press, in prep), showing that glaciers have lifted large slabs of the sedimentary bedrock and transported them over long distances. The slip planes at the base of the slabs tend to follow weak planes in the bedrock. Bluemle & Clayton (1984) concluded that most studied glacial thrust features in North Dakota are located over discrete aquifers. Sættem (1990) pointed out that any presence of gas or gas hydrates could have contributed to local glaciotectonic instability (e.g. Bugge 1983). Gas migrating into a confined aquifer under high pressure conditions beneath an ice cover, could give high pore pressure resulting in very low effective stress. High pore pressure due to excess pore water pressure or gas pressure, reduces the effective strength along possible slip planes. Migrating gas could therefore provide a particular failure mechanism during ice retreat. Oil staining could have a similar effect (Sættem in prep). Combination of high migration rate and gas pressure could therefore have assisted the glacier in releasing rocks from the craters before the glacier moved the slabs away.

It is reasonable to believe that the dissolution of potential gas hydrates occurred after the ice left the area in Late Pleistocene/Early Holocene time. The potential glaciotectonic activity could also have occurred in the Late Pleistocene. Both theories would therefore have the right timing as observed from the absence of the basal till from the depression. More data would be needed to decide if these processes formed the depressions or whether other processes were involved.

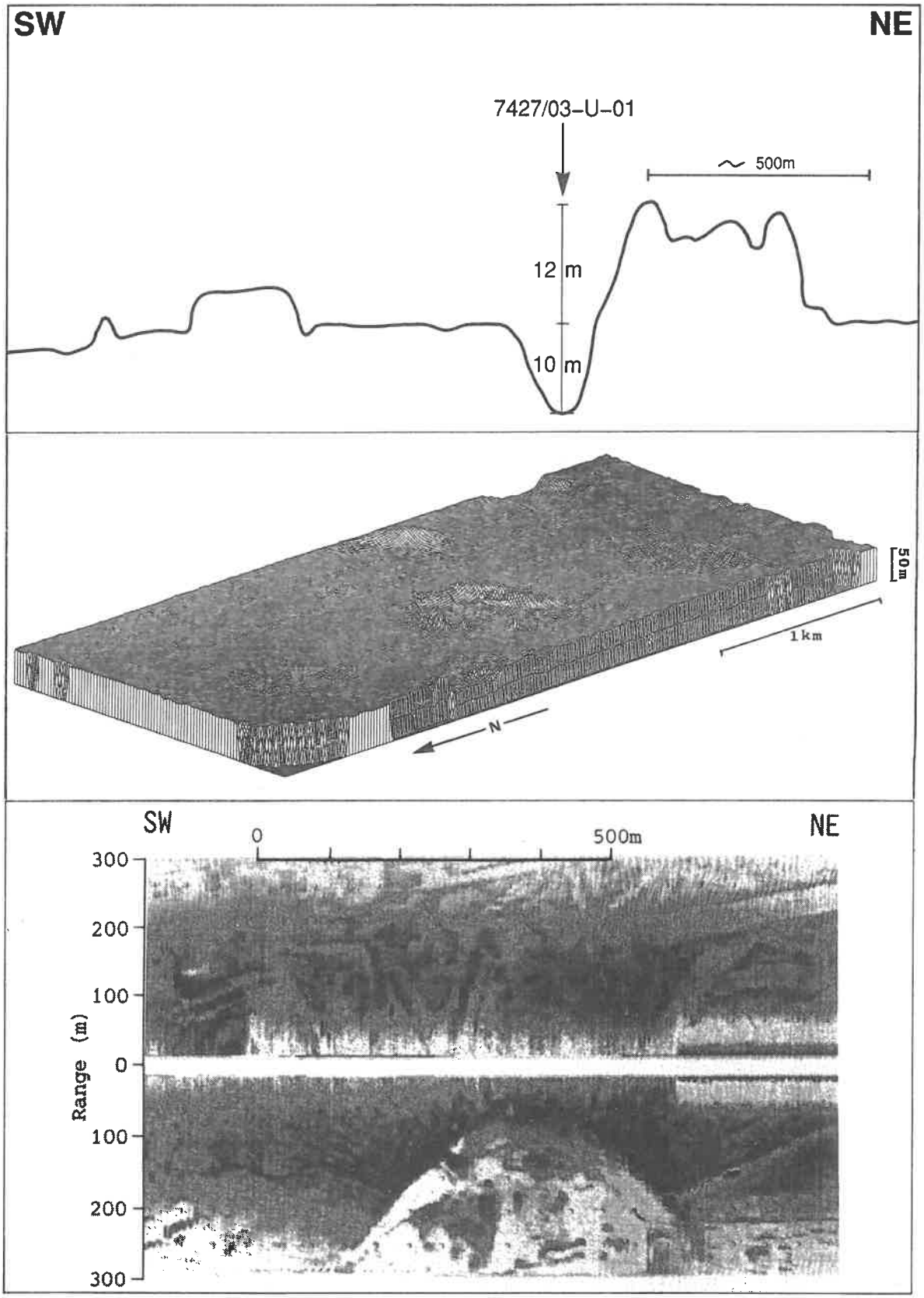

Figure 6.9 *Core 7427/03-U-01 was drilled within a 10 m deep depression on the sea floor.*
A. Echogramme across the depression. There is a 12 m high rim on the NE side of the depression.
B. The Norwegian Polar Research Insitute has mapped the bathymetry around some of the depressions in the area. They are typically 300-400 m wide, slightly elongate and 10-30 m deep.
C. Side-scan sonar of one depression.
Figures B and C are from Solheim et al. (1988).

6.3 Middle/Upper Jurassic - Lower Cretaceous

The Middle Jurassic - Lower Cretaceous succession is well known in the southwestern Barents Sea. North of 74°N, data are, however, more scattered.

This northern shelf area has been mapped seismically on a regional scale by the NPD. The Jurassic and Lower Cretaceous strata are outcropping in the Olga basin and on the Kong Karl platform. On the southern platforms, beds of these ages are separated by the more deeply eroded areas of the Sentralbanken high and the Gardarbanken high (Figure 6.1). In the areas where the Jurassic is preserved, the seismics indicates stable platform conditions in the late Jurassic, while tectonic movement of the anticlines apparently was initiated in the latest Jurassic or early Cretaceous (cfr. Section 6.1 and Figures 6.10 and 6.11).

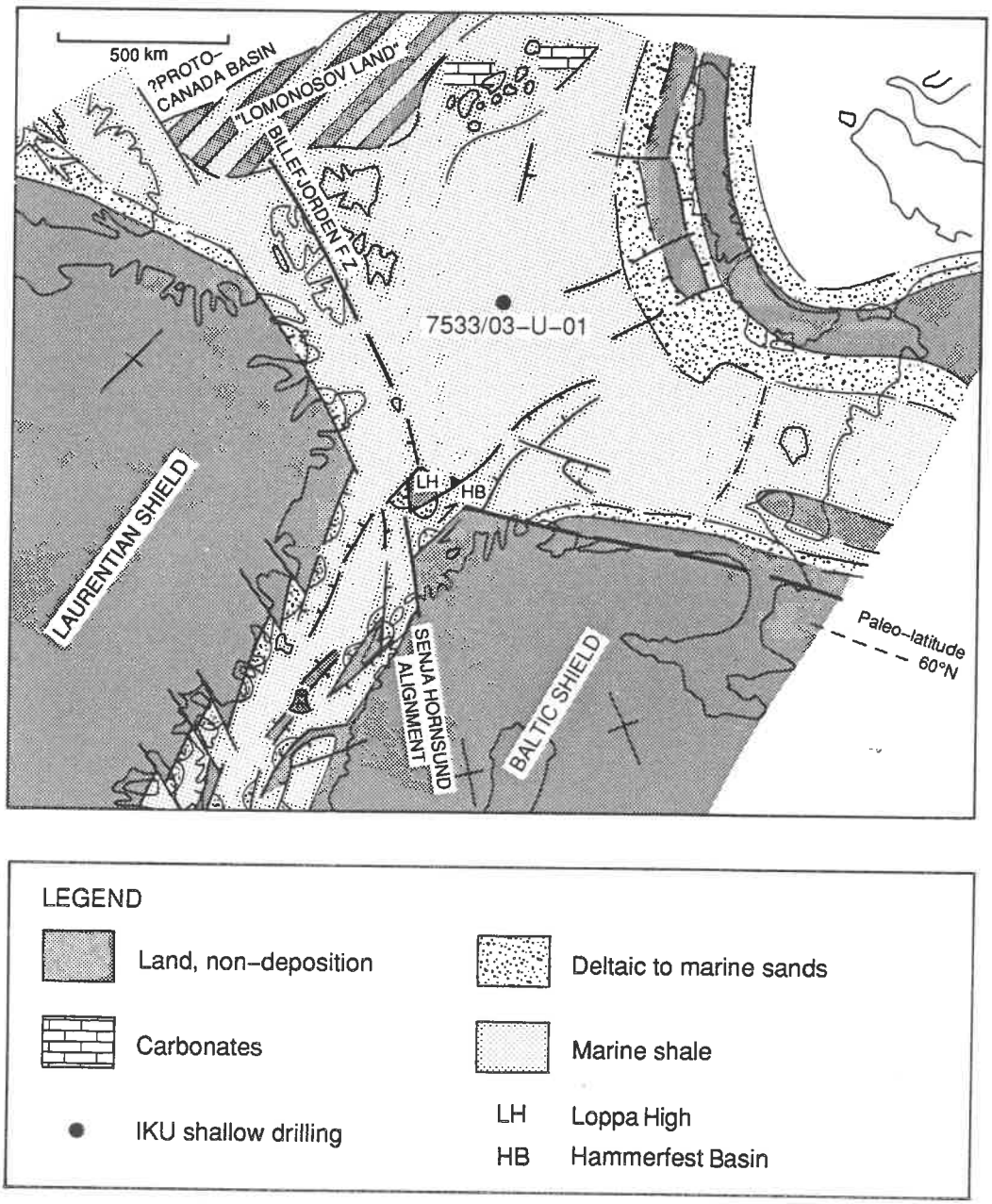

Figure 6.10 Paleogeographic reconstruction of the Late Jurassic (modfied from Doré in press).

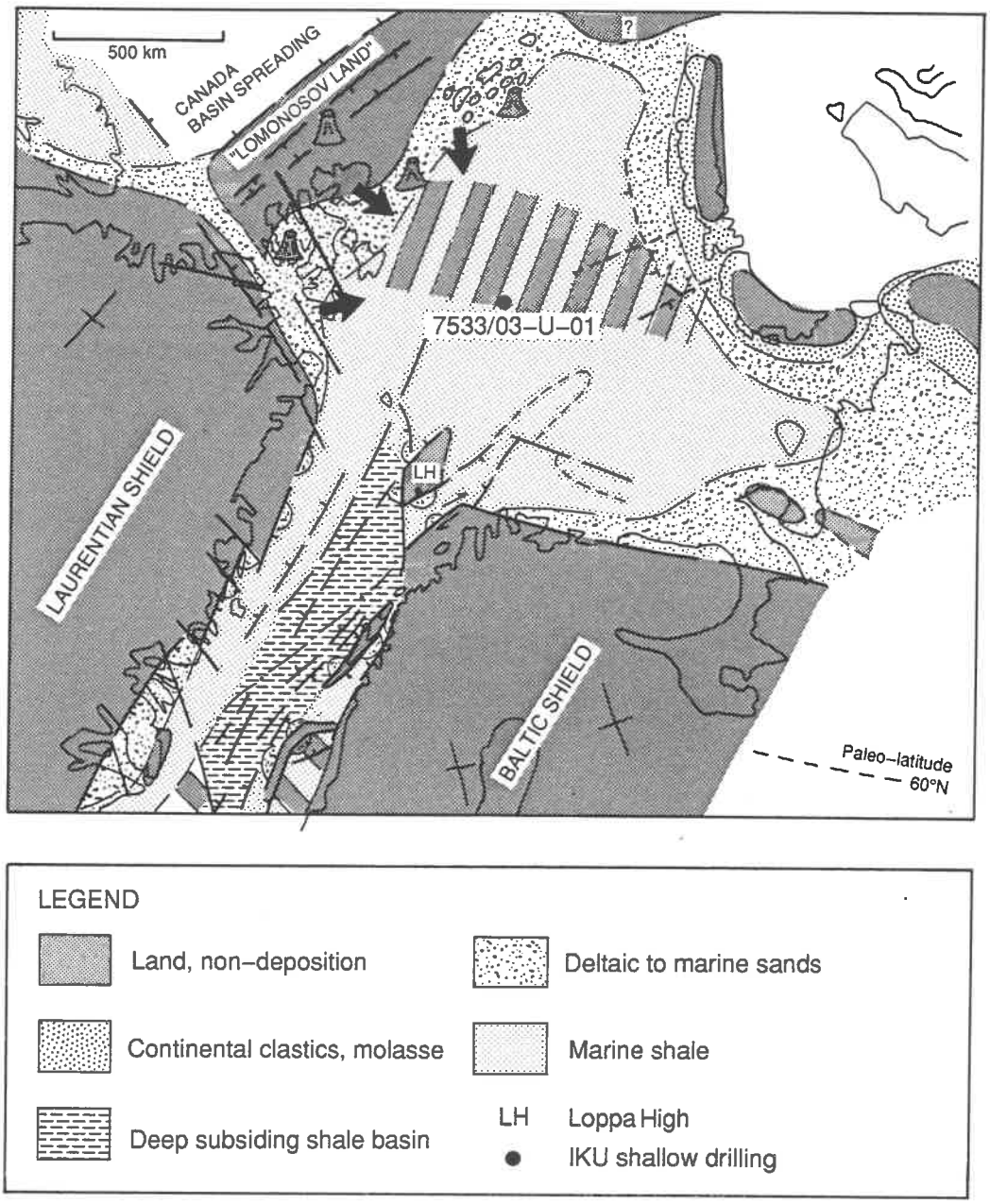

Figure 6.11 Paleogeographic reconstruction of the Early Cretaceous (modified from Doré in press).

Geological information exists from outcrops in the Svalbard Archipelago and on Franz Josef Land and from a few offshore shallow drillings to the west and south of Hopendjupet. In addition, The Norwegian Polar Research Institute (NPRI) has collected some seabed samples with Cretaceous clastic sedimentary rocks from the Olga basin as well as Barremian sandstones sampled close to core-hole 7533/03-U-01 (Elverhøi et al. 1988, Antonsen et al. in press). They also describe a shallow marine limestone which most likely correlates to Unit C encountered in core 7533/03-U-01.

Due to this relatively scattered data base, core 7533/03-U-01 provided an important contribution to our knowledge of the Middle Jurassic - Lower Cretaceous succession in the northern Barents Sea. The core has been divided

into four lithological units which can be related to the established lithostratigraphy in Svalbard and the Hammerfest Basin (Figure 6.12). The four lithological units are discussed in a regional context below.

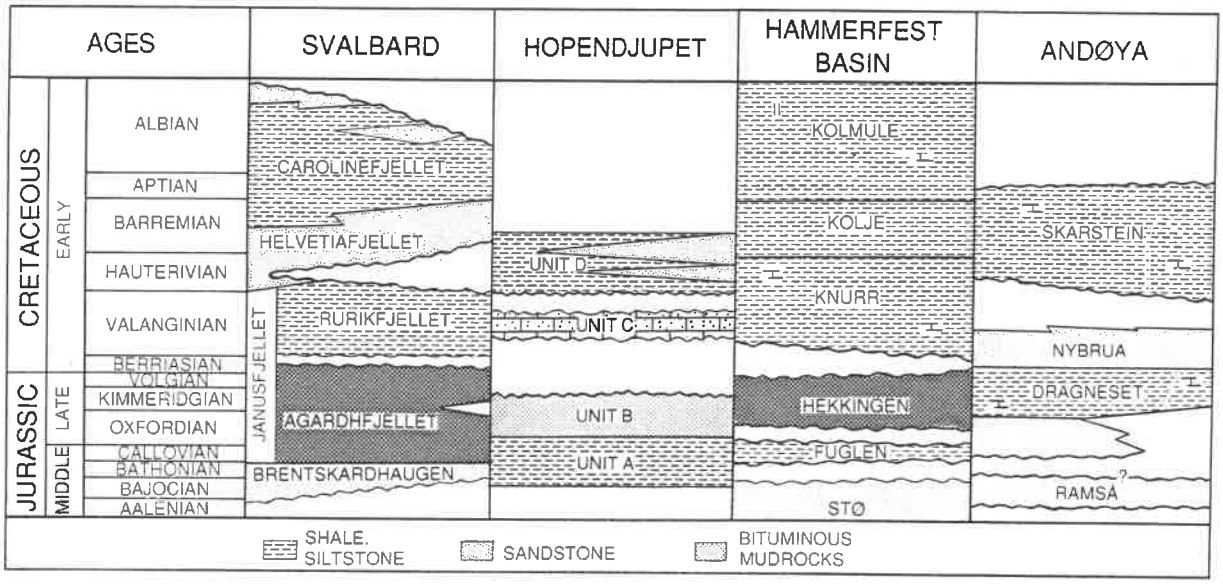

Figure 6.12 *Lithostratigraphical correlation scheme of Svalbard, the Hammerfest Basin and Hopendjupet. Based on Worsley et al. (1988), Leith et al. (in press), and data from the present project.*

Middle Jurassic

Unit A of core 7533/03-U-01 comprises brownish to medium grey mudstone, assigned a probable early Bathonian to earliest Oxfordian age.

The unit may be correlated with the lowermost part of the Janusfjellet Formation on Svalbard (Major & Nagy 1972) and with the Fuglen Formation in the southern Barents Sea (Worsley et al. 1988).

The Fuglen Formation consists of pyritic mudstone with interbedded thin limestone in the Hammerfest Basin. It is thin and condensed on the central highs, but increases in thickness towards the southwest. The most complete section of the Fuglen Formation is encountered in the fault blocks of the Ringvassøy-Loppa and Troms-Finnmark Fault Complexes. Normally, a hiatus is present between the Stø Formation and the Fuglen Formation, spanning the Bajocian to the Late Callovian in the Hammerfest Basin (Worsley et al. 1988).

The Fuglen Formation is there assigned a Late Callovian to Oxfordian age. Based on bio- and lithostratigraphy, we therefore tentatively correlate Unit A in core 7533/03-U-01 with the Fuglen Formation.

On Spitsbergen, the Brentskardhaugen Bed includes parts of the Toarcian - Bathonian succession between the Wilhelmøya Formation and the overlying Janusfjellet Formation of the Adventdalen Group (Figure 6.12). The hiatus is more pronounced in the western parts of Svalbard, where the Wilhelmøya Formation is developed as a condensed sequence capped by the Brentskardhaugen Bed.

The seismic data indicates that core-hole 7533/03-U-01 terminated a few metres or less above the top of another sequence (see Section 5.2). If the underlying sequence is an equivalent to the Stø and Wilhelmøya Formations, the Bathonian to Callovian sequence in Hopendjupet is more complete than its condensed correlatives on Svalbard and in most Barents Sea wells. Due to the well position believed to represent a stable platform area with little tectonic activity prior to the latest Jurassic, an eastward thickening of middle Jurassic strata is proposed.

Upper Jurassic

The Oxfordian to Ryazanian succession in the Barents Sea is characterized by dark grey to black organic rich shales. The Hekkingen Formation in the southwestern Barents Sea, is divided into a lower Alge and an upper Krill Member (Worsley et al. 1988). The Alge Member shows higher gamma readings and is more organic rich than the Krill Member.

The Upper Jurassic succession in the Hammerfest and Nordkapp Basins is thicker than in the platform areas farther to the north. This is believed to have been caused by differential subsidence related to fault activity. Seismic data indicates that the Hekkingen Formation generally is thin in all the platform areas, and a subdivision into Alge and Krill Members is difficult.

From well data it is indicated that the Krill Member in general is thin on the Bjarmeland Platform. The uppermost metres of the Hekkingen Formation in core 7430/10-U-01 can be assigned to the Boreal Berriasian. In this part of the section, a gradual transition from the dark shales typical of the Volgian, to the calcareous overlying Berriasian shales is reported. Organic

content and hydrogen indices are high in the Volgian section, and slightly lower in the uppermost 4 metres of core 7430/10-U-01.

The lowermost 7.5 m of Unit B in core 7533/03-U-01 consist of alternating light grey and black mudrocks, while the uppermost sixteen metres are comprised of black, organic-rich shale assigned a Kimmeridgian age. The black shale succession in the core is analagous both in age and thickness to the Alge Member of the Hekkingen Formation of the Troms area.

The shales of the Alge Member typically have TOC contents of ca 10 wt% in the Troms area (Weiss et al. 1991, IKU Shallow Drilling 1990). They are easily distinguishable from the shales of the overlying Krill Member, based on high gamma readings and TOC content. In the Upper Jurassic shales of the Nordkapp Basin and in core 7430/10-U-01 on the Bjarmeland Platform, organic carbon contents tend to be higher than in the Troms area showing little significant variation with depth. Mean TOC contents in these rocks are typically between 10 wt% and 15 wt%, and may exceed 20 wt% in individual samples.

With regards to kerogen quality, there appears to be a trend of increasing mean hydrogen index to the north and east away from the Troms area (Figure 6.3). A significant input of terrestrial material in the kerogen of the Hekkingen Formation is seen in the Nordkapp Basin and Troms III area reported in IKU shallow drilling programs in 1987, 1988 and 1990 (Elvebakk et al. 1988, Bugge et al. 1989, Weiss et al. 1991). It is interesting to note that the highest terrestrial kerogen contents observed in the Troms III Hekkingen Formation occurred in the more organic-rich Alge Member, decreasing upwards into the Krill Member. This variation was not evident from the hydrogen index data.

Terrestrial kerogen types, such as wood fragments, typically have a higher carbon content per unit mass than marine kerogen types, and may therefore be expected to influence TOC contents to a greater extent. The reverse is generally true regarding the hydrogen content of these kerogen types, certain algal and liptinitic macerals having a disproportionate influence on Rock-Eval character. Thus, it is possible to have radically different kerogen compositions with rather similar bulk chemistry.

In contrast to the Hekkingen Formation of the Troms III area and the Hammerfest Basin, which both appear to have been located in a more proximal position during deposition, the Hekkingen Formation of the Nordkapp Basin and Hopendjupet area shows a remarkably homogeneous bulk organic chemistry. The

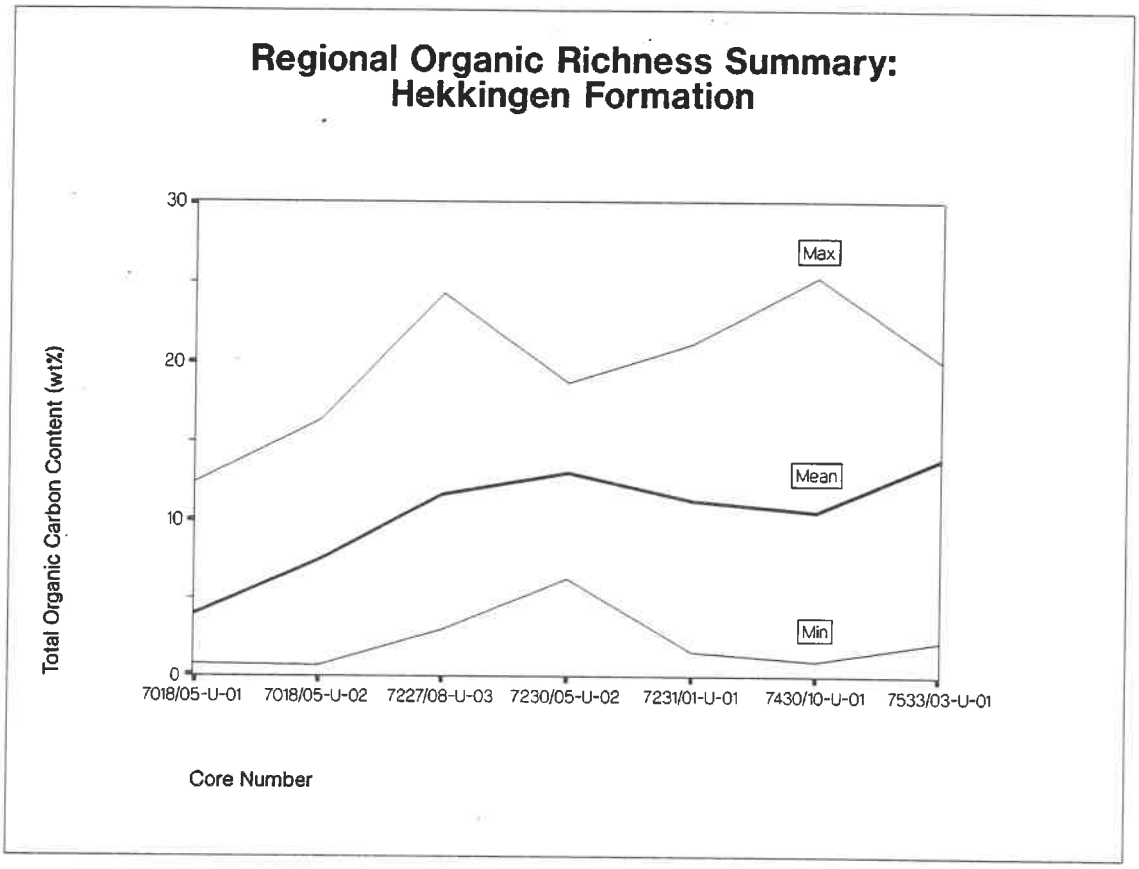

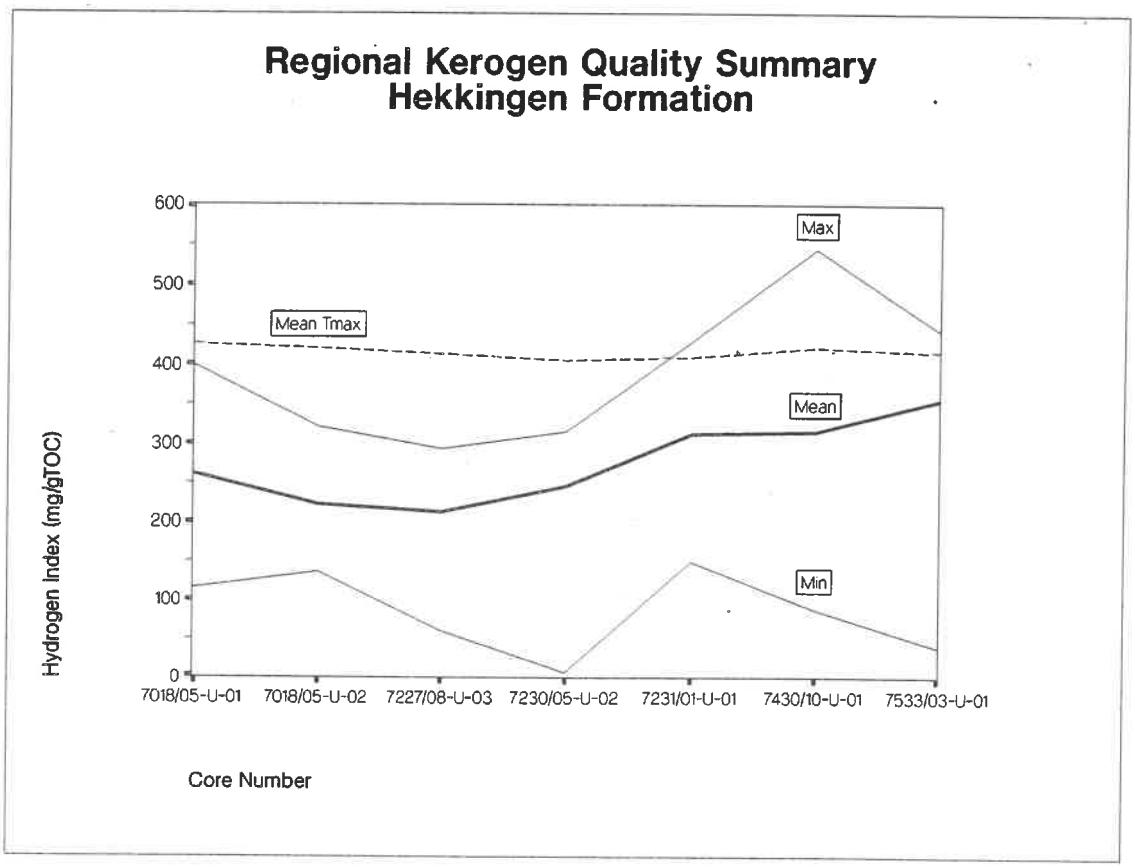

Figure 6.13 *Regional organic richness and kerogen quality summary for the Hekkingen Formation of the western Barents Sea.*

kerogen in these rocks is dominated by amorphous debris, in contrast to the Hekkingen Formation of Troms III, suggesting a more distal depositional setting.

Deposition of black organic rich shales was not synchronous in northwestern Europe as discussed by Doré (in press). The Late Jurassic organic rich shales were deposited in a complex system during a transgressive regime, where the conditions necessary for organic-rich shale deposition in the individual basins must have been related to local tectonics, overall geometry and position in the late Jurassic seaway. While there is general agreement that the Upper Jurassic shales of the Barents Sea were deposited in a dysoxic/anoxic marine shelf setting, Dypvik (1985), Gage & Doré (1986), Hvoslef et al. (1986) and Worsley et al. (1988) have suggested that the shales of the Agardhfjellet Member of the Janusfjellet Formation of Svalbard were deposited in a transgressive open shelf setting periodically influenced by anoxicity. In this case, low hydrogen indices associated with black shales were suggested as representing oxidation of the organic matter during transport in the water column followed by deposition in an anoxic water column.

Regarding the water depths associated with the deposition of marine organic-rich shales, there is more uncertainty. Detailed study of similar black shales adjacent to the North Sea area has provided evidence of deposition close to storm wave-base with estimated depths of ca 50-100 m (Myers & Wignall 1987, Oschmann 1988), although water depths may have been greater in the grabens. Surlyk (1989) and Stow et al. (1982) have postulated shallow water depths associated with organic-rich shale deposition and associated turbidite deposition. It is therefore important not to assume that "black shale deposition = deep anoxic basin deposition". Water depth has, however, a number of implications on the understanding of the geological development of the area, not least when combined with consideration of variations in sea level.

Lower Cretaceous

Geological information of the Lower Cretaceous from the northern Barents Sea is limited to the seabottom sampling carried out by the NPRI, mainly in the Olga basin (Elverhøi et al. 1988, Antonsen et al. in press). Farther south, a Lower Cretaceous section was cored by IKU in 1988 (core 7430/10-U-01) and in 1985 (core 7425/09-U-01). The latter comprised a brownish red, silty

claystone above a shallow marine limestone unit containing the bivalves *Inoceramus* and *Buchia*. In core 7430/10-U-01, a 5 m thick marly unit separates Berriasian and Barremian sediments (Bugge et al. 1989, IKU Shallow Drilling 1988).

In the Barents Sea south of 74°N, the Hauterivian section encountered in wells is in general made up of shale, marl and thin limestone units. Brownish and brick red colours are commonly reported from the cuttings material from the deep wells in the Hammerfest Basin.

In the Svalbard Archipelago a stable platform area existed at this time, influenced by NNW-SSE trending faults (e.g. the Billefjorden and Agardhbukta faults) controlling deposition locally. During the Callovian-Hauterivian, open marine organic rich shales were deposited, seen in the Janusfjellet Formation. During Barremian to ?Aptian deltaic sandstone of the Helvetiafjellet Formation (e.g. Steel & Worsley 1984) were deposited from deltaic complexes prograding southeast- and southwards from uplifted land areas in west and northwestern Spitsbergen, probably extending eastward to the Lomonosov High (Figure 6.11). Slumping of delta front blocks from the Hauterivian-Barremian section near Kvalvågen in eastern Spitsbergen is described by Nemec et al. (1988) who also indicated an extensive fluvio-deltaic system prograding to the south-southeast, across most of the southern Spitsbergen.

Probably related to the tectonic activity in connection with the opening of the Canada Basin in the north, basalts from Hauterivian - Barremian eruptions cover most of the Svalbard and Franz Josef Land archipelagoes. Basaltic lavas are also interbedded in deltaic sediments on Kong Karls Land and in non-marine Hauterivian - Barremian deposits on Novaya Zemlya (Kelly 1988).

On Kong Karls Land, Smith et al. (1976) reported Barremian continental sandy facies, and Verdenius (1978) has dated a marly clay to Valanginian based on calcareous nannofossils. The latter is correlated with the nodular limestone of Unit C in core 7533/03-U-01. This limestone unit represents a condensed and probably incomplete section, directly overlying the Kimmeridgian. This sequence may have been deposited on a relatively shallow oxygenated platform with very low sedimentation rate.

The light grey fossiliferous packstone of Valanginian age recorded in core 7533/03-U-01 is widely distributed (Århus in press), and seems easy to correlate over a wide area. Similar Valanginian-Hauterivian condensed

carbonate rich successions have been penetrated in the shallow cores 7425/09-U-01, 7320/03-U-01, 7231/01-U-01 and 7430/10-U-01 in the Barents Sea (Århus in press). A neighbouring area with comparable Valanginian lithology is Kongsøya in Kong Karls Land. In Spitsbergen and in sections along Izhma River in the Pechora Basin the Valanginian and Hauterivian section is thicker and dominated by claystones.

A paleogeographic model for this condensed carbonate-enriched interval probably implies deposition on a shallow marine shelf with low sedimentation rate and periodical storm influence. Deeper marine basins probably existed to the west in the Spitsbergen area and in the east towards Novaya Zemlya.

The clastic Unit D recorded in well 7533/03-U-01 is dated as Hauterivian - ?lower Barremian. It is composed of two main lithologies, reddish brown/greenish grey siltstone and the light grey sandstone referred to as lithofacies D1 and D2, respectively. These facies are interpreted to have different source areas and to represent different mechanisms of deposition, mud-/debris flows and turbidity currents, respectively (see Sections 5.3 and 6.3). We tentatively correlate the turbidite sands with the Festningen deltaic sandstone of the Helvetiafjellet Formation on Spitsbergen. The sandstones seem to be mainly coeval, although Unit D of core 7533/03-U-01 is more marine influenced than the Festningen sandstone. Alternatively, a Festningen equivalent could be situated above the section cored at site 7533/03-U-01.

Seismic data has been interpreted in order to study the seismic facies changes in the lowermost Cretaceous in the Olga basin area. Core-hole 7533/03-U-01 was in the southern part of this area.

Two of the boundaries of the lowermost Cretaceous section are interpreted as sequence boundaries. The lowermost correlates with the base of the marly limestone (Unit C) in core 7533/03-U-01 and is defined by onlap on the characteristic "Base of Cretaceous" reflector. The second one is defined by downlap of the overlying Lower Cretaceous section which shows progradation from a northerly direction. This sequence boundary was not penetrated in the well, but is supposed to be situated only a few metres above the top of the cored sandstone interval (see Section 5.2).

From seismic data, the sequence encountered as Hauterivian - lower Barremian sand-/siltstones in Unit D of core 7533/03-U-01 has been separated into two different seismic facies. Seismic facies I refers to a seismic sequence which in general shows increase in thickness to the east,

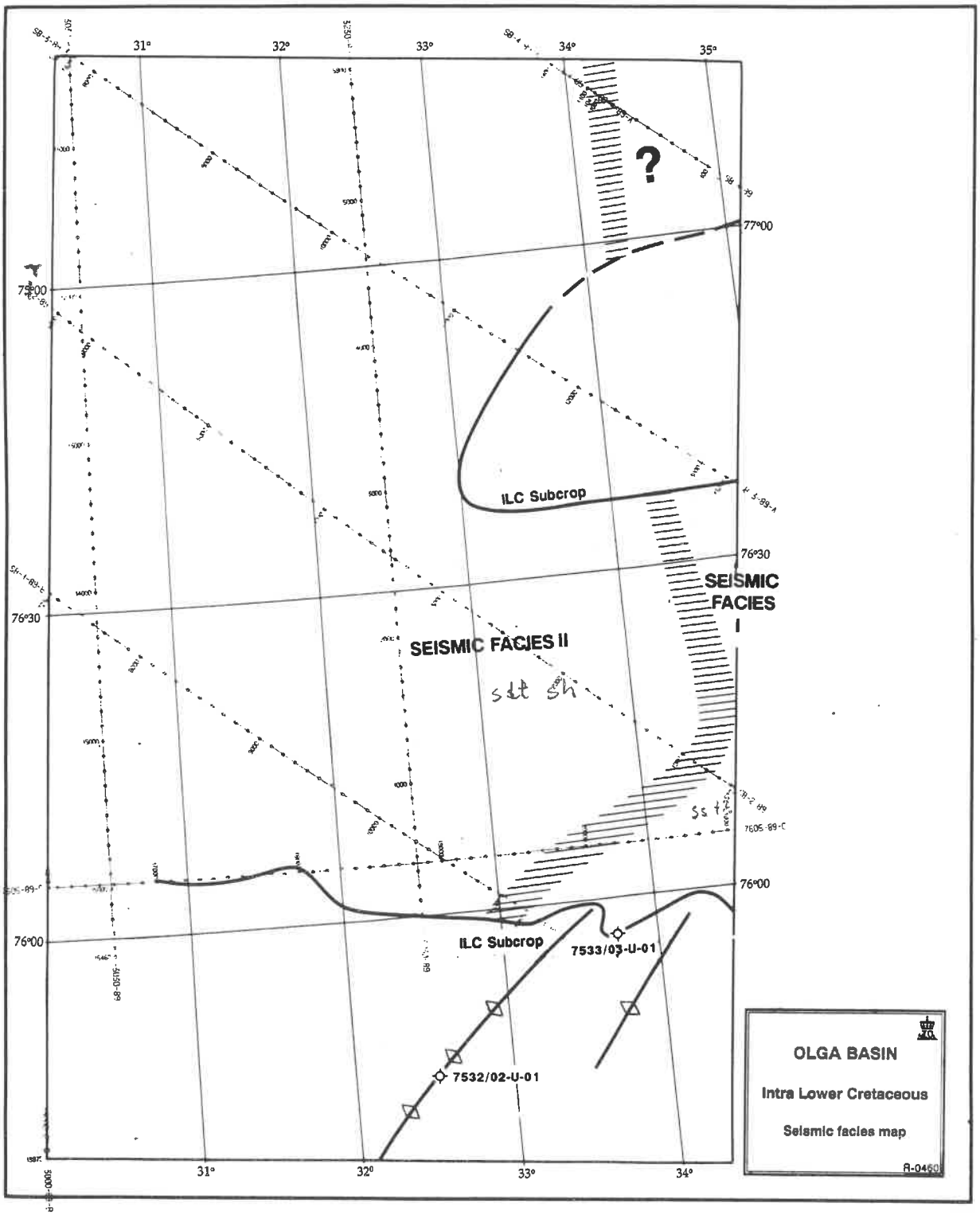

Figure 6.14 *Sketch map showing seismic facies of the Hauterivian - Barremian sequence in the Olga basin. Seismic facies I is interpreted as sandy and facies II as shaly.*

and which in some areas has a mounded structure. The reflection strength varies. In areas where the sequence outcrops to the sea floor, there is in

general a positive form with very little Quaternary cover (<1-2 m), suggesting more competent rocks than in the surrounding shales. At site 7533/03-U-01 also the Upper Jurassic shales show, however, specific competence against erosion and appear with a positive form on the seabed. Both core-hole 7533/03-U-01 and the NPRI samples are situated within the seismic facies I area (Figure 6.14), which is interpreted to consist mainly of sandstones with interbedded siltstones and claystones.

Seismic facies II is characterized by a sequence of parallel reflections with good continuity and with small changes in thickness (Figure 6.15). In general there is no positive form on the sea floor where this sequence outcrops, and the Quaternary thickness varies. Lithofacies within this seismic unit is interpreted to mainly consist of siltstones and claystones.

The sandy facies I seems to be limited to the eastern parts of the study area (Figure 6.14), shaling out to facies type II towards the west. It should, however, be noted that the definition of seismic facies II is less reliable to the north both due to poor data coverage, and due to the fact that the development of facies II is not so clear.

Seismic evidence indicates that at least some of the large anticlines in the Olga basin had a period of growth during the latest Jurassic/early Cretaceous. There is no such evidence for the main anticline where core 7533/03-U-01 was drilled, because of the deep erosion taking place after Cretaceous time. The shallow seismic lines crossing the large anticline structure farther north, in the central part of Kong Karl platform indicate, however, that the crest of the anticline was eroded in the early Cretaceous. Onlap of the Lower Cretaceous sequence onto the Jurassic rocks can be demonstrated in these lines, which also show thickening and facies change towards more laminated (shaly?) development away from the crest of the anticline (Figure 6.15).

Observation of growth in the lowermost Cretaceous section along the normal faults supports that such a tectonic activity took place, a fact also noted by Antonsen et al. (in press).

The major anticlines in the Olga basin, Kong Karl platform and the Sentralbanken high are thought to have a common history. Thus, in our tectonic model, movements in the latest Jurassic and early Cretaceous resulted in the formation of low relief NNE-SSW trending anticlines and NW-SE trending normal faults. The anticline crests were exposed to erosion in the

early Cretaceous, and their present shape was formed during later reactivation of the anticlines, probably some time during the Paleogene. A probable paleogeographic model for the lower Cretaceous section in core 7533/03-U-01 is presented below. Due to lack of intermixing of the sand prone turbiditic sediments and the reddish/greenish mud-/debris flow deposits in the core, we interpret the sediments to have been derived from two different source areas.

The reddish brown and greenish grey siltstone facies is interpreted to have been deposited by mud-/debris flows from a source area close to the well. This could be an island formed by tectonic uplift of the anticline where core 7532/02-U-01 was drilled (Figure 6.15). The massive sandstone is interpreted to have been deposited by turbidity currents derived from a different source area, most probably a delta front building out in the north and east (Svalbard - Franz Josef Land - Eastern Barents Sea).

The erosion of anticlines coincides with the above discussed tectonic history of the area, where the anticlines were exposed in the early Cretaceous (Figure 6.11) as a result of the tectonic movements in the latest Jurassic/-early Cretaceous. This tectonic activity could also have triggered the mass flows.

The source of the red coloured mud-/debris flow sediments had been subaerially exposed, and could still be partly above sea level when the anticlines were uplifted. Seasonal or unregular rainfall, could therefore have favoured generation of mud-/debris flows. In addition to being water saturated, the sediments may have collapsed because of earthquake activity. Although other agents such as wave abrasion and slope steepening, possible weak fault planes within the sediment etc. could have influenced the sliding, we believe water saturation and tectonic activity to be the most important causes for triggering the debris flows.

It is expected that the turbidites of lithofacies D2 had the ability of moving farther than the mud-/debris flows. They would probably need a slope of some 3-5° to be released, but could maintain their movement on a slope of even less than 1-2° (e.g. Bugge et al. 1987). Seismic data indicates a limited structural relief. As an example, a difference in elevation of 100 m corresponds to a distance of 6-12 km, given a slope of 0.5-1°. The anticlines are generally farther away (Figures 6.1 and 6.6). The delta front could have a regional extent and have moved over some distance, thus distributing the turbidite sand over a fairly wide area. Our seismic coverage is poor to the east and north, so any delta front has not yet been recognized seismically.

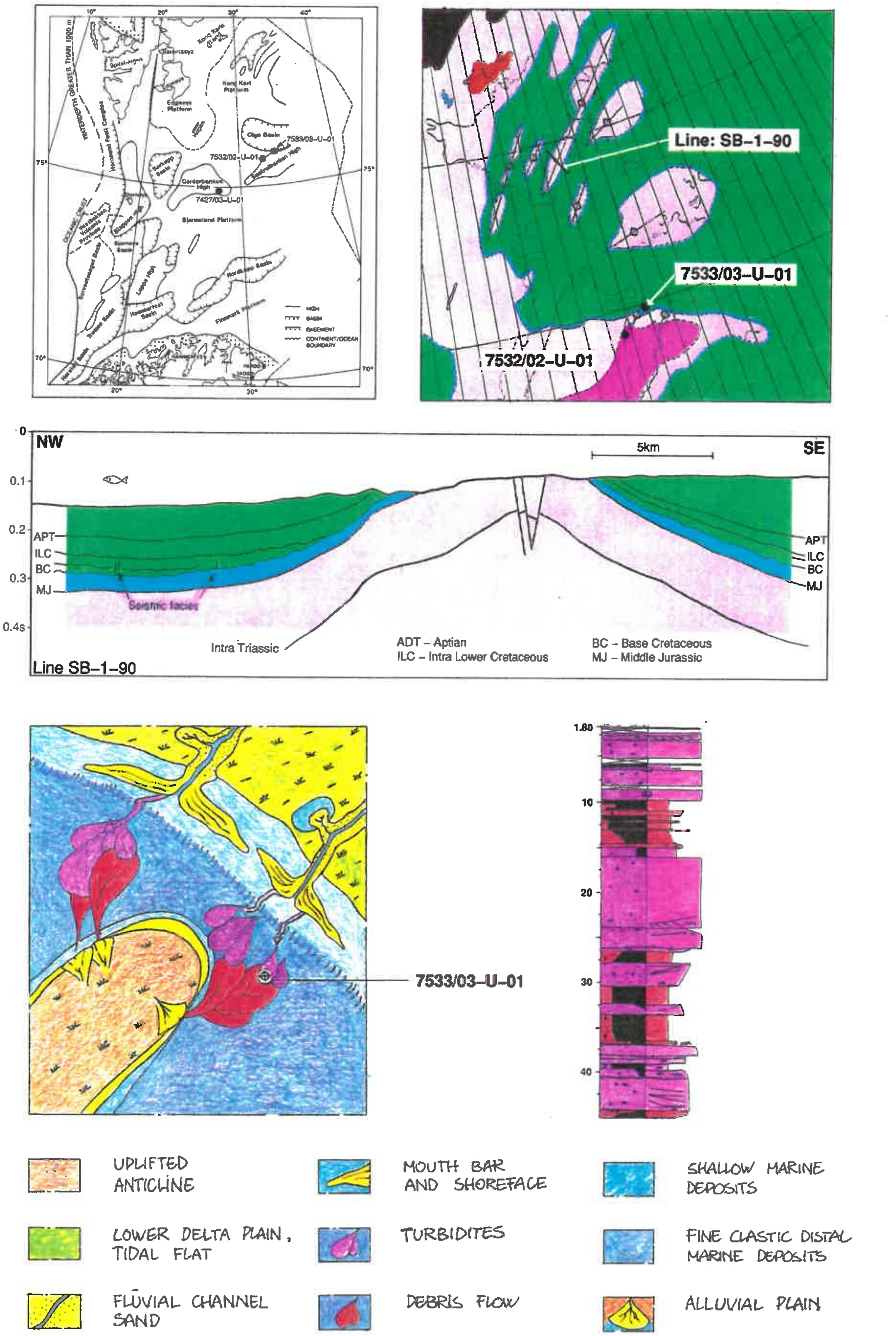

Figure 6.15 *Suggested depositional model for the Hauterivian - (early Barremian) sediments of Unit D of core 7533/03-U-01. The reddish brown/greenish grey siltstones are interpreted as mud flow/debris flow deposits derived from a subaerially exposed anticline. The light grey sandstones are interpreted as high density turbidites deposited from a prograding delta front. The sediment flows were probably triggered by earthquakes.*

The sandstones are interpreted as high density turbidites (transition to grainflow), derived from unstable sand rich mouth bars collapsing from time to time, and deposited in water depths below storm wave base in what was normally muddy environment.

We tend to associate the mouth bar/delta front failure and triggering of turbidites with seismic shocking. This mechanism is discussed by Nemec et al. (1988) in a relative time equivalent and comparable area in East Spitsbergen. They conclude that earthquakes induced the loss of strength in the detachment zone, thus triggering the collapse of the delta front.

IKU SINTEF GRUPPEN

7. REFERENCES

ANTONSEN, B., ELVERHØI, A., DYPVIK, H., SOLHEIM, A. in press: Shallow bedrock geology of the Olga Basin area, Northwestern Barents Sea. The American Association of Petroleum Geologists Bulletin.

BÄCKSTROM, S.A., NAGY, J. 1985: Depositional history and fauna of a Jurassic phosphorite conglomerate (the Brentskardhaugen Bed) in Spitsbergen, Norsk Polarinstitutts Skrifter, 183, 61p.

BIRKELUND, T., CALLOMON, J.H., CLAUSEN, C.K., NØHR-HANSEN, H., SALINAS, I. 1983: The Lower Kimmeridge Clay at Westbury, Wiltshire, England. Proceedings Geological Association (94(4), 289-309.

BIRKELUND, T., CALLOMON, J.H. 1985: The Kimmeridgian ammonite faunas of Milne Land, central East Greenland. Grønlands Geologiske Undersøgelse Bulletin 153, 56p.

BLUEMLE, J.P., CLAYTON, L. 1984: Large -scale glacial thrusting and related processes in North Dakota. Boreas 13, 279-299.

BUCHAN, S.H., CHALLINOR, A., HARLAND, W.B., PARKER, J.R. 1965: The Triassic stratigraphy of Svalbard. Norsk Polarinstitutt Skrifter 135, 94p.

BUGGE, T. 1983: Submarine slides on the Norwegian continental margin, with special emphasis on the Storegga area. Continental Shelf Institute Publication 110, 152p.

BUGGE, T., BEFRING, S., BELDERSON, R.H., EIDVIN, T., JANSEN, E., KENYON, N.H., HOLTEDAHL, H., SEJRUP, H.P. 1987: A Giant Three-Stage Submarine Slide Off Norway. Geo-Marine Letters, 7, 191-198.

BUGGE, T., ELVEBAKK, G., BAKKE, S., FANAVOLL, S., LIPPARD, S., LEITH, T.L., MANGERUD, G., MØLLER, N., NILSSON, I., RØMULD, A., SCHOU, L., VIGRAN, J.O., WEISS, H.M., ÅRHUS, N. 1989: Shallow Drilling Barents Sea 1988: Main Report. IKU Report 21.3444.00/03/89. Confidential.

CALLOMON, J.H. 1985: The evolution of the Jurassic ammonite family Cardioceratidae. Palaeontology Special Paper, 33, 49-90.

CARMAN, C.J., HARDWICK, P. 1983: Geology and regional setting of the Kuparuk oil field, Alaska. The American Association of Petroleum Geologists (AAPG) Bulletin, 67, 1014-1031.

CLEMMENSEN, L.B. 1980: Triassic rift sedimentation and palaeogeography of central East Greenland. Grønlands Geologiske Undersøgelse, Bulletin 136, 72p.

DALLAND, A., WORSLEY, D., OFSTAD, K. 1988: A lithostratigraphic scheme for the Mesozoic and Cenozoic succession offshore mid- and northern Norway. Norwegian Petroleum Directorate (NPD) Bulletin, 4, 65p.

DETTERMAN, R.L., REISER, H.N., BROSGE, W.P., DUTRO, J.T., 1975: Post-Carboniferous stratigraphy, Northeastern Alaska. USGS Prof. Paper 886, 46p.

DORÉ, A.G. in press: The structural foundation and evolution of Mesozoic Seaways between Europe and the Arctic Sea. In: Development of the Tethyan ocean. Palaeogeography, Palaeoclimatology, Palaeoecology, Special Issue. (Channell, Tansa & Winterer eds.).

DYPVIK, H. 1985: Jurassic and Cretaceous black shales of the Janusfjellet Formation, Svalbard, Norway. Sediment. Geol., 41, 235-248.

ELVEBAKK, G., BUGGE, T., EEM, J. V.D., FANAVOLL, S., FJERDINGSTAD, V., HAUGANE, E., LEITH, T.L., MØRK, A., RENDALL, H., SKARBØ, O., SMELROR, M., SÆTTEM, J., VIGRAN, J.O., WEISS, H.M., ÅRHUS, N. 1988: Shallow Drilling Barents Sea 1987: Main Report. IKU Report 21.3427.00/04/87. Confidential.

ELVERHØI, A., SOLHEIM, A. 1987: Shallow geology and geophysics of the Barents Sea - with special reference to the existence and detection of submarine permafrost. Norsk Polarinstitutt, No.37, 71p, 7 app.

EMBRY, A.F., in press: Mesozoic history of the Arctic Islands. In: Trettin, H.P, (ed.), Innuitian Orogen and Arctic Platform: Canada and Greenland. Geological Survey of Canada, Geology of Canada No. 3. (Also, The Geology of North America, Geological Society of America, v.E.).

EMBRY, A.F. 1989: Correlation of Upper Palaeozoic and Mesozoic sequences between Svalbard, Canadian Arctic Archipelago, and northern Alaska. In: Collinson, J.O. (ed.), Correlation in Hydrocarbon Exploration. Norwegian Petroleum Society. Graham & Trotman, 89-98.

ESHET, Y., COUSMINER, H.L. 1986: Palynozonation and correlation of the Permo-Triassic succession in the Negev, Israel. Micropaleontology, 32(3), 193-214.

ESPITALIE, J., DEROO, G., MARQUIS, F. 1986: La Pyrolyse Rock-Eval et ses Applications. Rev. Inst. Fr. Pét., v40, 755-784.

ESPITALIE, J., SENGA MAKADI, K., TRICHET, J. 1984: Role of mineral matrix in kerogen pyrolysis. Org. Geochem. 6, 365-382.

FISHER, M.J. 1979: The Triassic palynofloral succession in the Canadian Arctic Archipelago. AASP Contribution Series 5B, 83-100.

GABRIELSEN, R.H., FÆRSETH, R.B., JENSEN, L.N., KALHEIM, J.E., RIIS, F. 1990: Structural elements of the Norwegian continental shelf Part I: The Barents Sea region. Norwegian Petroleum Directorate (NPD) Bulletin 6, 33p, 16pls.

GAGE, M.S., DORÉ, A. 1986: A regional geological perspective of the Norwegian offshore exploration provinces. In: A.M. Spencer et al (eds.), Habitat of Hydrocarbons on the Norwegian Continental Shelf, Graham & Trotman, 21-38.

GRAMBERG, I.S. (ed.) 1988: The Barents Sea Shelf Plate. Trudy PGO'Sevmorgeologiya' L., Nedra, 196, 263p. (In Russian).

HALD, M., SÆTTEM, J., NESSE, E. 1990: Middle and Late Weichselian stratigraphy in shallow drillings from the southwestern Barents Sea: foraminiferal, amino-acid and radiocarbon evidences. Norsk Geologisk Tidsskrift 70, 241-257.

HOCHULI, P.A., COLIN, J.P., VIGRAN, J.O. 1989: Triassic biostratigraphy of the Barents Sea area. In: Collinson, J.O. (ed.), Correlation in Hydrocarbon Exploration, Norwegian Petroleum Society. Graham & Trotman, 131-153.

HVOSLEF, S., DYPVIK, H., SOLLI, H. 1986: A combined sedimentological and organic geochemical study of the Jurassic/Cretaceous Janusfjellet Formation (Svalbard), Norway. In: D. Leythaeuser & J. Rullkotter (eds.), Advances in Org. Geochem. 1985, Org. Geochem., 10, 101-111.

JACOBSEN, V.W., VAN VEEN, P. 1984: The Triassic offshore Norway north of 62°N. In: Spencer, A.M., et al. (eds.), Petroleum Geology of the north European Margin. Norwegian Petroleum Society, Graham & Trotman, 317-328.

KAR, R.K., KIESER, G., JAIN, K.P. 1972: Permo-Triassic subsurface palynology from Libya. Pollen & Spores, 14(4), 389-453.

KATZ, B.J. 1983: Limitations of 'Rock-Eval' pyroloysis for typing organic matter. Org. Geochem. 4, 195-199.

KELLY, S.R.A. 1988: Jurassic through Cretaceous stratigraphy of the Barents shelf. In: Harland, W.B. & Dowdeswell, E.K. (eds.), Geological evolution of the Barents Shelf Region, Graham & Trotman, 109-130.

KING, C., BAILEY, H.W., BURTON, C.A., KING, A.D. 1989: Cretaceous of the the North Sea. In: Jenkins, D.G. & Murray, J. (eds.), Stratigraphical Atlas of Fossil Foraminifera. (2nd ed). 372-417.

LEITH, T.L., WEISS, H.M., MØRK, A., ÅRHUS, N., ELVEBAKK, G., EMBRY, A.F., BROOKS, P.W., STEWART, K.R., PCHELINA, T.M., BRO, E.G., VERBA, M.L., DANYUSHEVSKAYA, A., BORISOV, A.V. in press: Mesozoic hydrocarbon source-rocks of the Arctic Region. Submitted to Proceedings of "Arctic Geology and Petroleum Geology" Conference, Tromsø, 1990.

LØVØ, V., ELVERHØI, A., ANTONSEN, P., SOLHEIM, A., BUTENKO, G., GREGERSEN, O., LIESTØL, O. 1990: Submarine permafrost and gashydrates in the northern Barents Sea. Norsk Polarinstitutt (NPI) Rapport Nr 56. 171p.

MAJOR, H., NAGY, J. 1972: Geology of the Adventdalen map area, with the geological map Adventdalen C9G 1:100 000 of Major from 1964. Norsk Polarinstitutt, skrifter 138.

MANGERUD, G., RØMULD, A. in press: Spathian-Anisian (Triassic) Palynology at the Svalis Dome, Southwestern Barents Sea. Accepted for publication in Review of Palaeobotany and Palynology.

MESEZHNIKOV, M.S. 1984: Kimmeridzskiy i volzhiskiy yarusi severa SSSR. 166p., Nedra, Leningrad.

MOE, A. 1983: Biostratigrafi i Tertiær og Kritt på Haltenbanken. Internal Norwegian Petroleum Directorate (NPD) report.

MYERS, K.J., WIGNALL, P.B. 1987: Understanding Jurassic Organic-rich Mudrocks - New Concepts using Gamma-ray Spectrometry and Palaeoecology examples from the Kimmeridge Clay of Dorset and the Jet Rock of Yorkshire. In: Leggat, J.K. & Zuffa, G.G., Marine Clastic Sedimentology, Graham & Trotman, 172-189.

MØRK, A., KNARUD, R., WORSLEY, D. 1982: Depositional and diagenetic environments of the Triassic and Lower Jurassic succession of Svalbard. In: Embry, A.F., Balkwill, H.R. (eds.), Arctic Geology and Geophysics, Canadian Society of Petroleum Geologists Memoir 8, 371-398.

MØRK, A., EMBRY, A., WEITSCHAT, W. 1989: Triassic transgressive-regressive cycles in the Sverdrup Basin, Svalbard and the Barents Shelf. In: Collinson, J.O. (ed.), Correlation in Hydrocarbon Exploration. Norwegian Petroleum Society. Graham & Trotman, 113-130.

MØRK, A., VIGRAN, J.O., HOCHULI, P.A. 1990: Geology and palynology of the Triassic succession of Bjørnøya. Polar Research 8, 141-163.

MØRK, A., VIGRAN, J.O., WEITSCHAT, W., KORCHINSKAYA, M.V., PCHELINA, T.M., FEFILOVA, L.A., VAVILOV, M.N. in press: Triassic rocks in Svalbard, the Arctic Soviet islands and the Barents Shelf; bearing on their correlations. Submitted to Proceedings of "Arctic Geology and Petroleum Geology" Conference, Tromsø, 1990.

NEMEC, W., STEEL, R.J., GJELBERG, J., COLLINSON, J.D., PRESTHOLM, E., ØXNEVAD, I.E. 1988: Anatomy of Collapsed and Re-established Delta Front in Lower Cretaceous of Eastern Spitsbergen: Gravitational Sliding and Sedimentation Processes. The American Association of Petroleum Geologists Bulletin, V.72, No.4, 454-476.

NJÅ, E. ROSENAU 1985: Lower Cretaceous Foraminiferal Stratigraphy. Part 1.Nof 62. Internal Norwegian Petroleum Directorate (NPD) report.

NOTH, R. 1951: Foraminifern aus unter- und oberkreide des Osterreichischen anteils an flysch, Helvetikum und Vorlandkommen. Jahrb. der Geol.Bundesant. Sonderb.3.

OSCHMANN, W. 1988: Kimmeridge Clay Sedimentation - A New Cyclic Model. Palaeogeography, Palaeoclimatology, Palaeoecology, 65, 217-251.

POULTON, T.P. 1987: Zonation and correlation of Middle Boreal Bathonian to Lower Callovian (Jurassic) ammonites, Salmon Cache Canyon, Porcupine River, northern Yukon. Geological Survey of Canada Bulletin 358, 155p.

RØNNEVIK, H., BESKOW, B., JACOBSEN, H. P. 1982: Structural and stratigraphic evolution of the Barents Sea. Canadian Society of Petroleum Geologists, Memoir 8, 431-440.

SCHOELL, M. 1983: Genetic Characterisation of Natural Gases. The American Association of Petroleum Geologists Bulletin, 67, 2225-2238.

SIGMOND, E. in prep: Berggrunnskart over norske land- og havområder, 1:3 mill. Norges Geologiske Undersøkelse.

SKARPNES, O. 1989: Tertiary uplift and erosion - effects on prospectivity. Proceedings of Int. Seminar on Seismic Stratigraphy of the Barents Sea Region, 183-192.

SMITH, D.G., HARLAND, W.B., HUGHES, N.F., PICKTON, C.A.G. 1976: The geology of Kong Karls Land, Svalbard. Geological Magazine 113, 193-232.

SOLHEIM, A., ELVERHØI, A., FINNEKÅSA, Ø. 1988: Marine geophysical/-geological cruise in the Northern Barents Sea 1987 - Cruise Report.

SOLHEIM, A., ELVERHØI, A., ANTONSEN, P., NYLAND BERG, M., RUSSWURM, L. 1990: "Krater-strukturer" på havbunnen i Barentshavet, mulige dannelsesmekanismer og deres betydning for forståelsen av Barentshavets glasial-geologiske historie. Geonytt 1/90, abstract.

STEEL, R.J., WORSLEY, D. 1984: Svalbard's post-Caledonian strata. An atlas of sedimentational patterns and palaeogeographic evolution. In:Spencer, A. M. et al. (eds.), Petroleum Geology of the north European Margin. Norwegian Petroleum Society, Graham & Trotman, 109-135.

STOW, D.A.V., BISHOP, C.D., MILLS, S.J. 1982: Sedimentology of the Brae Oil-field, North Sea: Fan Models and Controls. Journal Petroleum Geol., 5, 129-148.

SURLYK, F. 1989: Mid-Mesozoic syn-rift turbidite systems: controls and predictions. In: J.D. Collinson (ed.), Correlation in Hydrocarbon Exploration. Graham & Trotman, 231-242.

SYKES, R.M., CALLOMON, J.H. 1979: The Amoeboceras zonation of the boreal Upper Oxfordian. Palaeontology 22, 4, 839-903.

SÆTTEM, J. 1988: Varmestrømsmålinger i Barentshavet. Extended abstract from paper presented at the 18th. Geological winter meeting in Copenhagen, 1986.

SÆTTEM, J. 1990: Glaciotectonic forms and structures on the Norwegian continental shelf: observations, processes and implications. Norsk Geologisk Tidsskrift 70, 81-94.

SÆTTEM, J. in press.: Glaciotectonic structures along the margin of the southern Barents shelf. Submitted for publication in the proceedings from the INQUA Commission on the formation and Properties of Glacial Deposits. Balkema.

SÆTTEM, J. in prep.: Glaciotectonism - an important process in Late Cenozoic erosion in the southwestern Barents Sea? Manuscript prepared for publication.

TETRA TECH 1982: Petroleum Exploration of NPRA, 1974-1981, Tetra Tech Report no. 8200, Energy Management Division, Tetra Tech Inc., Anchorage, Alaska, 183p.

THOMPSON, K.F.M. 1987: Fractionated aromatic petroleums and the generation of gas-condensates. Org. Geochem., 11, 573-590.

ULMISHEK, G. 1985: Geology and petroleum resources of the Barents - northern Kara Shelf in light of new geologic data. Argonne National Laboratory ANL/ES-148, 1-89.

VAN DER ZWAN, C.J. 1990: Palynostratigraphy and Palynofacies Reconstruction of the Upper Jurassic to Lowermost Cretaceous of the Draugen Field, Offshore Mid Norway. In: Review of Palaeobotany and Palynology, 62, 157-186.

VERDENIUS, J. 1978: A Valanginian calcareous nannofossil association from Kong Karls Land, Eastern Svalbard. Norsk Polarinstitutt Årbok 1977, 350-352.

VIGRAN, J.O., ELVEBAKK, G., BUGGE, T., FJERDINGSTAD, V., GOLL, R.M., KONIECZNY, R., MØRK, A., LEITH, L., HAUGEN, G., BERG, T., THORVALDSEN, B. 1986: Dia-Structure shallow drilling 1986 Main data report. Appendix - Organic geochemical data. IKU Report 21.3420.00/04/86, 229p. Confidential.

VIGRAN, J.O., VAN DER EEM, J., WEITSCHAT, W., MANGERUD, G., RØMULD, A., MØRK, A. 1988: Follow-up studies Dia-structure shallow drilling 1986 Documentation of fossils. IKU Report 23.1316.01/01/88, 93p., 2 apps. Confidential.

VISSCHER, H., BRUGMAN, W.A. 1981: Ranges of Selected Palynomorphs in the Alpine Triassic of Europe. In: Review of Palaeobotany and Palynology, 34, 115-128.

WEISS, H.M., BAKKE, S., BUGGE, T., HANSEN, J.W., LØSETH, H., MØRK, A., MØRK, M.B.E., RITTER, U., SMELROR, M., VERDENIUS, J.G., VIGRAN, J.O., ÅRHUS, N. 1991: Shallow Drilling Troms III 1990: Main Report. IKU Report 23.1433.00/02/91. Restricted.

WHITAKER, M.F. 1984: The usage of palynostratigraphy and palynofacies in definition of Troll Field geology. In: Offshore Northern Seas - Reduction of Uncertainties by Innovative Reservoir Geomodelling. Norsk Petroleumsforening. Article G6.

WIERZBOWSKI, A. 1989: Ammonites and stratigraphy of the Kimmeridgian at Wimanfjellet, Sassenfjorden, Spitsbergen. Palaeontologica 34, 4, 355-378.

WIERZBOWSKI, A., ÅRHUS, N. 1990: Ammonite and dinoflagellate cyst succession of an Upper Oxfordian - Kimmeridgian black shale core from the Nordkapp Basin, southern Barents Sea. Newsletters on Stratigraphy 22, 1, 7-19.

WORSLEY, D., JOHANSEN, R., KRISTENSEN, S.E. 1988: The Mesozoic and Cenozoic Succession of Tromsøflaket. In: Dalland, A., Worsley, D. & Ofstad, K. (eds.), A lithostratigraphic scheme for the Mesozoic and Cenozoic succession offshore mid- and northern Norway. Norwegian Petroleum Directorate (NPD) Bulletin No. 4, 42-61.

ÅRHUS, N. in press: The Transition from Deposition of Condensed Carbonates to Dark Claystones in the Lower Cretaceous Succession of the Southwestern Barents Sea. Norsk Geologisk Tidsskrift.